NANOSTRUCTURED GRAPHENE NANOPLATELETS FOR ENERGY STORAGE APPLICATIONS

By

Anchita Monga

A DISSERTATION

Submitted to
Michigan State University
in partial fulfillment of the requirements
for the degree of

Chemical Engineering-Doctor of Philosophy

2013

ABSTRACT

NANOSTRUCTURED GRAPHENE NANOPLATELETS FOR ENERGY STORAGE APPLICATIONS

By

Anchita Monga

There is an increasing demand for high performance compact batteries for diverse applications ranging from portable electronics to electric automotive vehicles. This need has driven the direction of research towards newer materials, improved synthesis and architectured assembly. This research addresses the gravimetric and volumetric density challenges as well as the cost issues faced by energy storage devices by developing structured graphitic materials, aiming at better electrochemical performance, improved energy density and reduced cost.

The few layer graphene nanoplatelets (GnP) used in this study can be produced from natural graphite in thicknesses from 1-10 nm and in widths from 0.3 to 50 microns via an acid intercalation/thermal exfoliation process. The GnP serves as an inexpensive alternative to carbon nanotubes and single graphene sheets. The ability to nanostructure GnP and tailor its inherent properties for lithium storage and electrical conductivity, allows it to be used for customized applications in three different lithium ion battery components viz., active anode material, current collector and conducting additive.

Metal nanoparticle doped GnP in which nanosized metal particles are coated onto the GnP basal surface, have been assembled to make a 'pillared' nanostructure in which the

particles maintain a fixed distance between adjacent GnPs facilitating improved transport and enhanced lithium storage capacity, especially at faster charge rates. Graphene nanoplatelets synthesized with different sizes of metal nanoparticles effectively create a nano-architectured GnP multilayer assembly with flexible interlayer spacing. The creation of a lithium ion battery anode with controllable GnP interlayer spacing facilitates lithium ion diffusion through the electrode, and this in turn leads to improved transport and enhanced capacity.

Graphene nanoplatelets are also intrinsically excellent electrical conductors, which can be assembled into continuous conductive thin films to replace metal foils as current collectors for electrochemical applications. Self-standing, binder-free, flexible and porous paper is prepared by a simple filtration process using an aqueous suspension of GnP. This GnP paper is an attractive alternative current collector to replace copper in lithium ion batteries, because of its lower areal density, desirable electrical conductivity and good electrochemical stability. The performance of GnP as a current collector with different electrode materials and its role in reducing the overall battery cell weight has been investigated.

The third application combines the benefits of electrical conductivity and nanostructuring of GnP to function as a conducting additive for different electrode materials. An investigation of the use of different sizes of GnP as a conducting additive for lithium titanate electrodes and as a conducting host/matrix for lithium sulfur batteries has demonstrated its applicability here also.

Dedicated to my parents and to my sister

ACKNOWLEDGEMENTS

First of all, I would like to express my sincere gratitude and appreciation to my research advisor, Prof. Lawrence T. Drzal, for his patience, guidance and support through the course of my Ph.D. program. I am deeply thankful to him for the encouragement and numerous opportunities given to me, which helped me, showcase my research and develop my potential.

I am very thankful to my Committee members Prof. Martin Hawley, Prof. Jeff Sakamoto and Prof. Phillip Duxbury for their kind support and valuable suggestions. I am also grateful to Prof. Jeff Sakamoto and Ezhiyl Rangasamy for helping me with the experiments and technical nuances of this research field.

I would like to extend a sincere thanks to all the research staff at CMSC, Mike Rich, Brian Rook, Per Askeland, Hazel Ann Hosein and Ed Drown for always being there and for providing their endless help, patience, efforts and support for my research. Also, I would like to thank Hiroyuki Fukushima, Inhwan Do, Wanjun Liu, Hwanman Park, Xiaobing Li, Saswata Bose and Frederic Vautard for their valuable inputs and feedback. Also, my deepest appreciation goes to Karen Lillis, Inger Weitlauf, Shirley Wohlfert, Joann Peterson, Lauren Brown and Danielle Murphy for their assistance in making this journey smooth.

A special thanks goes to my colleagues and officemates through these years, Xian, Jinglei, Dee, Yan , Pat , Sanjib, Huang, Tao , Deb, Dana, Steve, Eeshwar, Markus, Keith, Albert

and Isabel David, for providing me the best workplace possible. I will always remember the smiles, conversations, serious discussions and celebrations, experienced in your company.

A special acknowledgement goes to my friends Durga, Anbu, Raghav, Madhumitha, Abinand, Ezhiyl, Rengarajan, Nikita, Prachi, Leo, Venkat and Sudhanwa for being my support system and my extended family. Thank you for always being there through all the ups and downs and making my stay at MSU a memorable one.

Life in US, away from home, would not have been easy without my family in Iowa and I can't imagine taking this step without the support of my brother Amit, my sister in law Sonia and my nieces Soumya and Anya.

Finally, I would like to thank my parents, Mr. B D Monga and Dr. Kanchan Monga and my sister, Samita for their unconditional love, support and encouragement at every step, in making me who I am today. Also, I would like to thank my brother-in-law Atin and my adorable niece Azalea for bringing endless joy to our lives.

TABLE OF CONTENTS

LIST OF TABLES

LIST OF FIGURES

1 INTRODUCTION

DEMAND FOR ENERGY STORAGE

With the finite availability of fossil fuels and the imbalance in demand and replenishment of coal and petroleum based reserves, there has been immense focus on alternative energy resources for catering to the increasing power demands. The utilization of alternative energy sources such as solar, wind, water or nuclear based energy have been critically evaluated by their availability, sustainability, efficiency, environmental impact and need for energy storage and transmission. The first three are very attractive but limited by their availability at certain times and locations thus necessitating the additional need for energy storage and transmission. However nuclear energy requires a sophisticated setup and complicated disposal due to the hazardous nature of the reactants involved leading to a high capital investment. Moreover, with advancements in technology, diverse high power and high-energy requirements for portable applications has been created. Electrochemical energy storage is a potential solution that can meet these requirements in an efficient and environmentally friendly manner if gravimetric, volumetric and economic metrics can be achieved.

LITHIUM BASED BATTERIES

Lithium based rechargeable batteries have emerged as the most promising solution to the increasing energy needs, ever since its advent in 1970s. Firstly their use as primary

batteries, and then their use as rechargeable batteries (after commercialization by Sony in 1990), lithium ion batteries were the preferred choice for diverse portable applications. They had significant advantages over other battery technologies because of high energy density (Figure 1-1), lower weight and good cycle life. These advantages can be attributed to high electropositive nature and low weight of lithium[1]. The potential of these batteries extends over a wide domain of mobile applications ranging from small portable electronic appliances such as cell phones, iPods and laptops to their use in hybrid electric vehicles.

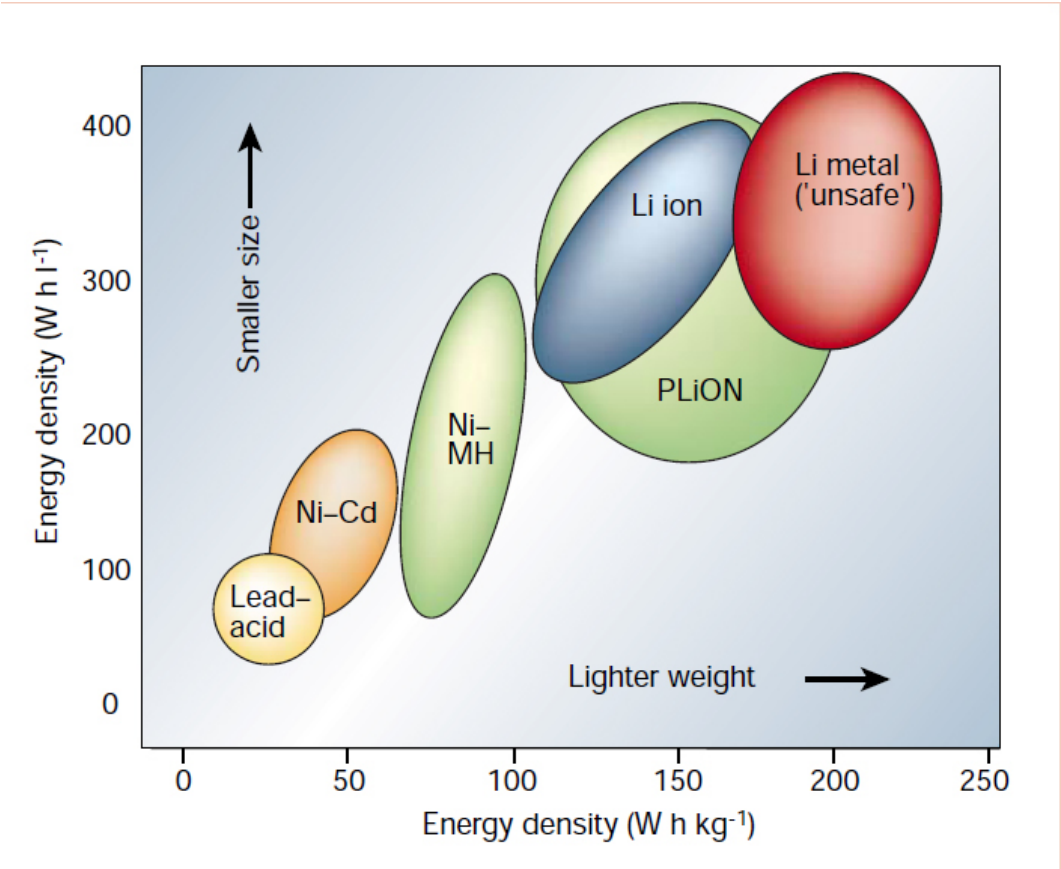

Figure 1-1: Gravimetric and Volumetric energy density of different battery systems [2]

"For interpretation of the references to the color in this and all other figures, the reader is referred to the electronic version of this dissertation"

LITHIUM-ION BATTERIES

A commercial lithium ion battery involves a graphitic anode with a lithium metal oxide ($LiMO_2$) cathode, sandwiched in a cell with a porous non-conducting separator and $LiPF_6$ electrolyte in a mixture of organic solvents (Ethylene Carbonate + Dimethyl Carbonate). The lithium ions shuttle between the two electrodes during charge and discharge, with a corresponding exchange of electrons through the external electrical circuit. During discharge, the lithium ions travel from the graphite anode to the cathode through the electrolyte, and the process is reversed in the charging step, where lithium ion migrate from cathode and move towards the anode, and re-intercalate between the layers of graphite.

In the first cycle, a thin film called Solid Electrolyte Interface (SEI) is formed on the surface of electrodes, due to the high field strength at the surface resulting in the degradation of the electrolyte. This passivated electrically insulated film is comprised of lithium organic and inorganic compounds and consumes lithium in the first cycle, resulting in irreversible loss of capacity. However, the SEI layer does not decompose on charging and can be beneficial in stabilizing the electrode-electrolyte interface and avoid further electrolyte degradation[3,4]. Though, for high surface area electrode materials, there can be significant SEI film formation, which can result in a battery temperature increase (exothermic reaction) and hindered charging and discharging kinetics. Many different electrode materials can be used as cathode, and anode materials for lithium ion batteries. Different cathode and anode materials corresponding to their potential and capacity valueshave been studied and summarized in detail by Tarascon et. al[2]. Some of the most popular electrode materials are described briefly in the next section.

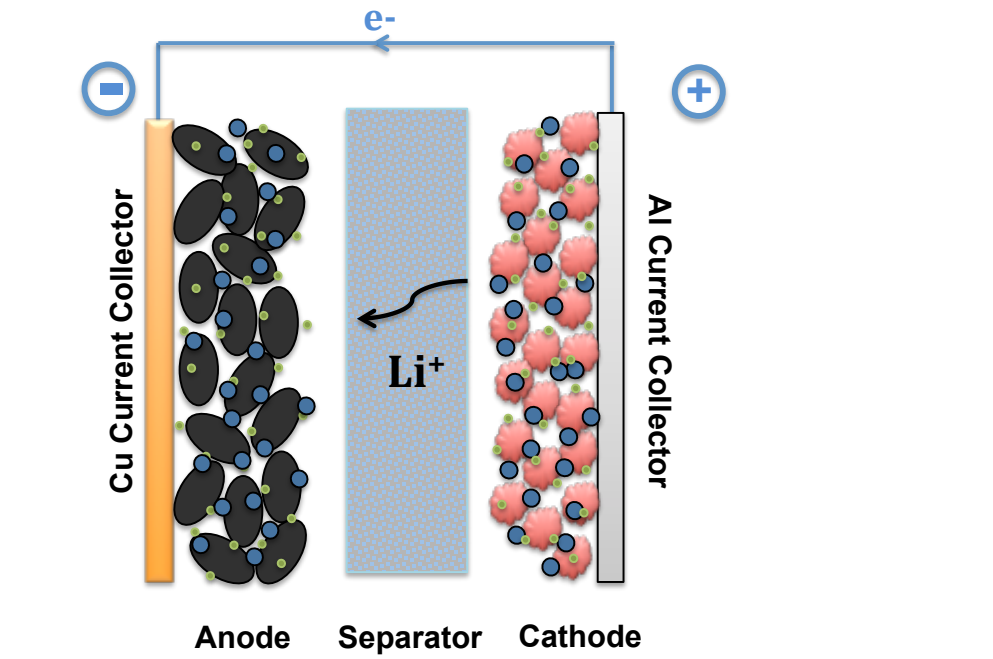

Figure 1-2 : Schematic showing the working of lithium ion battery (Adapted from http://bestar.lbl.gov/venkat/files/batteries-for-vehicles.pdf)

$$6C + LiCoO_2 \leftrightharpoons Li_xC_6 + Li_{1-x}CoO_2$$

Anodes

Metallic lithium could have been the ideal choice for anode material, because of its high energy density and maximum potential difference with respect to the cathode, however its usability has not been realized because of its high reactivity, dendrite formation and low melting point, thus raising concerns about safety[5]. Some common anode materials that are being considered for these batteries include:

Graphite

Graphite is the most commonly used anode material for lithium ion batteries due to its abundance, good cycle life, reasonable capacity and low cost. These electrodes operate by an intercalation mechanism based on stepwise insertion of lithium ions in between the graphene layers[6] (staging).

$$C_6 + Li^+ + e^- \leftrightarrow LiC_6.$$

The theoretical storage capacity of graphite is 372 mAh/g and it has a nominal volume expansion of 10 % in the direction perpendicular to the graphene plane after lithium intercalates in between graphene layers[7].

Nano-carbon materials such as carbon nanotubes and graphene have been a subject of interest in recent years, and have been known to deliver significantly higher capacity in comparison to graphite powder. These materials are discussed in detail in a later section.

Transition Metal Oxides

Lithium titanate is another promising anode material, which operates by intercalation approach. Despite of its low storage capability 170mAh/g , LTO has shown potential because of its high rate performance, zero strain with intercalation and excellent cycle life.

$$Li_4Ti_5O_{12} + 3Li^+ + 3e^- \rightarrow Li_7Ti_5O_{12}$$

Moreover, LTO operates at relatively higher potential, at which there is no electrolyte decomposition and hence, is safer and more reliable.

Several other metal oxides based on conversion reactions such as NiO, MnO_2, Co_3O_4 and Fe_2O_3, are being explored as anode materials[5,8].

Metal Anodes / Alloying Anodes

Other anode materials such as Si, Sn, and Ge are based on alloying interaction with lithium and hence can deliver significantly higher capacity (4200 mAh/g, 990 mAh/g and 1600mAh/g respectively)[8,9]. However they undergo a significant volume change during the alloying-dealloying process, which can result in material failure, loss of conductivity and electrode pulverization. The current research focus is on developing nanostructured composite electrodes of these high capacity materials with a flexible conducting matrix, so as to ensure high capacity without loss of electrode conductivity and act as a buffer for accommodating strain during volume expansion.

Cathodes

Cathodes are the limiting factor so far that are restricting any drastic improvements in the performance of lithium-ion batteries. The selection of cathode materials is evaluated on the basis of its storage capacity, rate performance and thermal stability, which in turn affects the safety of the batteries[10]. The different categories of cathode materials currently being investigated are briefly described below.

Layered Lithium Transition Metal Oxides

$LiCoO_2$ is the most popular cathode material for lithium ion batteries because of good cycling stability, and easy synthesis. Because of concerns about the cost, toxicity and availability of cobalt, other layered systems such as $LiMnO_2$ and $LiNiO_2$ are also being explored[11]. The layered structure of these materials is attractive for easy accessibility of lithium ions. However these materials suffer from the problems of low tap density("amount of material that can be loaded into a specific volume[10]"), lower power performance and capacity fade on cycling.

Lithium transition metal oxide Spinels

Spinel $LiMn_2O_4$ is another potential candidate for cathodes for lithium in batteries and has attractive features such as eco-friendly, high power capability, abundance, low cost and better safety[2]. But it has a high reactivity with non aqueous electrolytes, which can cause the Mn^{2+} ions to dissolve in the electrolyte, and get deposited on the anode, thus degrading the

performance and causing capacity fade[10]. This problem is being addressed by nanostructuring, developing new materials and use of electrolyte additives[10].

Lithium transition metal phosphates Olivines

$LiFePO_4$ has emerged to be a promising cathode material primarily because of its low cost, thermal stability and good cycle performance. In the initial studies of $LiFePO_4$ starting 1997, several challenges such as low electronic and ionic conductivity and low energy density were faced, which limited its potential[10]. However, these drawbacks were taken into account by developing nanomaterials for improved ionic mobility and conductive surface coatings for enhanced conductivity[7]. Recent studies have explored alternate transition metals such as Mn, Ni, Co to replace Fe, which can increase the operating potential of this material.

Electrolytes

Conventionally, Lithium hexafluorophosphate ($LiPF_6$) is used as the electrolyte salt in a combination of organic solvents (Ethylene carbonate, Dimethyl carbonate, Propylene carbonate). These electrolytes pose a potential safety hazard in unusual situations of short-circuits, leakage, overcharging and thermal runaway reactions, because of their high reactivity and corrosive nature.

In addition to developing new electrode materials, there has been a tremendous interest in exploring electrolyte improvements, to enable the applications of lithium ion batteries for diverse high power and high energy applications. The progress in this direction is

directed towards solid polymer electrolytes, which are advantageous due to their higher energy density, no leakage or explosion problems, ease in manufacturing and low cost. However, these materials are still restricted due to low conductivities at room temperature, thus making them applicable only to slow charge rate systems[2,10]. Gel electrolytes are the intermediate answer to these two categories, having leakage free properties with good ionic conductivity.

LITHIUM-SULFUR BATTERIES

Lithium-sulfur batteries offer a promising solution for high energy density applications. They are of particular interest due to low cost, non-toxicity, abundance and high theoretical capacity of sulfur. These batteries are based on the redox reaction mechanism for conversion of Sulfur (S_8 molecule) to Li_2S. Theoretically these batteries are capable of delivering 2500 $Wh.kg^{-1}$ and 2800 $Wh.l^{-1}$ gravimetric and volumetric energy density respectively[12]. However, they suffer from serious limitations, such as poor conductivity of sulfur and polysulfides, dissolution of reaction intermediates into the electrolyte, thus compromising the efficiency and reversibility of these electrodes[12–14]. The high order polysulfides formed at the cathode, which are soluble in the electrolyte, can migrate to the anode, get converted to the low-order polysulfide and transport back to the cathode, where they get oxidized and return back to anode. This shuttle mechanism leads to capacity fade and loss of active electrode area when the reaction proceeds to form insoluble and insulating Li_2S. Significant research is being done in the recent times, trying to overcome these challenges by developing conducting matrices,

which are partially restrictive to polysulfides, and by exploring alternative electrolytes which don't react with polysulfide compounds[14].

$$2\,\mathrm{Li} + 2\,e^- + \mathrm{S} \rightleftharpoons \mathrm{Li_2S}$$

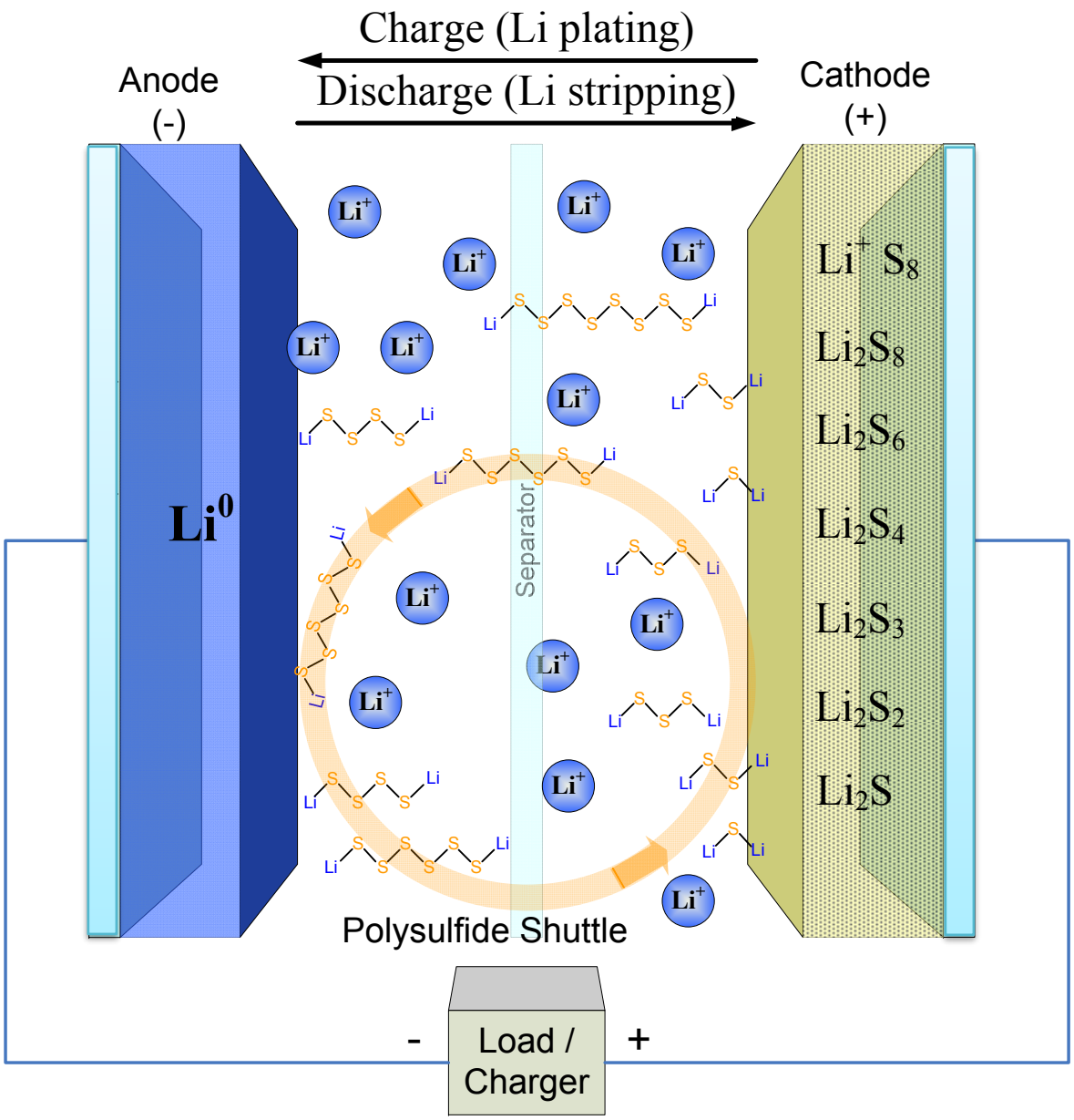

Figure 1-3: Schematic showing the working of Lithium-Sulfur Battery [15]
Text within figure is not meant to be readable and is for visual reference only.

Anode

Lithium metal is used as the anode for lithium sulfur battery and accounts for their high performance, because of the high theoretical specific energy of lithium. However, there is a necessity to use excessive lithium, since complete utilization of its capacity is not achieved. This inefficiency results from two factors, repeated formation of SEI layer in every cycle and parasitic consumption of Lithium in polysulfide reaction to form Li_2S on the anode (polysulfide shuttle)[16,17]. Also, dendrite formation is another problem, that can lead to short-circuits, and hence the failure of the batteries. To address these issues, different approaches such as improved SEI layer formation, electrolyte additives for protective films and polymer protection layer for lithium anode protection, are being explored[18]. These disadvantages, safety concerns and limited amount of Lithium resources has prompted the need for alternative anode materials[16,18].

Alloying anodes, such as Sn or Si can be used as anode options; however, their usage in this system will either involve prelithiation before cell-assembly or the use of Li_2S as the cathode[16,19].

Cathode

Sulfur composites with carbon materials are used as the cathode for this system. The poor conductivity of sulfur and the polysulfide compounds makes the presence of a conducting material indispensable. Porous carbon frameworks, mesoporous carbon materials and other

nano carbon materials like carbon nanotubes, graphene, carbon fibers etc. are evaluated for their role in imparting necessary conductivity and restraining polysulfide dissolution[12,13,20]. The morphology and structure of electrode can make a significant impact here, and hence different nanostructures such as template structures, mesoporous frameworks, porous /tubular hosts and hierarchical structures, are being evaluated[21]. This approach is discussed in detail in Chapter 5.

Electrolyte

Electrolyte is one of the most crucial components for practical development of efficient lithium-sulfur batteries. The problem of dissolution of polysulfides in the liquid electrolyte is a major challenge, which results in parasitic consumption of lithium, loss of sulfur and capacity fade. Selection of appropriate liquid electrolytes, use of ionic liquids and additive materials such as $LiNO_3$, can help in protecting lithium anode by forming a passivating layer and reducing polysulfide dissolution[13,18]. Various polymer electrolytes, and gel–electrolytes and ceramic electrolytes are being explored, owing to slow dissolution of polysulfides and better separation of lithium anode from the cathode[16,17]. However, these alternatives are still facing challenges of low ionic conductivity, electrode-electrolyte interface and reactivity with lithium metal[13].

LITHIUM-AIR/OXYGEN BATTERIES

Lithium –air batteries are being envisioned as a future alternative to high performance energy solution, since their theoretical and also estimated practical energy density are significantly higher than all other battery systems[5,10]. The technology has been explored for primary batteries for a while, however its application for rechargeable batteries gained attention after reports of reversibility were shown by the use of MnO_2 as catalyst[10,14]. These batteries have been investigated for aqueous as well as non-aqueous electrolytes. Figure 1-4 below shows the schematics of lithium-air batteries in both setups. The anode here is Lithium metal, which gets oxidized on discharge and forms Li^+, which is transferred through the electrolyte. On the cathode, which is a porous carbon network, oxygen from the atmosphere dissolves in the electrolyte and interacts with the lithium ion and is reduced. Different reaction products are formed based on the kind of electrolyte used as shown below.

$$2Li^+ + 2\,e^- + O_2 \leftrightharpoons \mathrm{Li_2}O_2$$

$$2Li^+ + 2\,e^- + \frac{1}{2}O_2 + H_2O \leftrightharpoons 2LiOH$$

These batteries face significant hurdles before they can be used for commercial applications. Some of them involve the dendritic formation and safety issues associated with lithium metal anodes. Other challenges involve use of suitable electrolytes to avoid any

precipitation, and selectivity of cathode materials allowing O_2 but restricting CO_2 and H_2O[10,14,22].

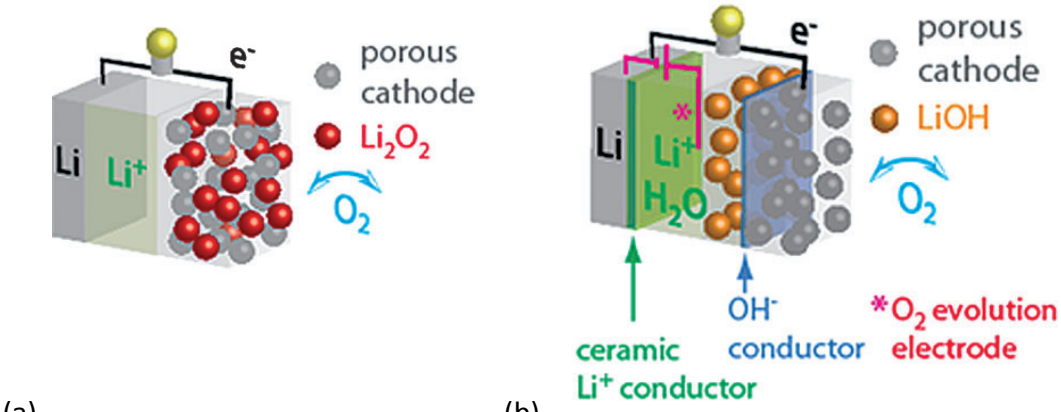

Figure 1-4: Schematic showing the setup of Lithium-air (O_2) batteries (a) non-aqueous electrolyte (b) aqueous electrolyte[10]

CHALLENGES ASSOCIATED WITH LITHIUM BATTERIES

Performance

To cater to the increased energy and power requirements, new materials with higher capacity, better rate performance and high coulombic efficiency are needed. This need motivates the development of new chemistry, new materials and new morphologies (nano), which will have inherently better storage capabilities. In addition to high storage capacity, reversibility, cell voltage and rate capability are crucial factors governing the application of a material for desired applications. However, complete utilization of theoretical capacity can be a challenge. Such situations can arise due to incomplete accessibility, low conductivity and undesirable side reactions. Another challenge faced in the performance is in case of gravimetric energy density

of the battery. This entails the use of inactive components in the battery such as conducting additives, binders, current collectors and packaging materials. Hence, there is a focus on reducing the dead weight in the cell by reducing the weight of conducting additives and binders in the electrodes. Also, self-standing and lightweight current collectors are being investigated to improve the gravimetric energy density of these electrodes.

Ionic transport

In all different types of active materials for cathode and anodes, lithium ion diffusion is one of the most critical factors that impact the performance of the electrode. This problem is mainly addressed by developing nanosized material or nanostructured electrode, which will result in reduced diffusion length and hence shorter diffusion time of lithium ions, especially during charge.

Electrical Conductivity

Many of these electrode materials such as silicon, lithium transition metal compounds for cathodes and anodes have inherently lower electrical conductivity, which can affect its high rate capability and high power performance. Such materials require the addition of a conducting supplement, which can ensure good electrical contact through fast and long term cycling. This can be done by doping, conductive coating, use of conducting templates or by addition of conducting additives in the electrode.

Volumetric expansion

Some of the electrode materials undergo significant expansion and contraction during the charge-discharge process, which eventually has a negative effect on the mechanical

integrity of the electrode. In particular the electrode materials based on alloying mechanisms such as Si, can increase in volume as much as 300%. Repeated changes in volume can exert high stresses on the electrode, thus causing cracking, delamination or pulverization. In addition, this will cause discontinuity in the conducting network of the electrode, thus resulting in higher resistance and inefficient utilization of the electrodes. To tackle this problem, design of electrodes utilizing nanomaterials organized into a more robust network allowing for flexibility without fracture is considered. Various nanosize active materials of different shapes and morphologies have shown good prospects in resolving this problem. Porous or hollow nanostructures (such as nanotubes or template mesoporous structures), accommodate a volume change without affecting the electrode structure. Other approaches involve use of composite electrodes with porous conducting matrices and addition of high aspect ratio conducting additives to ensure conductivity. The distribution of nanoparticles within the structure does not change the overall volumetric change but does distribute it is such a way as to avoid failure of the overall electrode structure.

Side Reactions and Insulating products

There are some side reactions that happen during the process of potential change during cycling, which can pose a challenge to the performance of electrode materials. For example, a passivating SEI layer is formed in the first cycle of carbon anodes, which is a result of electrolyte degradation. Despite of its benefit in stabilizing the electrode-electrolyte interface, increased SEI formation can lead to low conductivity, reduced kinetics, and loss of active surface area [3]. Also, there are some intermediate reaction products, which are insulating in

nature, and hence can inhibiting the further reaction by blocking ion transport or by loss of electrical contact. Such a phenomenon is observed in Lithium sulfur batteries, where insulating intermediate polysulfides products can deposit on the electrode surface, thus restricting the availability and efficiency of the active material[14]. A similar problem is experienced in lithium-air batteries also, where insoluble Li_2O_2 can deposit on the active electrode material, reducing the electron and ion transport, thus decreasing the efficacy of active material[5,14].

Safety

Safety is one of the most important concerns restricting the usage of lithium ion batteries for some applications such as automobiles. The electrolyte currently being used can cause serious problems such as high vapor pressure, high flammability, and environmental and health hazards, in case of a runaway reaction or leakage[10,22]. The use of Li metallic electrode is restricted due to the risk of dendrite formation or lithium plating. Other safety issues revolve around the thermal stability of the electrode materials (particularly lithium transition metal cathodes and high surface area carbon electrodes)[10] and the chances of short circuit in the batteries.

GOING THE NANO-ROUTE

To satisfy the increasing performance requirements of the lithium based batteries, drastic changes in the existing technology are required. The solution is moving to the "Nano" dimension, i.e., developing nano-scale materials or doing nano-architectured assembly. The concepts, efficacy and challenges associated with the development of nanomaterials have been

well studied and comprehensively reviewed[1,8,11,23–25]. Some of the important advantages and disadvantages of nanomaterials are described below.

With nano-features, unique behavior of material is observed which can be attributed to the combination of bulk and surface properties. Developing materials at the nanoscale can result in the prominence of reactions, which are restricted on a macroscopic scale[23]. The increased surface area enhances electrode-electrolyte interaction, thus improving the performance of the reaction.

Another significant advantage of using nano-size particles is the resulting shorter path length between constituents, resulting in improvements in electron and lithium ion transport[25]. The effect of enhanced diffusion on nanostructuring can be understood by looking at the basic equation for solid state diffusion

$$\tau = L^2/2D,$$

where τ is the mean diffusion time, L is the diffusion length, D is the diffusion coefficient.

The diffusion length can play a crucial role in reducing the diffusion time, which corresponds to fast transport of lithium ions in and out of the system. Based on diffusion models, it can be seen that a change in L from 10 μm to 100 nm can bring about a change of 4 orders in magnitude in diffusion time[24]. The effect of fast diffusion of lithium ions translates into improved capacity at faster charge rates. In a real system, various other parameters such

as nature of electrolyte, size of active materials, tortuous pathway and solid-liquid interface, which will play a role in diffusion of lithium ions. Based on a simplified estimation, it has been observed that specific capacity will depend on volume ratio, $\{r^3-(r-L)^3\}/r^3$ where r is the radius of the active particle[25]. Using this parameter, it has been estimated that for a charge discharge cycle of 1 min, the particle size of active material should be 2 nm in dia[25].

In addition to improved diffusion, nanostructuring can also play a role in improving the mechanical integrity of the electrode. This is particularly advantageous in the case of alloying anodes, which can undergo a high volume change, (as high as 300% for Silicon) during the charge-discharge process. Nanomaterials, even if they undergo the same relative volume expansion, don't undergo a huge change in the absolute size, and hence are better capable of handling strain. Thus, reducing the active material to nanoscale and encapsulation in a flexible conducting matrix, can allow buffer for volume expansion without loss of conductivity, thus holding the electrode together and solving the problem of electrode pulverization[8].

However, there are some critical disadvantages of nanomaterials, which can restrict their efficacy for energy storage applications[26]. First and foremost, the synthesis methods are complex, not well understood and require sophisticated techniques, which increases the difficulty level and cost involved in the large scale synthesis of the material. Also, the attractive feature of a high interfacial area can be disadvantageous by providing more area for undesirable side reactions. Excessive SEI layer formation can occur because of high surface area availability, which can lead to temperature elevation and capacity degradation[3]. In addition, the

poor compaction of smaller particles results in lower volumetric energy densities. Hence, the development of nanomaterials requires significant consideration of the pros and cons, thus demanding careful optimization of morphology, to achieve the desired performance.

One way of approaching this situation is to develop nano/micro hierarchial structures such as self-assembled nano/micro materials, nanostructured composites, mesoporous materials, hierarchical 3-D mixed conducting network[24]. Such a structure can encompass the benefits of easy synthesis, good conductivity & mechanical integrity of the microstructure and fast diffusion and better performance of nanostructure.

SIGNIFICANCE OF NANOSTRUCTURING

In conjunction to developing new materials with a nanodimension, structuring of electrodes to facilitate electron and ion transport is the next step towards achieving the performance targets in this field. Developing well-architectured nanostructures in different ordered shapes can enable benefits such as high surface area, short diffusion length, ordered porosity and interconnectivity. These features are crucial for getting good electrode electrolyte contact area, thus resulting in more active sites and hence improved performance. An ordered, well- connected structure will help maintain good cycle life by absorbing volumetric strain and maintaining conductivity, thus maintaining electrode integrity. Some common approaches used for nanostructuring are described below:

Template-Directed Materials

One of the most facile methods of developing controlled structures with desired functionality is by the templating method. Anodic aluminum oxide (AAO) and MCM-silica are commonly used

templates, owing to their availability in different shapes and pre sizes. The resulting structure is generally the inverse of the template structure and hence the choice of template scaffold can decide the morphology and dimensions of the resulting nanostructure[27]. Nanowires, nanotubes or rod-shaped structure can be created using an AAO template with isolated pores, and 3-D porous structures can be created with templates with continuous pores[27]. This technique is very versatile and can be used to synthesize any type of electrode material, ranging from carbon nanotube, carbon fibers, silicon forest, to lithium transition metal compounds and sulfur cathodes.

Sol-Gel

Sol-gel is a well understood and popular synthesis technique, particularly for synthesis of lithium transition metal compounds for cathode for lithium ion batteries. This method offers better control over synthesis procedure because of homogeneous mixing and lower heating temperature, thus yielding nanometer size uniform particles. This technique is widely used to synthesize most of the cathode materials[28,29] and some anode materials[29] (SnO_2, TiO_2, LTO etc.) . It has been demonstrated that materials prepared by sol-gel method have shown improved capacity, cycle life and rate performance[28–32].

Self-Assembly

Self-assembly of two components in a composite electrode is another technique being explored to develop uniform, well-connected electrodes for batteries applications The assembly is driven by use of appropriate surfactants, opposite charged polyelectrolytes, resulting in the formation

of ordered structure with alternating layers of active components. This methodology is widely used to make graphene-metal oxide composite material for anodes[33,34], and for making conductive additive and lithium metal compounds for cathodes. In addition to the benefits of the two components in the composite, such electrodes have demonstrated a better and faster rate performance, reduced capacity fade and improved cycle life.

Layer by layer (LBL) assembly

Another methodology of developing structured electrodes is by LBL technique, in which repeated sequential immersion of substrate into polycation or polyanion solution alternatively can result in an well-organized assembled structure[35]. This method is advantageous due to its versatility with different types of materials, environmentally friendly and inexpensive process.

Carbon nanotubes and graphene composite electrodes with metal nanoparticles can be synthesized effectively using this technique with less aggregation, no polymeric binder and high packing density[35]. However, this process involves multiple steps and can be time consuming, from the perspective of commercial applications.

Using these techniques, we can synthesize diverse nanostructured architectures, such as nanoparticles, nanorods, nanotubes, core-shell nanostructures, 3-D pillared architectures, mesoporous 3-D structure[5,36]. These approaches to tailor-made structure have shown improved performance and have opened the way forward for addressing the challenges faced by the rechargeable lithium battery scenario.

CARBON BASED NANOMATERIALS

Nano-scale materials such as carbon nanostructures show distinct thermodynamic and kinetic properties in comparison to their bulky counterparts. This miniaturization also results in unique properties, which can be suitably modified when required. The reduced length scale improves the kinetics by increasing the diffusion rate and decreasing the diffusion length.

Graphitic materials are currently being used as anode materials in commercial lithium ion batteries because of their good performance and exceptional properties such as electrochemical stability, cycle life and low cost. Graphene, the 2-D carbon nanostructure, has been an active material of interest for energy applications, because of its high surface area and excellent electronic conductivity over its other carbon counterparts[37]. After its discovery in 2004, the potential for graphene as an anode material in itself and its composites with different metal oxides and silicon has been a focus of research in the development of new materials. In addition to individual graphene sheets, other graphene nanostructures such as carbon nanotubes, graphene nanoribbons and graphene nanoplatelets have been the subject of interest and have been evaluated based on their performance, safety, feasibility and scalability.

GRAPHENE BASED MATERIALS

Graphene is the single atom layer of hexagonally packed sp^2 carbon atoms[38], which forms the building block for many carbon materials. This two- dimensional monolayer of carbon atoms can be wrapped up into 0D fullerenes, rolled into 1D nanotubes or stacked into 3D graphite as shown in Figure 1-5. Graphene, as a stable material was extracted/obtained for the

first time by the Scotch-tape method by Geim and Kostya in 2004 [39], and this brought about a revolution in terms of nano-graphitic applications. Since then numerous studies have been done to synthesize large quantities of graphene sheets by different methods viz., Scotch tape, chemical vapor deposition, oxidation and exfoliation, thermal exfoliation, sonication etc[38,40,41]. However, the variation in synthesis procedure can result in considerable differences in the physical properties of graphene.

Graphene is a really thin flexible material with a large surface area (up to 2600 m^2/g), chemical inertness, good mechanical strength and excellent electrical and thermal conductivity, which makes it very desirable for several electrochemical applications. There are multiple literature reports showing the use of graphene in lithium ion batteries, fuel cells, transparent films for solar cells, conductive support for platinum catalyst for DSSC[40,42,37,43].

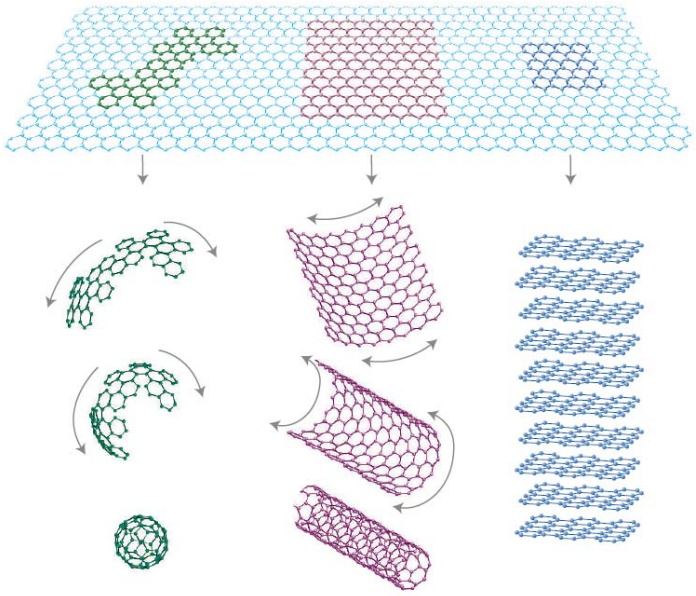

Figure 1-5 : Nanostructures based on graphene (a) 0-D fullerene (b) 1-D carbon nanotube (c) 3-D graphite [44]

GRAPHENE USE IN LITHIUM BATTERIES

Anode Material

Graphene sheets because of its nano dimension thickness and high electrical conductivity was expected to be an excellent anode material for lithium ion batteries. Lithium storage capability of graphene sheets was reported in the range of 500-1500 mAh/g[45,46]. This was a significant improvement over the theoretical 372 mAh/g lithium storage capacity of carbon materials. Different explanations have been proposed to explain the increase in storage capacity and since the synthesis methodology is varied, there is no consensus on what might be the primary reason behind the improved performance

Graphene sheets are known to have high surface area, since both sides of every sheet are available, hence lithium interaction on both sides has been projected as a possible

explanation for higher storage capacity. Also, because of its nano-dimensions, graphene electrodes will have shorter diffusion pathway, and improved transport, which can enhance its storage capability. Other hypotheses revolve around increases in lithium insertion active sites, due to high surface area, defects, nano cavities, edge sites[45], and functionality on the graphene[46]. Suitable modifications in graphene sheets such as pillaring of graphene sheets with CNTs or fullerenes[47] or metal nanoparticles to avoid agglomeration[38] or creating nanopores[38] and holes[48] in graphene sheets to allow facile Li+ ion diffusion, has also shown improved high rate capacity performance.

However, for most of the graphene based systems, because of large surface area and more edge sites, increased SEI formation has been observed, which results in high first cycle capacity loss[49]. In addition, poor rate performance, hysteresis, capacity fade, large scale production and high synthesis cost are some of the deterrents towards the commercial application of graphene as anode material[47,49].

Graphene Composites with metal/metal oxides as Anode Material

Metal anodes (Si, Ge, Sn) and the metal oxides (TiO_2, Co_3O_4, etc.) are alternate anode materials for lithium ion batteries. However, most of these materials suffer from low electronic conductivity. In addition, metal anodes based on an alloying mechanism such as Si, Ge , Sn are also prone to huge volume changes, resulting in loss of conductivity and electrode degradation. Making a composite of these materials with graphene can impart the necessary electronic

conductivity coupled with high storage capacity[49,50]. Also, appropriately nanostructured electrodes, such as graphene–Si[51,52] and graphene–SnO_2 [53,54,55] composites can form an expandable structure, which can adjust for the mechanical strain during alloying process.

Graphene as Conducting Additive for Anode and Cathodes

Graphene has been used as a conducting additive for lithium titanate electrodes[56,57,58]. It has been shown that a graphene aided nanostructure can improve performance by reduced polarization[56], improved conductivity and reduced impedance[58].

Similar phenomenon was observed for different cathode materials, such as LiCoO2 and LiFePO4 [59,60], where the desired conductivity can be observed at a lower percolation in comparison to commercial Super P.

GRAPHENE NANOPLATELETS (GNP): OUR MATERIAL OF INTEREST

Graphene nanoplatelets (GnP) are an inexpensive alternative to other carbon nanomaterials such as carbon nanotubes and single graphene sheets[61]. These nanoplatelets are a few sheets of graphene stacked together and have micron range diameter, thus giving it the beneficial high aspect ratio.

GnP is synthesized from natural graphite by a simple acid intercalation and exfoliation procedure[62], which is schematically represented in Figure 1-6. Graphite intercalated compounds (GICs), synthesized by intercalating a combination of sulfuric and nitric acid, are

obtained commercially from Asbury Carbons. This acid intercalated material is subjected to microwave irradiation, which results in rapid heating. This sudden increase in temperature vaporizes the acid trapped in graphite galleries, thus causing expansion and ultimate exfoliation of graphite, forming an expanded "worm" like structure. These worms are then further subjected to a combination of sonication and milling procedures to form graphene nanoplatelets of different dimensions. These nanoplatelets can be produced with dimensions ranging from 50 microns to 0.1 micron in diameter and thicknesses ranging from 20 nm to 3 nm. Correspondingly the surface area can be modified from 20 m^2/g to 200 m^2/g. The GnP platelets have a pristine basal plane with few carboxylic and amine functional groups on the edge.

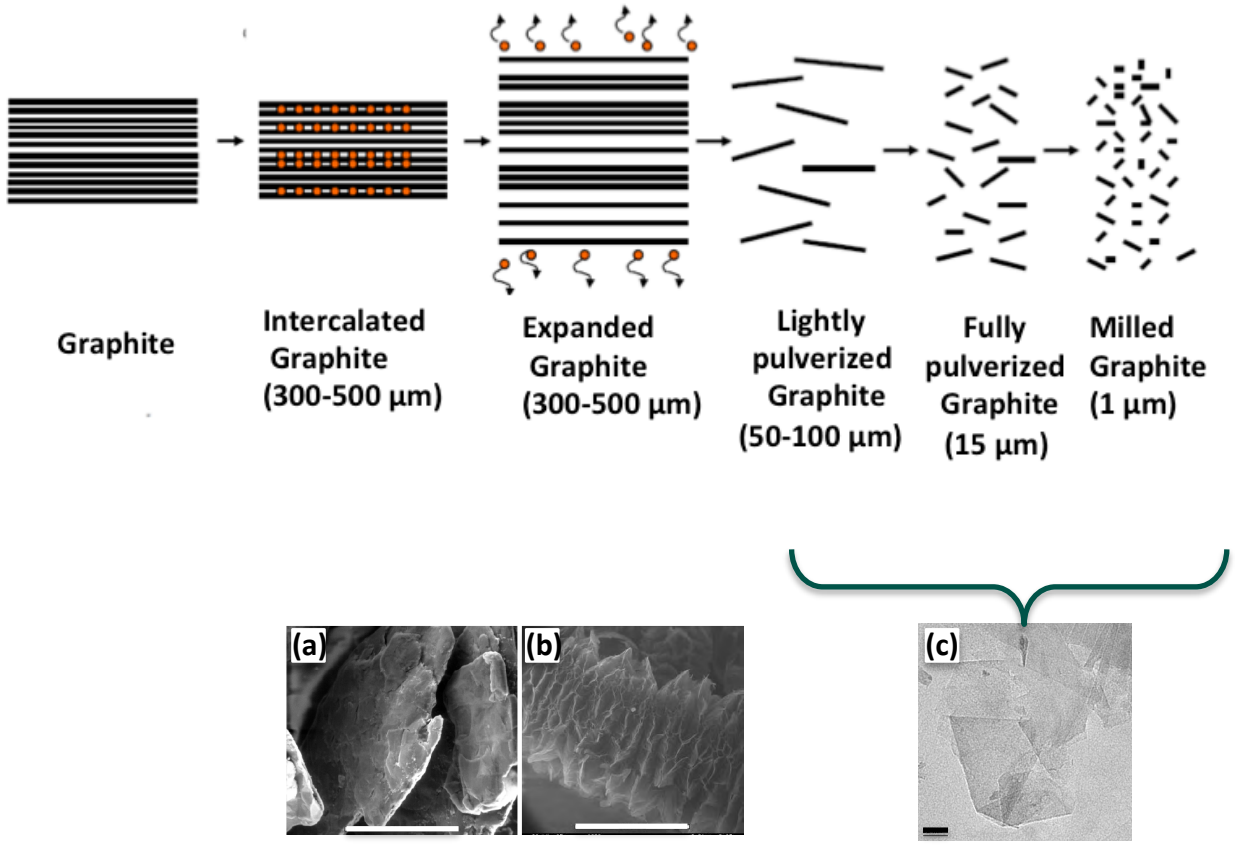

Figure 1-6 : Schematic showing synthesis of Graphene nanoplatelets (GnP) by intercalation and exfoliation procedure and SEM images of the corresponding stages [61] *(Scale bar : (a) 300 µm, (b) 500 µm, (c) 50 nm)*

The high aspect ratio and nano thickness of these platelets impart excellent electronic, mechanical and transport properties associated to these platelets. Also, GnP platelets have good thermal stability and chemical inertness, which makes it an attractive candidate for myriads of applications ranging from polymer composites to electrochemical energy storage.

Due to their comparable properties and simple, cost effective synthesis procedure, these platelets are a promising candidate for carbon nanomaterials for electrochemical energy storage applications.

DISSERTATION OBJECTIVE

This dissertation is focused on nanostructuring graphene nanoplatelets (GnP) by taking advantage of its inherent properties of lithium storage capability and electrical conductivity, and tailoring GnP for different applications for lithium-based secondary batteries.

In the first part of this dissertation we are evaluating the potential of GnP as anode active material for developing nanoarchitectured electrode structure, aiming at increase in energy density, reduction of cost and improvement in performance. Graphene platelets doped with different size of nickel metal nanoparticles are used to tailor-made different structured electrodes with improved transport and enhanced capacity.

In the next section, we have investigated the role of different sizes of GnP as a conducting additive in lithium titanate electrodes for lithium ion batteries. This work is focused on providing alternative to commercial carbon black materials, focused on reducing the additive concentration without compromising performance.

Further on, we are capitalizing on the high in-plane electrical conductivity of these platelets, to form current collector for electrochemical applications. The underlying fundamentals are to arrange these platelets in a structured manner, to optimize desirable properties of electrical conductivity and mechanical integrity.

In the last section we have explored the effect of GnP as a conducting matrix for sulfur electrodes for lithium sulfur batteries. Based on the results from the prior work, we have developed GnP-sulfur electrodes, targeted at achieving maximum capacity with long term cyclability. Two different approaches of using GnP as conducting additive and using GnP paper as conducting template are assessed.

REFERENCES

REFERENCES

1. Kumar, H., Rajan, S. & Shukla, A. K. Development of lithium-ion batteries from micro-structured to nanostructured materials: its issues and challenges. *Science Progress* **95**, 283–314 (2012).

2. Tarascon, J. M. & Armand, M. Issues and challenges facing rechargeable lithium batteries. *Nature* **414**, 359–67 (2001).

3. Liu, D. & Cao, G. Engineering nanostructured electrodes and fabrication of film electrodes for efficient lithium ion intercalation. *Energy & Environmental Science* **3**, 1218–1237 (2010).

4. Li, H., Wang, Z., Chen, L. & Huang, X. Research on Advanced Materials for Li-ion Batteries. *Advanced Materials* **21**, 4593–4607 (2009).

5. Song, M., Park, S., Alamgir, F. M., Cho, J. & Liu, M. Nanostructured electrodes for lithium-ion and lithium-air batteries : the latest developments , challenges , and perspectives. *Materials Science & Engineering* **72**, 203–252 (2011).

6. Winter, B. M., Besenhard, J. O., Spahr, M. E. & Novuk, P. Insertion Electrode Materials for Rechargeable Lithium Batteries . *Advanced Materials* **10**, 725–763 (1998).

7. Rev, A. *et al.* Materials for Rechargeable Lithium-Ion Batteries. *Annu. Rev. Chem. Biomol. Eng.* **3**, 445–471 (2012).

8. Bruce, P. G., Scrosati, B. & Tarascon, J. Lithium Batteries Nanomaterials for Rechargeable Lithium Batteries. *Angewandte Chemie* **47**, 2930–2946 (2008).

9. Mukherjee, R., Krishnan, R., Lu, T.-M. & Koratkar, N. Nanostructured electrodes for high-power lithium ion batteries. *Nano Energy* **1**, 518–533 (2012).

10. Choi, N. *et al.* Challenges Facing Lithium Batteries and Electrical Double-Layer Capacitors . *Angewandte Chemie* **51**, 9994–10024 (2012).

11. Alc, R., Lavela, P. & Carlos, P. Nanostructured Electrodes for Lithium Ion Batteries. *Solid State Electrochemistry II: Electrodes, Interfaces and Ceramic Membranees* 383–413 (2011).

12. Evers, S. & Nazar, L. F. New Approaches for High Energy Density Lithium Sulfur Battery Cathodes. *Accounts of chemical research* , (2012). **DOI:** 10.1021/ar3001348

13. Su, Y. Challenges and Prospects of Lithium Sulfur Batteries. *Carbon*, (2012). **DOI:** 10.1021/ar300179v

14. Bruce, P. G., Freunberger, S. A., Hardwick, L. J. & Tarascon, J. Li – O 2 and Li – S batteries with high energy storage. *Nature materials* **11**, 19–30 (2012).

15. Mikhaylik et. al., High Energy Rechargeable Li-S Cells for EV Application. Status, Challenges and Solutions. Available from http://sionpower.com/pdf/articles/SionPowerECS.pdf

16. Bruce, P. et al., Li – O 2 and Li – S batteries with high energy storage. *Nature Materials* **11**, 19–30 (2012).

17. Song, M.-K., Cairns, E. J. & Zhang, Y. Lithium/sulfur batteries with high specific energy: old challenges and new opportunities. *Nanoscale* **5**, 2186–204 (2013).

18. Zhang, Y., Zhao, Y., Sun, K. E. & Chen, P. Development in Lithium / Sulfur Secondary Batteries. *The Open Materials Science Journal*, 215–221 (2011).

19. Yang, Y. *et al.,* New nanostructured Li2S/silicon rechargeable battery with high specific energy. *Nano letters* **10**, 1486–91 (2010).

20. Xin, S., Guo, Y.-G. & Wan, L.-J. Nanocarbon networks for advanced rechargeable lithium batteries. *Accounts of chemical research* **45**, 1759–69 (2012).

21. Evers, S. & Nazar, L. F. New Approaches for High Energy Density Lithium-Sulfur Battery Cathodes. *Accounts of chemical research* , (2012). **DOI:** 10.1021/ar3001348

22. Scrosati, B. & Garche, J. Lithium batteries : Status , prospects and future. *Journal of Power Sources* **195**, 2419–2430 (2010).

23. Bruce, P. G., Scrosati, B. & Tarascon, J.-M. Nanomaterials for rechargeable lithium batteries. *Angewandte Chemie* **47**, 2930–46 (2008).

24. Guo, Y.-G., Hu, J.-S. & Wan, L.-J. Nanostructured Materials for Electrochemical Energy Conversion and Storage Devices. *Advanced Materials* **20**, 2878–2887 (2008).

25. Jiang, C., Hosono, E. & Zhou, H. Nanomaterials for lithium ion batteries. *Nano Today* **1**, 28–33 (2006).

26. Aricò, A. S., Bruce, P., Scrosati, B., Tarascon, J.-M. & Van Schalkwijk, W. Nanostructured materials for advanced energy conversion and storage devices. *Nature materials* **4**, 366–77 (2005).

27. Cheng, F., Tao, Z., Liang, J. & Chen, J. Template-Directed Materials for Rechargeable Lithium-Ion. *Chemistry of Materials* **20**, 667–681 (2008).

28. Liu, H., Wu, Y. P., Rahm, E., Holze, R. & Wu, H. Q. Cathode materials for lithium ion batteries prepared by sol-gel methods. *Journal of Solid State Electrochemistry* **8**, 450–466 (2004).

29. Fu, L. J. *et al.* Electrode materials for lithium secondary batteries prepared by sol – gel methods. *Progress in Materials Science* **50**, 881–928 (2005).

30. Hu, Y., Doeff, M. M., Kostecki, R. & Fiñones, R. Electrochemical Performance of Sol-Gel Synthesized LiFePO[sub 4] in Lithium Batteries. *Journal of The Electrochemical Society* **151**, A1279 (2004).

31. Choi, D. & Kumta, P. N. Surfactant based sol–gel approach to nanostructured LiFePO4 for high rate Li-ion batteries. *Journal of Power Sources* **163** (2), 1064–1069 (2007).

32. Rho, Y. H. *et al.* Preparation of Li 4 Ti 5 O 12 and LiCoO 2 thin film electrodes from precursors obtained by sol – gel method. *Solid State Ionics* 151–157 (2002).

33. Wang, D. *et al.* Ternary self-assembly of ordered metal oxide-graphene nanocomposites for electrochemical energy storage. *ACS nano* **4**, 1587–95 (2010).

34. Cassagneau, B. T. & Fendler, J. H. High Density Rechargeable Lithium-Ion Batteries Self-Assembled from Graphite Oxide Nanoplatelets and Polyelectrolytes . *Advanced Materials*, **10** (11),877–881 (1998).

35. Lee, S. W., Gallant, B. M., Byon, H. R., Hammond, P. T. & Shao-Horn, Y. Nanostructured carbon-based electrodes: bridging the gap between thin-film lithium-ion batteries and electrochemical capacitors. *Energy & Environmental Science* **4**, 1972–1985 (2011).

36. Liu, C., Li, F., Ma, L.-P. & Cheng, H.-M. Advanced materials for energy storage. *Advanced materials* **22**, E28–62 (2010).

37. Brownson, D. a. C., Kampouris, D. K. & Banks, C. E. An overview of graphene in energy production and storage applications. *Journal of Power Sources* **196**, 4873–4885 (2011).

38. Pumera, M. Electrochemistry of graphene: new horizons for sensing and energy storage. *Chemical record* **9**, 211–23 (2009).

39. Novoselov, K. S. *et al.* Electric field effect in atomically thin carbon films. *Science* **306**, 666–9 (2004).

40. Zhu, Y. *et al.* Graphene and graphene oxide: synthesis, properties, and applications. *Advanced materials* **22**, 3906–24 (2010).

41. Choi, W., Lahiri, I., Seelaboyina, R. & Kang, Y. S. Synthesis of Graphene and Its Applications: A Review. *Critical Reviews in Solid State and Materials Sciences* **35**, 52–71 (2010).

42. Geim, a K. Graphene: status and prospects. *Science* **324**, 1530–1534 (2009).

43. Sun, Y., Wu, Q. & Shi, G. Graphene based new energy materials. *Energy & Environmental Science* **4**, 1113–1132 (2011).

44. Geim, a K. & Novoselov, K. S. The rise of graphene. *Nature materials* **6**, 183–191 (2007).

45. Lian, P. *et al.* Large reversible capacity of high quality graphene sheets as an anode material for lithium-ion batteries. *Electrochimica Acta* **55**, 3909–3914 (2010).

46. Wang, G., Shen, X., Yao, J. & Park, J. Graphene nanosheets for enhanced lithium storage in lithium ion batteries. *Carbon* **47**, 2049–2053 (2009).

47. Yoo, E. *et al.* Large reversible Li storage of graphene nanosheet families for use in rechargeable lithium ion batteries. *Nano letters* **8**, 2277–2282 (2008).

48. Zhao, X., Hayner, C. M., Kung, M. C. & Kung, H. H. Flexible holey graphene paper electrodes with enhanced rate capability for energy storage applications. *ACS nano* **5**, 8739–8749 (2011).

49. Liang, M. & Zhi, L. Graphene-based electrode materials for rechargeable lithium batteries. *Journal of Materials Chemistry* **19**, 5871-5878 (2009).

50. Yang, S., Feng, X., Ivanovici, S. & Müllen, K. Fabrication of graphene-encapsulated oxide nanoparticles: towards high-performance anode materials for lithium storage. *Angewandte Chemie* **49**, 8408–8411 (2010).

51. Zhou, X., Yin, Y.-X., Wan, L.-J. & Guo, Y.-G. Facile synthesis of silicon nanoparticles inserted into graphene sheets as improved anode materials for lithium-ion batteries. *Chemical communications* **48**, 2198–2200 (2012).

52. Lee, J. K., Smith, K. B., Hayner, C. M. & Kung, H. H. Silicon nanoparticles-graphene paper composites for Li ion battery anodes. *Chemical communications* **46**, 2025–2027 (2010).

53. Du, Z. *et al.* In situ synthesis of SnO2/graphene nanocomposite and their application as anode material for lithium ion battery. *Materials Letters* **64**, 2076–2079 (2010).

54. Wang, G. *et al.* Sn/graphene nanocomposite with 3D architecture for enhanced reversible lithium storage in lithium ion batteries. *Journal of Materials Chemistry* **19**, 8378-8384 (2009).

55. Wang, X., Zhou, X., Yao, K., Zhang, J. & Liu, Z. A SnO2/graphene composite as a high stability electrode for lithium ion batteries. *Carbon* **49**, 133–139 (2011).

56. Shi, Y., Wen, L., Li, F. & Cheng, H.-M. Nanosized Li4Ti5O12/graphene hybrid materials with low polarization for high rate lithium ion batteries. *Journal of Power Sources* **196**, 8610–8617 (2011).

57. Zhu, N. *et al.* Graphene as a conductive additive to enhance the high-rate capabilities of electrospun Li4Ti5O12 for lithium-ion batteries. *Electrochimica Acta* **55**, 5813–5818 (2010).

58. Zhang, B. *et al.* Percolation threshold of graphene nanosheets as conductive additive in Li 4 Ti 5 O 12 anodes of Li-ion batteries. *Nanoscale* **5**, 2100–2106 (2013).

59. Su, F.-Y. *et al.* Could graphene construct an effective conducting network in a high-power lithium ion battery, *Nano Energy* **1**, 429–439 (2012).

60. Su, F.-Y. *et al.* Flexible and planar graphene conductive additives for lithium-ion batteries. *Journal of Materials Chemistry* **20**, 9644-9650 (2010).

61. Drzal, L. T. *Exfoliated Graphite Nanoplatelets: A Carbon Nanotube Alternative*. Available from http://www.xgsciences.com/docs/xGnP_tech_overview_web.pdf.

62. Fukushima, H. Graphite Nanoreinforcements in Polymer Nanocomposites. Chemical Engineering & Materials Science Department, Michigan State University, East Lansing (2003).

2 METAL DOPED GRAPHENE NANOPLATELETS AS ANODE MATERIAL

SIGNIFICANCE

Nanographitic materials such as nanotubes and graphene nanosheets have gained considerable attention as potential energy storage materials, because of their desirable properties such as high surface area, good conductivity, and significant mechanical and electrochemical stability. Particularly, anodes made of graphene sheets and their composites have shown a significant increase in specific capacity (nearly 100%) by careful control of interlayer spacing [1].

Another category of anode material, which is of prime significance, is the metal nanoparticles, which have excellent storage capacity but are restricted in their use due to poor mechanical integrity and high cost. The focus of this research in developing anode materials for lithium ion batteries is to integrate the two different materials, and develop a metal-nanographite composite, thereby achieving the benefits from both constituents. Such electrodes capitalize on the benefit of high lithium storage capability from metals and their oxides and combine it with excellent conductivity and mechanical robustness of the graphitic systems[2–6].

There are numerous reports on combining SnO_2, silicon and other metal oxides with graphene to form a high capacity nanostructures with a highly conductive support. These metal-based electrode materials interact with lithium via alloying mechanism and undergo

huge volume change during cycling. Making a composite structure with high aspect ratio graphene helps to sustain the strain due to lithium alloying/dealloying process of the metal component [3,7–9].

APPROACH

Our approach is to develop a 3 dimensional layered graphene nanoplatelet structure where the addition of metal nanoparticles allows for the construction of a tailorable nano-architecture. The schematic illustration shown in Figure 2-1 gives an overview of the concept behind the technique

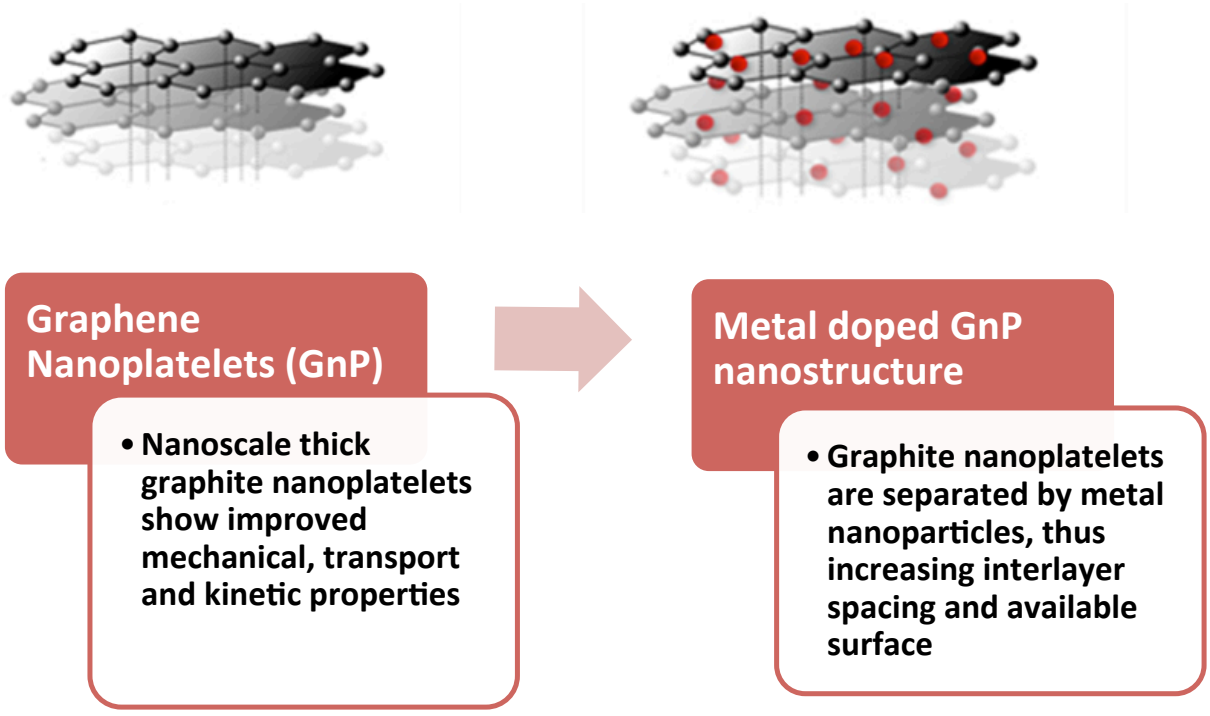

Figure 2-1: Schematic showing the potential of metal-doped carbon as anodes for lithium ion batteries

Based on the concepts discussed in the introduction, having a nanostructured electrode will have the benefits of fast Li ion diffusion coupled with better mechanical robustness. The

addition of these nanoscale metal particles results in a structured nanographite assembly that can potentially have the following advantages:

1. Metal nanoparticles will act as spacers, increasing interlayer spacing and thus allowing easy diffusion of lithium ions in and out of the electrode thereby enhancing the reaction rate.
2. Metal nanoparticles will act as conducting additive, thereby reducing the electric resistance of the electrode.
3. Metal nanoparticle dopants, such as nickel, tin, antimony and silicon, can contribute to the cell capacity because of their inherent interaction with lithium, thereby augmenting the specific capacity of the anode
4. Compared to monolithic metal anodes, improved cycle should be achieved by restricting the extent of volume expansion in the nanographitic matrix.

EXPERIMENTAL SECTION

SYNTHESIS

Graphene Nanoplatelets

Graphene Nanoplatelets were synthesized by a well-established microwave exfoliation and sonication procedure from acid intercalated graphite[10]. Around 1 g of acid intercalated graphite material from Asbury (A3772) placed in a 600 ml beaker was heat-treated in a kitchen microwave at 1000 W for 1 min. During the microwave heating, the acid vaporizes and tries to escape the galleries of graphite, thus resulting in rapid volumetric expansion, exfoliation and

formation of GnP worms. This procedure was repeated with intermittent stirring 3 times, to ensure complete exfoliation and acid removal. The obtained GnP worms were then dispersed in isopropanol and ultrasonicated at 100 W for 2 hours to separate the GnP worms into individual nanoplatelets and to reduce their overall lateral dimensions. . The solution was air dried, followed by vacuum drying at 100 C to obtain GnP platelets of ~15 µm diameter and with a surface area of 25-30 m^2/g.

Nickel doped GnP materials

Three different sizes of nickel nanoparticles supported on GnP, were synthesized by different procedures. The summary of the synthesis methodology, conditions and concentration details are summarized below in Table 2-1. The nomenclature used to denote different materials is GnP_Ni-x, where x is indicative of the size of nickel nanoparticles.

Table 2-1: Summary Table for different nickel doped GnP materials synthesized

Material (Nomenclature)	**Methodology**	**Nickel nanoparticles size**	**Starting Concentration of Nickel in precursors**	**Actual concentration of Ni nanoparticles (TGA Analysis)**
GnP_Ni-5	Polyol Method	5 nm	10%	2.5%
GnP_Ni-30c	Solventless	30 nm clusters	10%	10 %
GnP_Ni-60	Solventless	60-80	10%	10 %

Microwave Assisted Polyol Method

The GnP nanoplatelets were acid treated in H_2SO_4 + HNO_3 (1:3) mixture to oxidize the nanoplatelet edges which can aid in interaction with glycols and metal salts. 1 g oxidized GnP was dispersed in 80 ml triethylene glycol with the aid of ultra sonication and mechanical stirring. A nickel salt, nickel nitrate, was dissolved separately in 40 ml triethylene glycol at appropriate concentration (10%). The two solutions were then stir mixed overnight to ensure good interaction. The mixed solution was heated to 270 °C in a programmable Ethos Microwave (5 min ramp). The resulting solution was centrifuged three times with acetone to remove excess salt and triethylene glycol. The final solution was dried in air and then heated at 100 °C to evaporate acetone and to produce GnP doped with 5 nm nickel nanoparticles (denoted as GnP_Ni-5).

Solventless Method

The synthesis of two other GnP-Ni materials (GnP_Ni-30c, GnP_Ni-60) was done by a simple procedure involving reduction of nickel salts on the graphene surface by heat treatment in an inert environment[11]. GnP and the appropriate concentration of nickel acetate were weighed and put in a ball mill chamber of 65 ml size. The mixture was milled with the aid of 5 g PP balls for 20 minutes using a SPEX 8000 M Mixer Mill. The obtained mixture was heated for 3 hours in a tube furnace under Argon flow at temperatures of 350 °C and 600 °C to obtain nickel nanoparticles supported on GnP, of 30 nm clusters and 60 nm size (GnP_Ni-30c and GnP_Ni-60)

respectively. GnP_Ni-30c materials has small nanoparticles combined together to form 30 nm clusters, hence the notation c for clusters.

MORPHOLOGY OBSERVATION

The characterization of GnP_Ni-5 material was done using a JEOL 2200 FS Transmission Electron Microscope (TEM), at an accelerating voltage of 200 kV. The sample preparation involved creating a dilute suspension of GnP_Ni powder in acetone by tip sonication for 2 minutes, followed by drop casting on a Cu TEM grid.

The morphology of other Ni doped GnP materials prepared from the solventless approach and the electrode morphologies were observed by JEOL JSM 7500-F Field Emission SEM at an accelerating voltage of 15 kV. For cross-section observation of electrodes, Cu foil was etched from the electrodes with a mild acid treatment for 2 days.

The morphology of GnP_Si paper was observed by Focused Ion Beam (FIB) Milling technique using the Carl Zeiss Auriga® CrossBeam scanning electron microscope. This technique helps in eliminating the artifacts in the morphology due to epoxy embedding and polishing.

The details of the procedure of the two sample preparation techniques for viewing the cross-section are described below:

Epoxy Embedding and Polishing

A small piece of electrode was cut and mounted to a clip with the electrode edge facing upwards. The clip was placed in a ring holder, and a slow cure room temperature epoxy was poured around the sample. After curing, polishing of the epoxy embedded sample was done by

the Abramis polisher, in multiple steps starting with 320 grit sandpaper, followed by 600 grit, 1200 grit, and finally 4000 grit sand paper. Material removal rates for the graphene are very slow compared to the epoxy. The polished sample was then exposed to oxygen plasma for 30 minutes to etch residual epoxy on the surface, thus enhancing the contrast between the sample and epoxy matrix. The samples were lightly gold coated prior to SEM observation to eliminate charging.

Focused Ion Beam (FIB) Milling/Sectioning

The cross-section morphology of LTO electrodes were studied using (FIB)-SEM (Carl Zeiss Auriga® CrossBeam) instrument. The cross-section of the electrode is exposed for observation by a systematic process of milling from the surface through the thickness of the electrode, using a focused gallium ion beam. Figure 2-2 shows the layout of the sectioning setup in the FIB-SEM column. As shown, the electron and ion beam are inclined at an angle of 36° in the vacuum column. Thus, the sample is inclined to 54° to ensure that the ion beam is hitting the sample at 90 degrees thus exposing the true nature of electrode cross-section. For SEM observation, the image is tilt corrected (by the software) to account for the 36° angle between the electron beam and the sample. The milling process is a multiple step procedure, to make sure the section is exposed well and the sputtered material doesn't redeposit back on the sample surface. First, a large beam of 30 kV, 20 nA is used to cut out a trapezoid. Two further rectangular fine sections with smaller beams (30kV, 4nA and 30 kV, 2nA) are done on the small parallel side of the trapezoid, removing any redeposited material, and exposing the cross-sectional electrode surface.

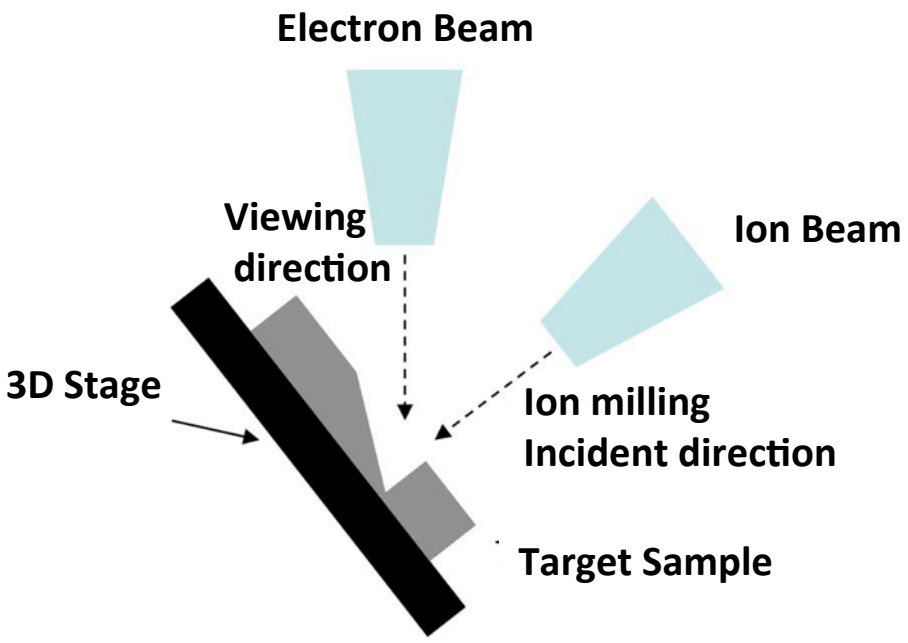

Figure 2-2: Schematic of FIB-SEM setup[12]

PHYSICAL CHARACTERIZATION

The concentration of nickel nanoparticles was evaluated by using a TA Instruments thermogravimetric analysis (TGA) instrument by heating up to 900C in air at a ramp rate of 10 C/min.

The X-ray diffraction (XRD) analysis of different materials was obtained on a Philips Rigaku Rotaflex 200B X-ray powder diffractometer using Cu-Kα radiation to determine the composition of metal nanoparticles in the 2θ range of 10° to 80°.

The Raman spectra of the undoped and Ni doped GnP materials was obtained using the Lab RAM ARAMIS instrument from Horiba. The powders were dispersed in acetone with tip sonication and drop cast on a glass slide to make a thick film. All the materials were analyzed with the 532 nm 50 mW DPSS laser in the range of 0 - 4000 cm^{-1}.

ELECTROCHEMICAL CHARACTERIZATION

Electrodes were prepared from the undoped GnP, GnP_Ni-5, GnP_Ni-30c and GnP_Ni-60 materials by spreading its slurry with N-Methyl-2-pyrrolidone and PVDF as the binder (5%), on the copper substrate using a microfilm applicator. These anodes were then characterized in a three electrode Swagelok cell setup (Figure 2-3) with lithium foil as counter and reference electrode. The separator used was a glass microfiber filter. 1M $LiPF_6$ in equivolume of ethylene carbonate-dimethyl carbonate (EC-DMC) solution was used as the electrolyte. The galvanostatic performance of these electrodes was evaluated using an Arbin BT 2000 Battery Analyzer by the protocol adopted shown below in Figure 2-16. The galvanostatic cycling was done at different rates for every 5 cycles, keeping the rate identical for both charge and discharge. Further electrochemical characterization, viz. cyclic voltammetry and electrochemical impedance spectroscopy was done with a Versa STAT MC instrument. The CV for all the electrodes was collected from 0-2.0V at a scan rate of 0.05mV/s. AC impedance spectra were obtained by applying a sine wave of 5 mV amplitude in the frequency range of 100 kHz to 0.01 Hz.

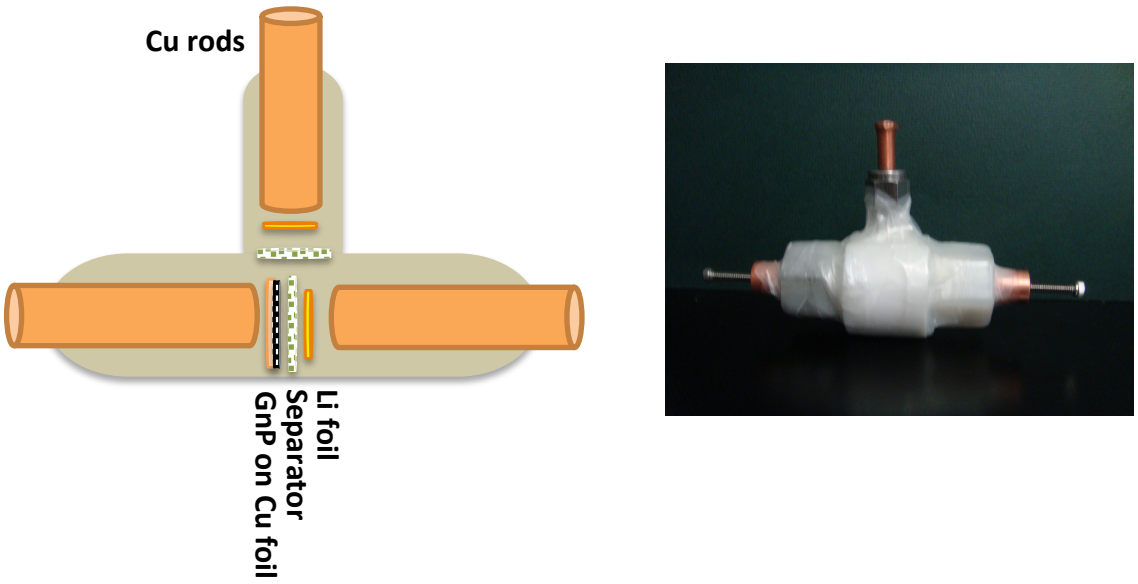

Figure 2-3: Schematic & Picture of Three electrode Swagelok type T- cell for electrochemical measurements

RESULTS & DISCUSSION

MORPHOLOGY OBSERVATION OF NICKEL DOPED GNP

The synthesis of small size metal doped GnP by the microwave assisted polyol process has the advantages of rapid, homogeneous heating coupled with enhanced reaction rates, thus facilitating synthesis of small size uniform metal doping. Figure 2-4 shows the TEM images of nickel nanoparticle doped GnP-15 platelets at different magnifications, from which we can see that the average size of these nickel nanoparticles is in the range of 3-4nm. Despite the fact that we start with a high metal concentration in the reactants, the actual concentration of nickel nanoparticles was found to be 2.5% by XPS (as confirmed by the TGA (Figure 2-6). This might result from insufficient GnP surface area available for nickel particles to attach, nucleate and grow with the excess nickel compound washed off during repeated centrifugation separation with acetone.

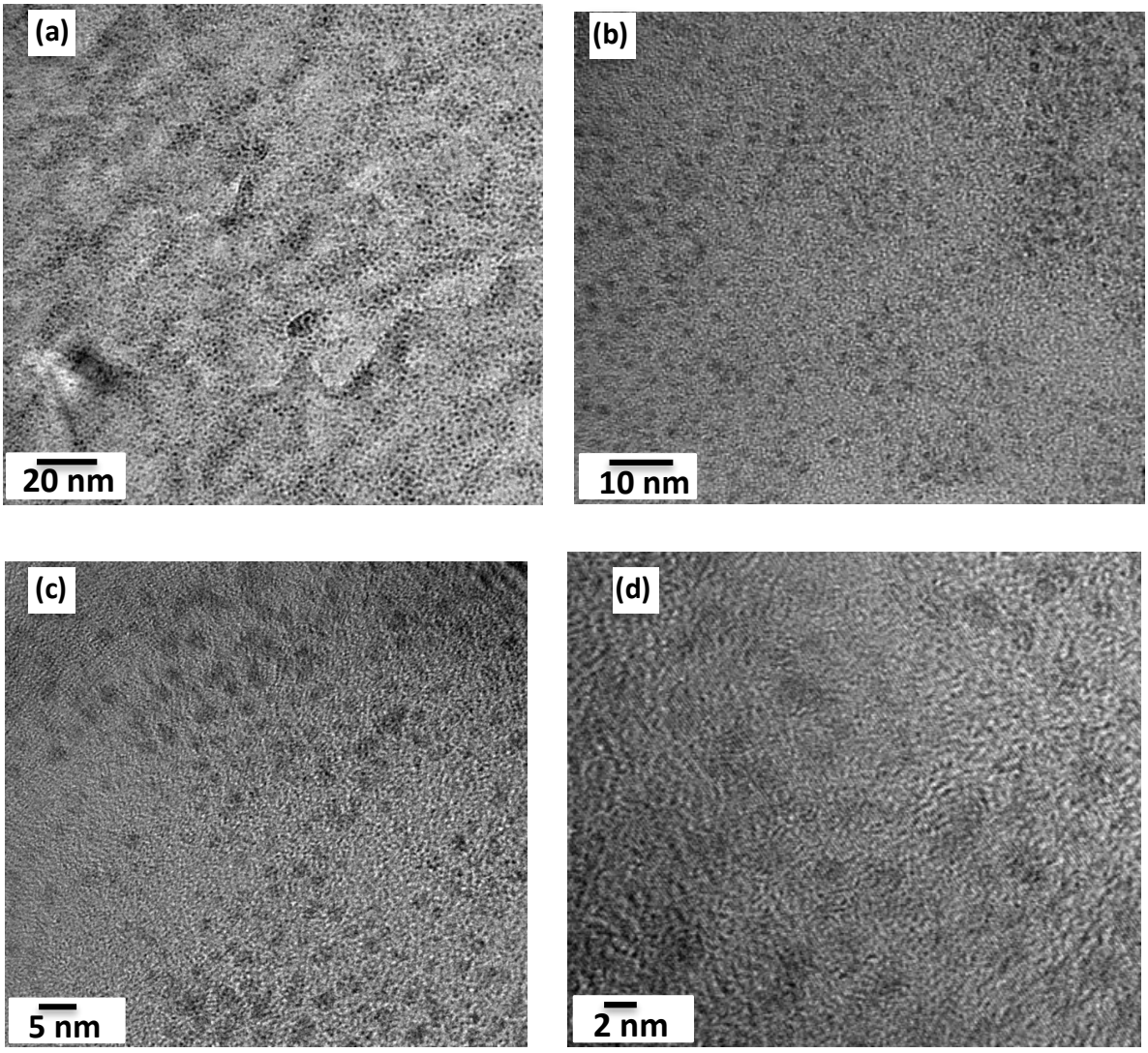

Figure 2-4: Nickel nanoparticle doped GnP synthesized by Polyol assisted microwave process

To confirm the identity of the doped nanoparticles, Scanning Transmission Electron Microscopy (STEM) combined with energy dispersive x-ray spectroscopy (EDS) was done. In the results shown in Figure 2-5, we see a copper signal throughout the line scan analysis due to signal from the grid. There is a constant signal from carbon, which is the signal reflected from GnP platelets. Nickel is clearly seen in the spectra as nanoparticles on the GnP surface. In the nickel spectrum, we can notice the bump in the line scan corresponding to the nanoparticle.

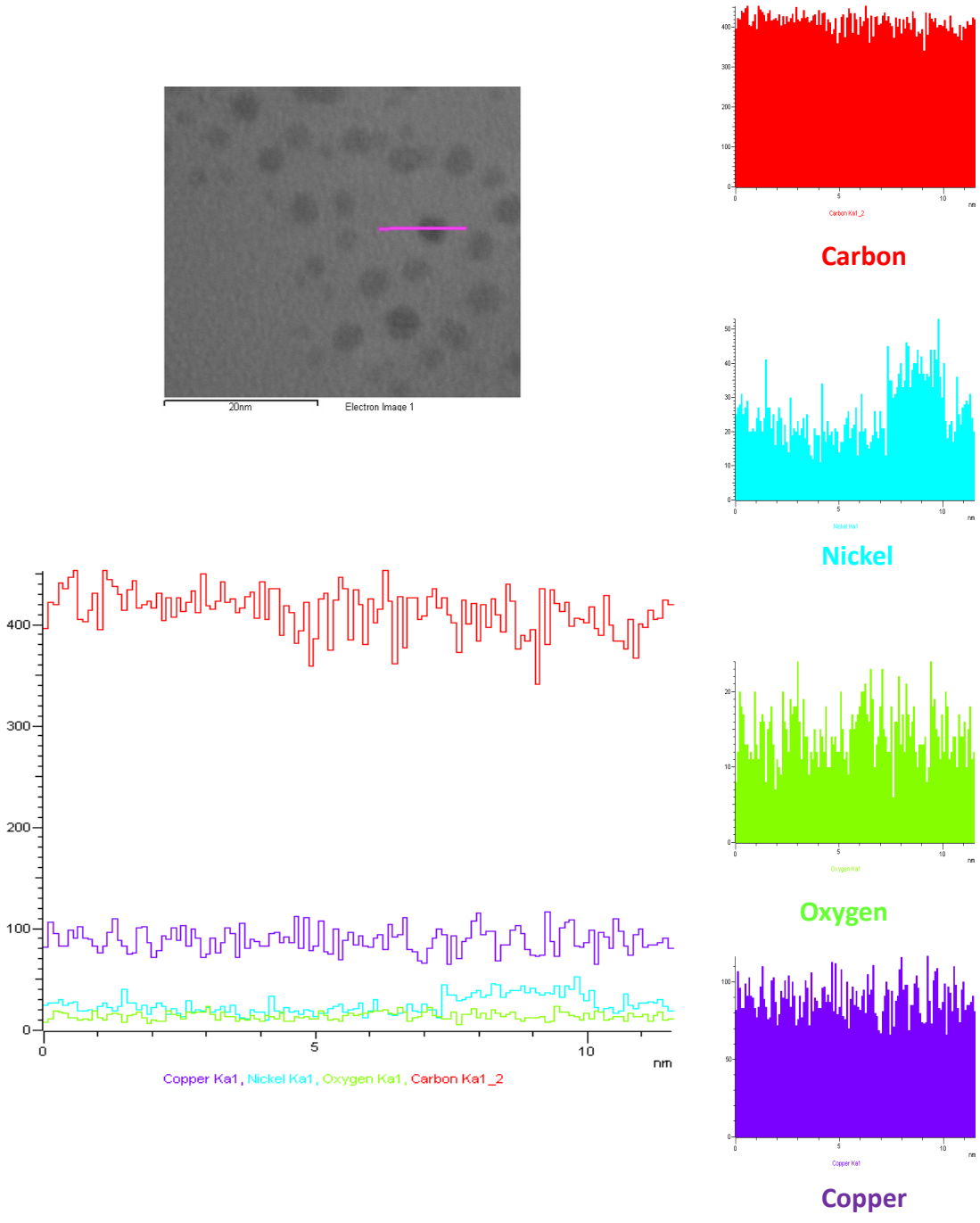

Figure 2-5: STEM-EDS Analysis of GnP_Ni-5 nanoparticles. Text within figure is not meant to be readable and is for visual reference only.

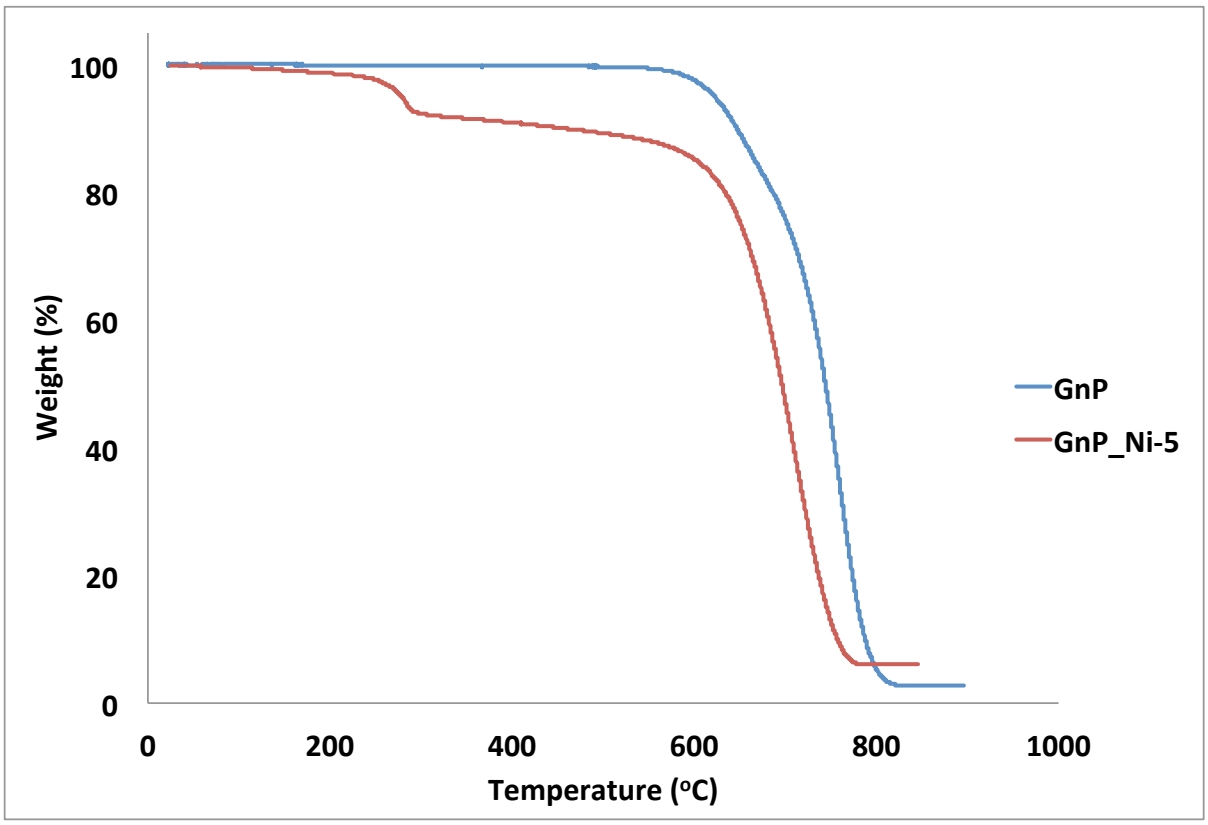

Figure 2-6: TGA Analysis of GnP_Ni-5 showing the concentration of metal nanoparticles

The other nickel nanoparticle doped GnP materials which were obtained by a solventless method using solid mixing and inert heat treatment procedure have larger size nanoparticles and were characterized using SEM. Figure 2-7 and Figure 2-9 below shows the images of nickel nanoparticle doped GnP-15 platelets with metal nanoparticles of 30 nm clusters and 60 nm respectively. From the SEM images, we can observe that the metal nanoparticles are uniform and are well distributed over the GnP platelets. The concentration of the metal doping is verified by the TGA data shown in Figure 2-8 and Figure 2-10.

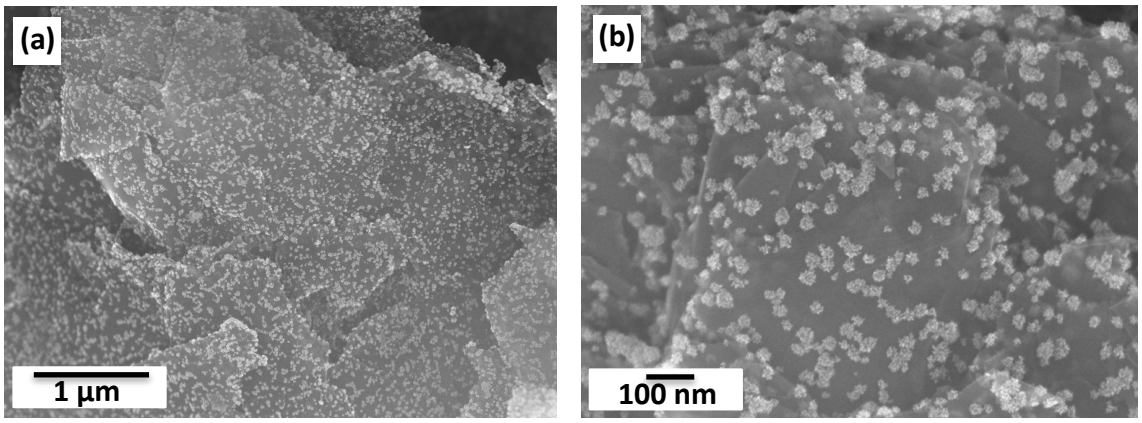

Figure 2-7: GnP nanoparticles doped with nickel NPs clusters of 30-40nm

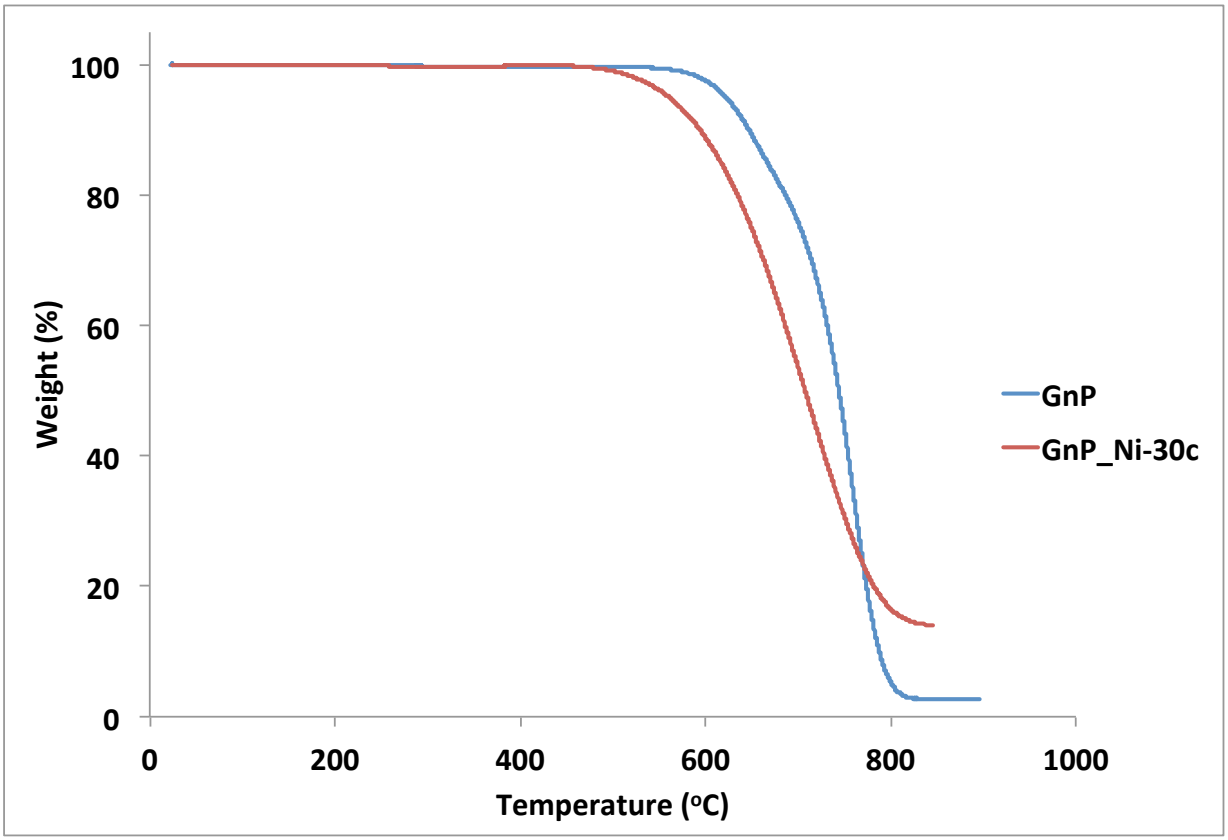

Figure 2-8: Thermogravimetric analysis of GnP_Ni-30c material

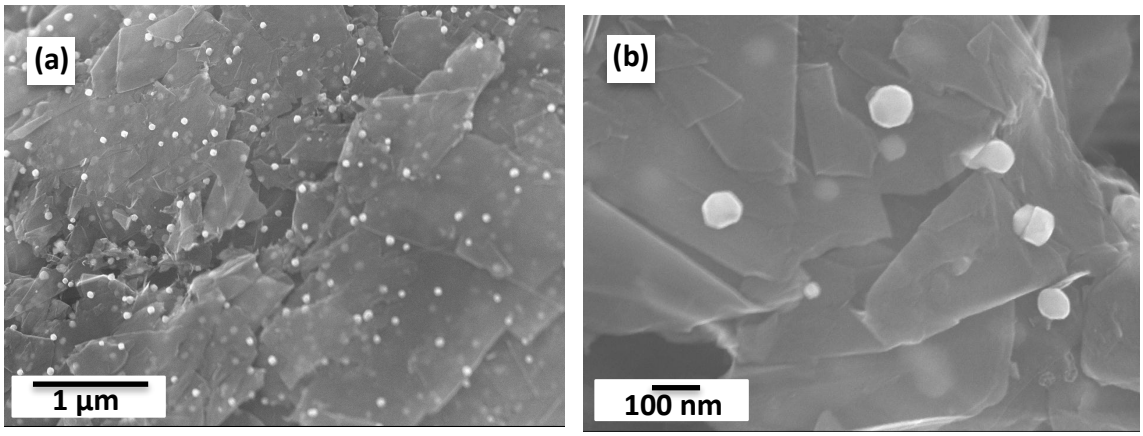

Figure 2-9: GnP nanoplatelets doped with nickel NPs of size 60-80 nm

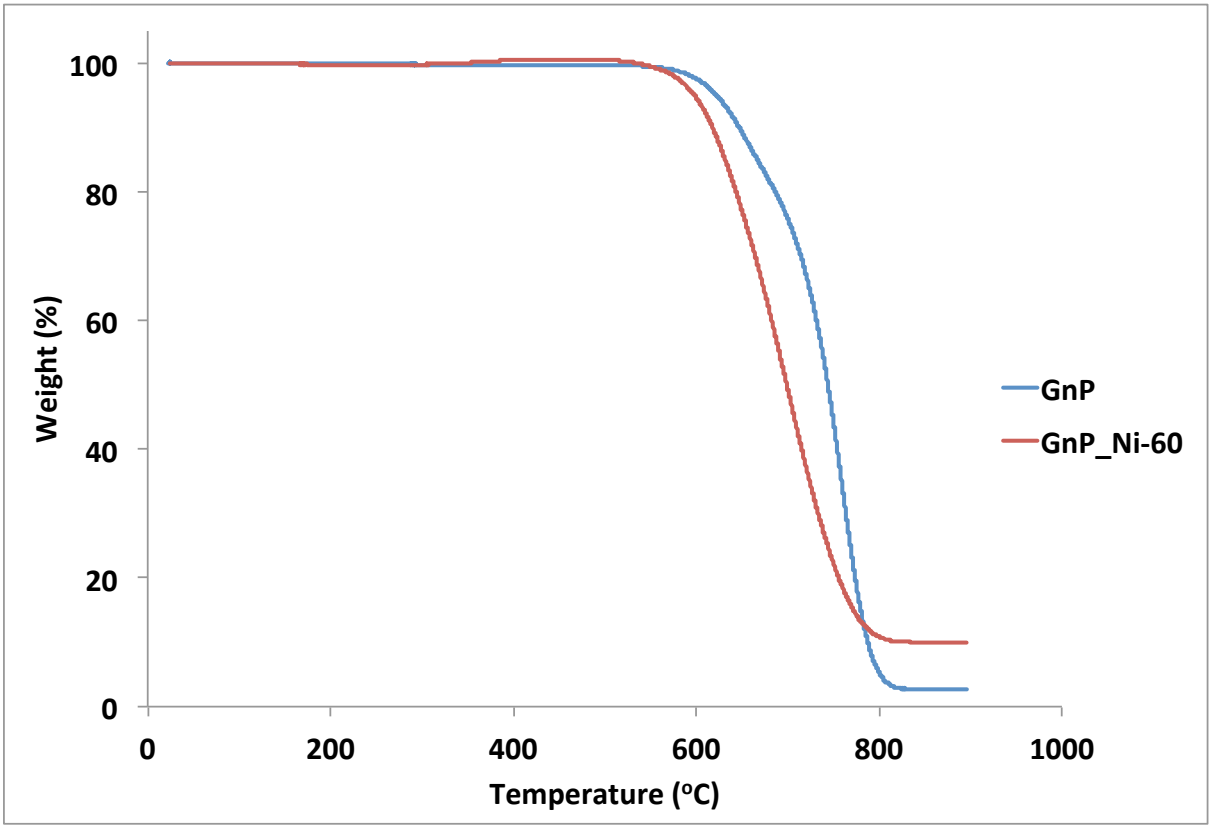

Figure 2-10: Thermogravimetric analysis of GnP_Ni-60 material

The Ni-GnP materials synthesized by the solventless approach can be produced in different concentrations. Figure 2-11 below shows the GnP_Ni-60 material at different concentrations of Nickel doping. The distribution of nanoparticles is very uniform, however, we can see that at higher concentration of 15 wt% Ni, there is some evidence of agglomeration. The concentration of metal nanoparticles in the composite was confirmed by doing TGA analysis by heating in air to 900°C (Figure 2-12). The GnP platelets decompose around 800°C, leaving behind the metal nanoparticles. From the weight percentage of the residual material, we can verify the metal concentration in different GnP_Ni material of different concentrations.

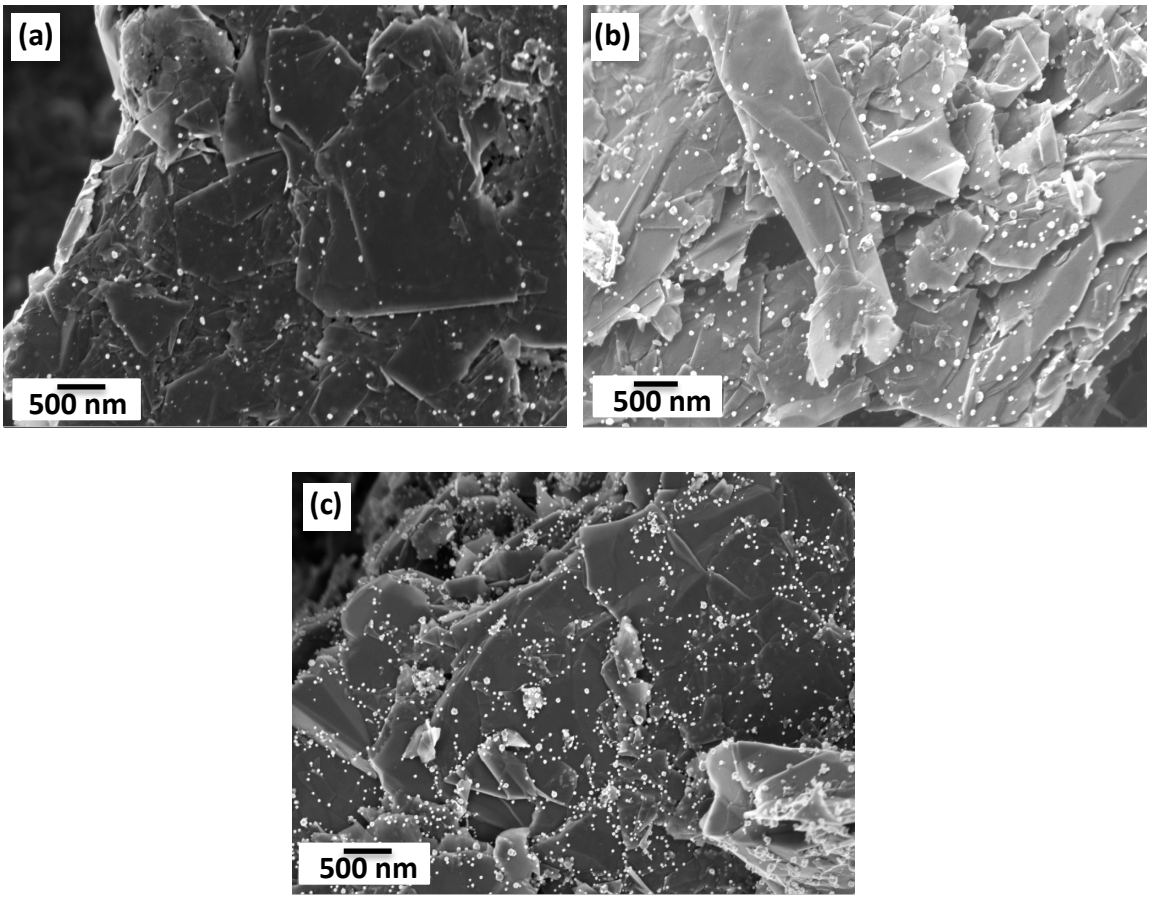

Figure 2-11: SEM Images of GnP_Ni-60 at different concentrations:(a) 5%,(b) 10%,(c)15%

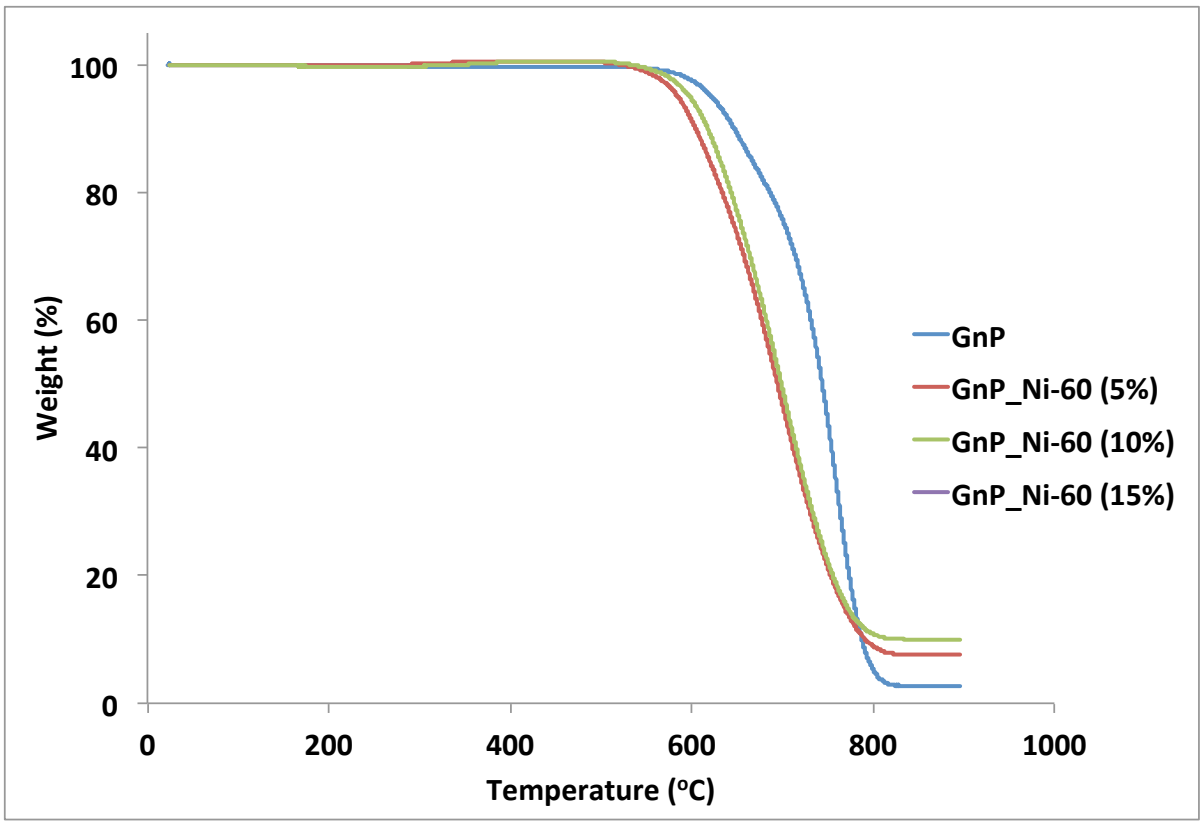

Figure 2-12: Thermogravimetric Analysis (TGA) of GnP-Ni materials showing the concentration of nickel nanoparticles in the sample

X-RAY DIFFRACTION ANALYSIS

XRD analysis was conducted to analyze and confirm the composition of metal nanoparticles. The XRD pattern for different nickel doped materials is shown below in comparison with undoped GnP. As seen from Figure 2-13, the characteristic graphitic peaks at 26° and 55° are observed in all the materials. The characteristic peaks of Ni occur at 2Θ= 44.5°, 51.86°, 76.39° [13] and for NiO at 2Θ: 37.26°, 43.29°, 62.88°, 75.42°, 79.41° [9,14]. From Figure 2-13(b), we can see that all the materials show a mixture of Ni/NiO peaks, which indicates the possibility of partial oxidation of the nanoparticles. From the analysis, the presence of metal nanoparticles is very clearly distinguishable with the peak widths corresponding to the invesrse relationship between peak width and particle size as shown by the Scherrer equation.

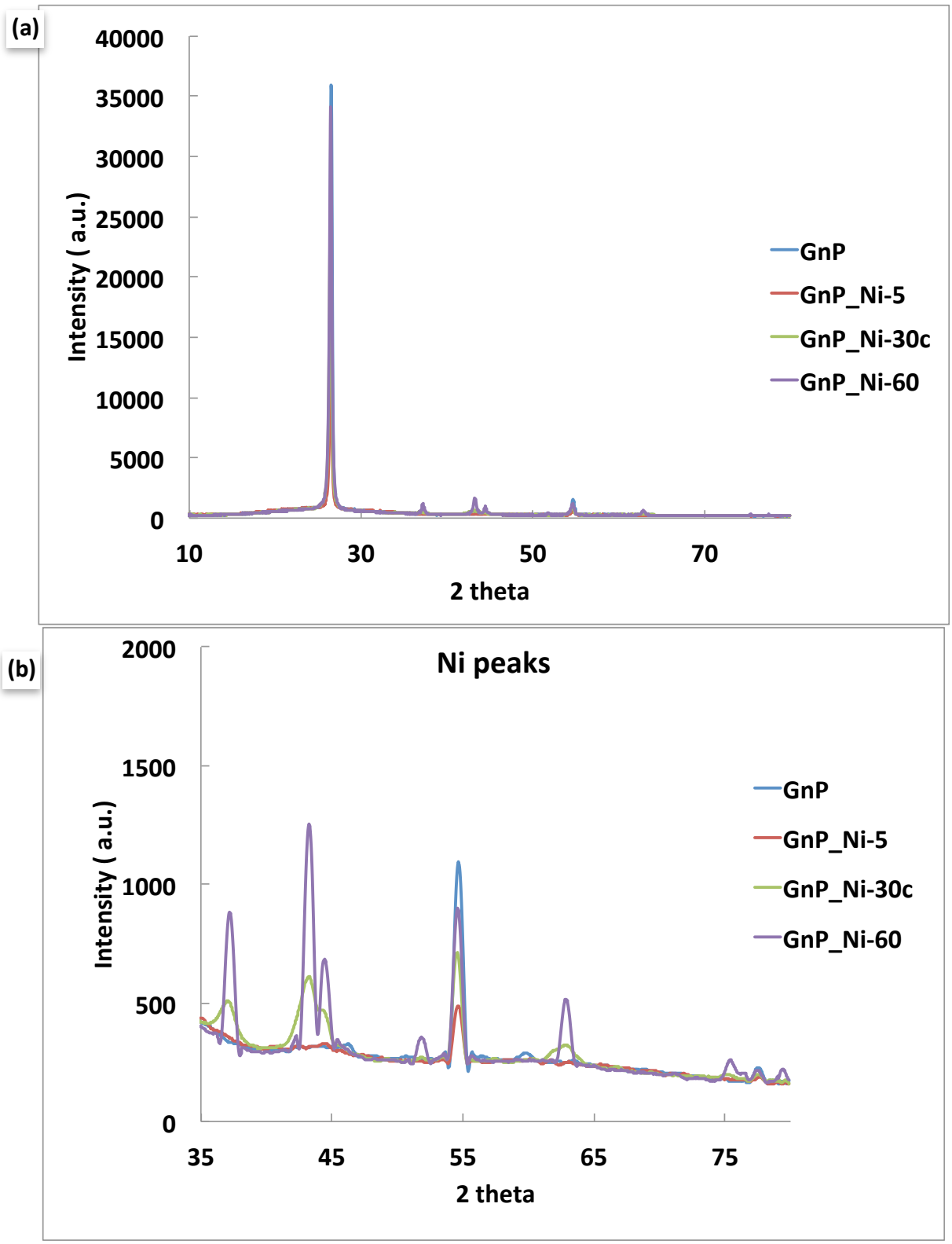

Figure 2-13: XRD pattern of nickel doped materials in comparison with undoped GnP (a) Full spectra (b) Ni peaks

RAMAN SPECTROSCOPY CHARACTERIZATION

To understand the effect of doping on GnP and evaluate the interaction of nickel nanoparticles with GnP, further characterization was done using Raman spectroscopy. The G band at 1580 cm^{-1}, known as the graphite or tangential band, is indicative of the in-plane stretching of the C-C carbon bond[15,16]. The D band, known as the defect or disorder band, around 1350 cm-1 corresponds to visible laser excitation, and can give us useful information about disorder in the graphitic materials[15,16]. The peak at 2700 cm-1 is referred to as 2D or G' peak, which is attributed to second order two phonon process[15,16]. From Figure 2-14 (b) we can observe slight downshift in the G peak for all nickel doped GnP materials which is an indication of charge transfer, the possibility being the electrons are being transferred from metal dopants to GnP platelets[17]. These two parameters can give us useful information about the graphitic character of the material viz., I_D/I_G ratio, which is an indication of the impurity in the material and disorder parameter: $I_D/(I_D+I_G)$.

Table 2-2 shows the values of these two parameters, and we can see that no significant change was observed. This implies that the nickel particles are not intercalated in between the graphene layers and there isn't any damage to the inherent structure of the graphene nanoplatelets.

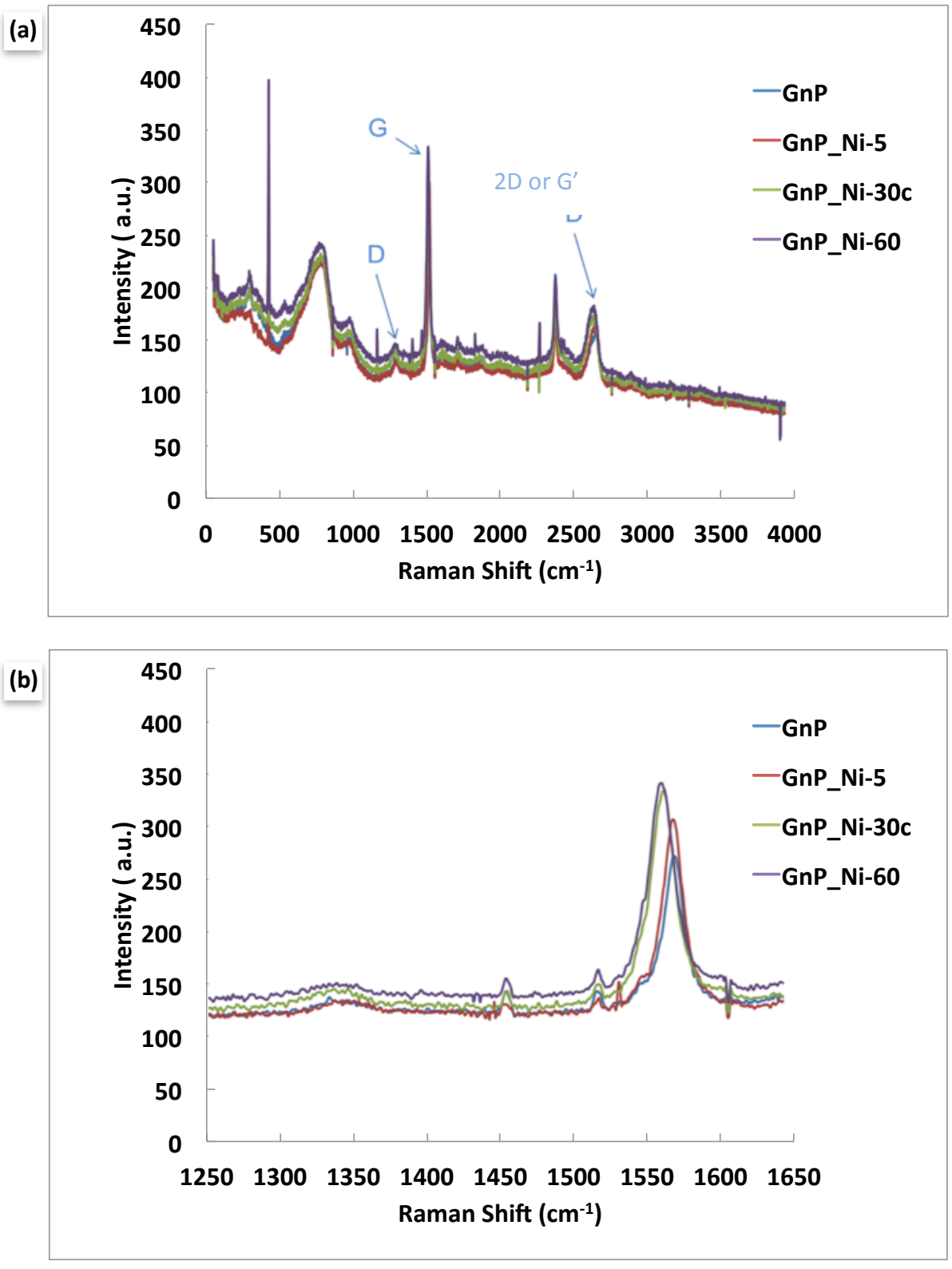

Figure 2-14: Raman Spectroscopy Analysis of different GnP_Ni materials

Table 2-2: Intensity values I_D, I_G, I_D/I_G and disorder parameter of GnP_Ni Materials

	I_D	I_G	I_D/I_G	Disorder Parameter
GnP	147	302	0.49	0.33
GnP_Ni-5	143	297	0.48	0.33
GnP_Ni-30c	168	340	0.49	0.33
GnP_Ni-60	351	351	0.46	0.31

ELECTRODE MORPHOLOGY

The morphology of the electrodes was observed both from the top view and cross-section by scanning electron microscopy (Figure 2-15). The cross-section view of the GnP electrode shows that it consists of the nanoplatelets arranged next to each other and formed into an aligned network. This can be due to the π-π interactions of the GnP basal plane. The interconnected matrix of GnP platelets imparts good conductivity and strength to the electrode in the in-plane direction.

For GnP_Ni-5, we can see that the platelets are well-connected but not perfectly aligned. This is possibly related to the interaction of metal nanoparticles with the π electrons of the basal plane. For both the nickel doped GnP materials made by solventless approach (GnP_Ni-30c and GnP_Ni-60), the electrode morphology is the same. The GnP platelets have experienced a morphology change and size reduction during the ball milling process. The electrode cross-section shows well-connected but a relatively random and disordered arrangement of the nanoplatelets. This change on electrode structure can explain the difference in electrochemical performance of these electrodes.

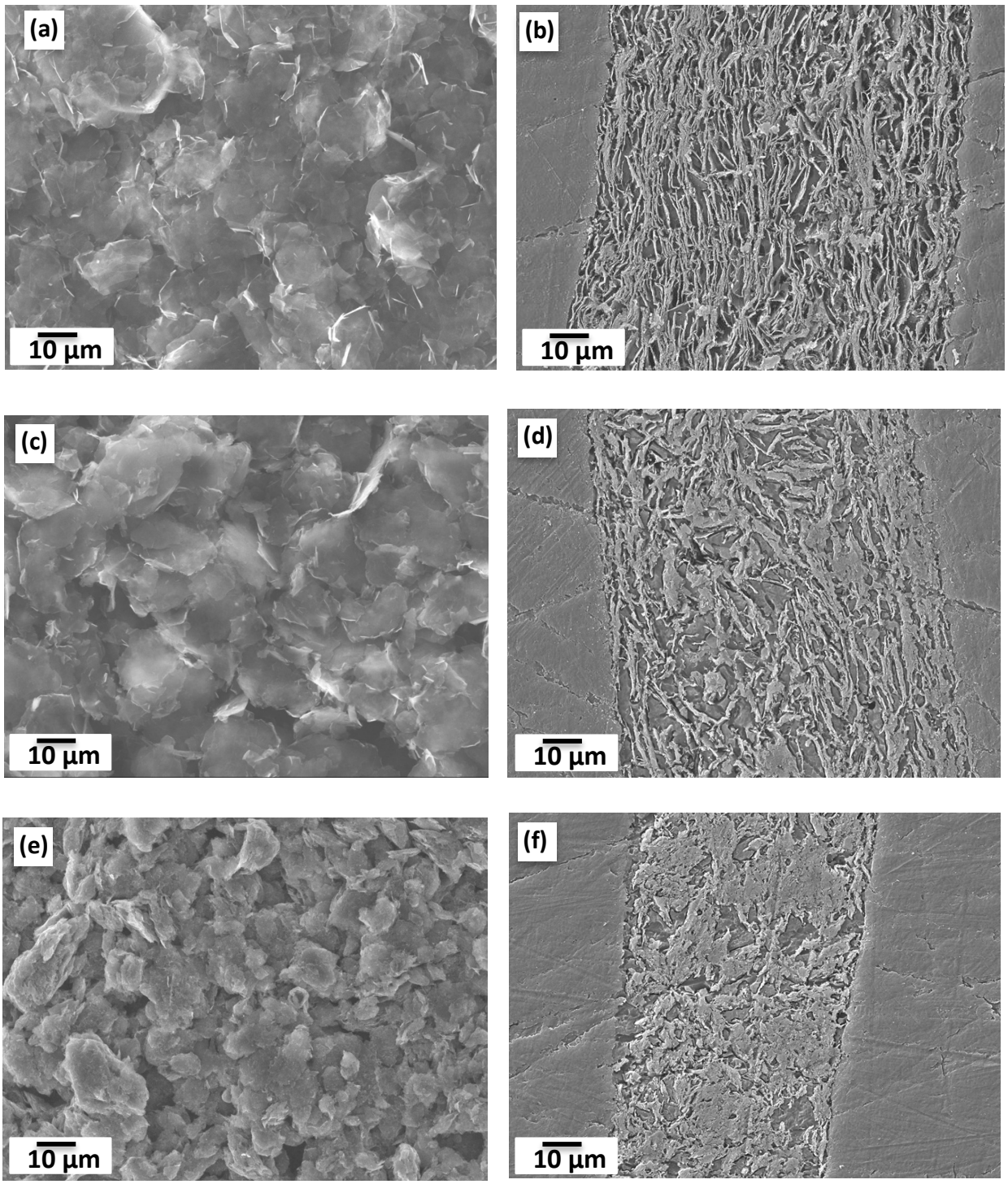

Figure 2-15: Electrode Morphology of top-view and cross-section view (respectively) of Undoped GnP [(a), (b)]; GnP_Ni-5 [(c), (d)]; GnP_Ni-30c, GnP_Ni-60 [(e), (f)]

ELECTROCHEMICAL CHARACTERIZATION

Galvanostatic Cycling

Figure 2-17 (a) shows that the capacity values of baseline GnP-15 without any metal nanoparticles at different charge rates as per the protocol. The capacity of GnP electrode is around 330 mAh/g at C/5 charge rate and a decrease in the capacity values is observed at faster charge rates, as expected in graphitic systems. Also, the highly aligned structure of the GnP electrode might hamper the diffusion of Li^+ ions through the thickness of the electrodes, particularly at faster charge rates. The storage capacity of the GnP electrode decreases significantly at faster charge rates of C & 2C, however it recovers back to high capacity when we cycle the electrode at the slower rate. This is a verification of the fact that the decrease in capacity is due to restricted kinetics, and there is no permanent degradation of the electrode. Also, we can see the discharge and charge capacity of the electrode is very close, translating to a high coulombic efficiency of > 98 %.

For the GnP doped with small size nickel nanoparticles (GnP_Ni-5), the performance is the same as the undoped GnP. This suggests that there is no role of nanoparticles towards capacity contribution, neither as active material nor as nanostructuring agent. The size of nickel nanoparticles is probably too small to make an impact on creating a nanostructured electrode that can influence performance. For the second set of Ni doped systems prepared by solventless approach mentioned above, the performance is shown in Figure 2-17 (c) and (d) for GnP_Ni-60 and GnP_Ni-30 respectively. The capacity of the electrode was maintained at the same value even when the charge rate was varied from C/5 to C/2, C and 2C. This demonstrates

the potential of the metal doped material to perform very well even at faster charge rates. This change in performance can be attributed to the connected but random arrangement of active material in the electrode. Also, the metal doping will aid in keeping the GnP platelets apart and will prevent agglomeration. These two factors combined together promote fast diffusion of lithium ions and better access to the graphitic surface at faster charge rate, thus showing improved performance.

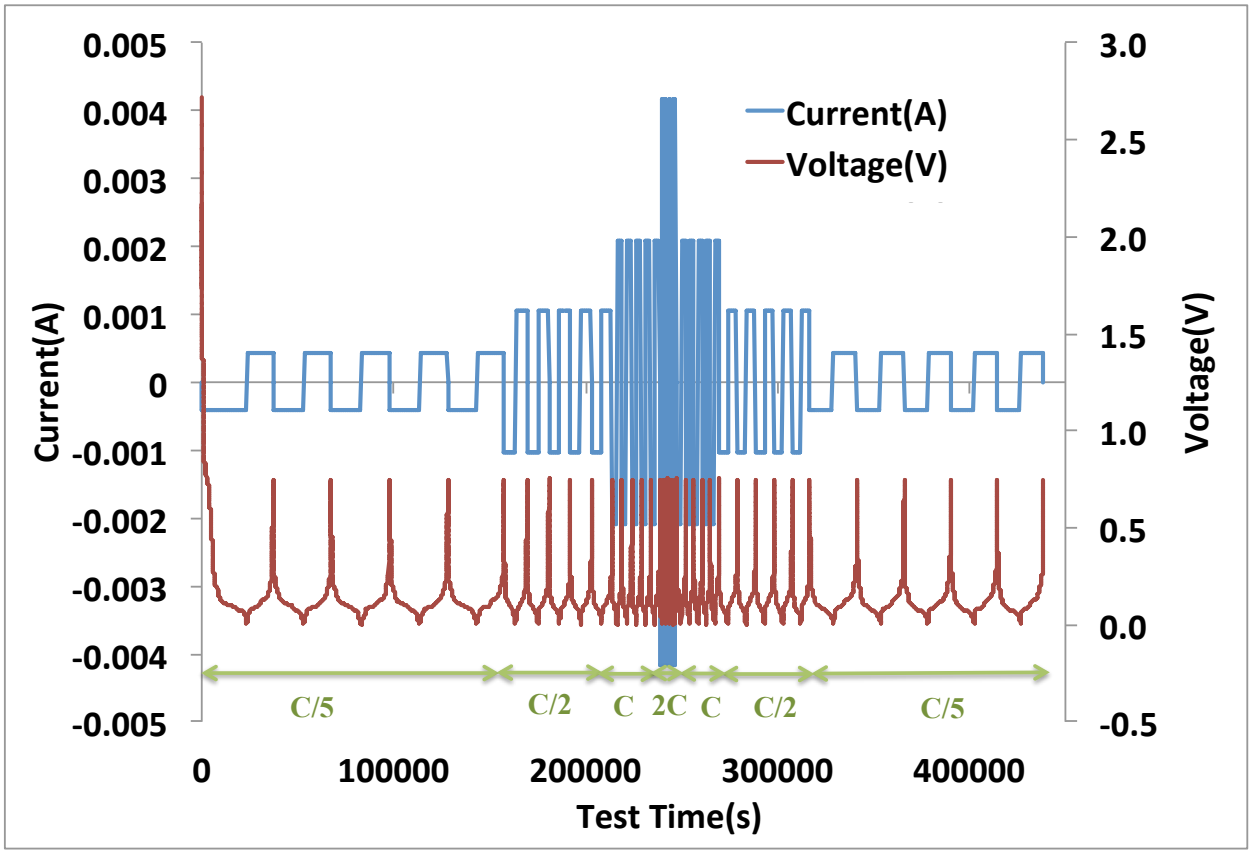

Figure 2-16: Testing Protocol for galvanostatic analysis of electrodes

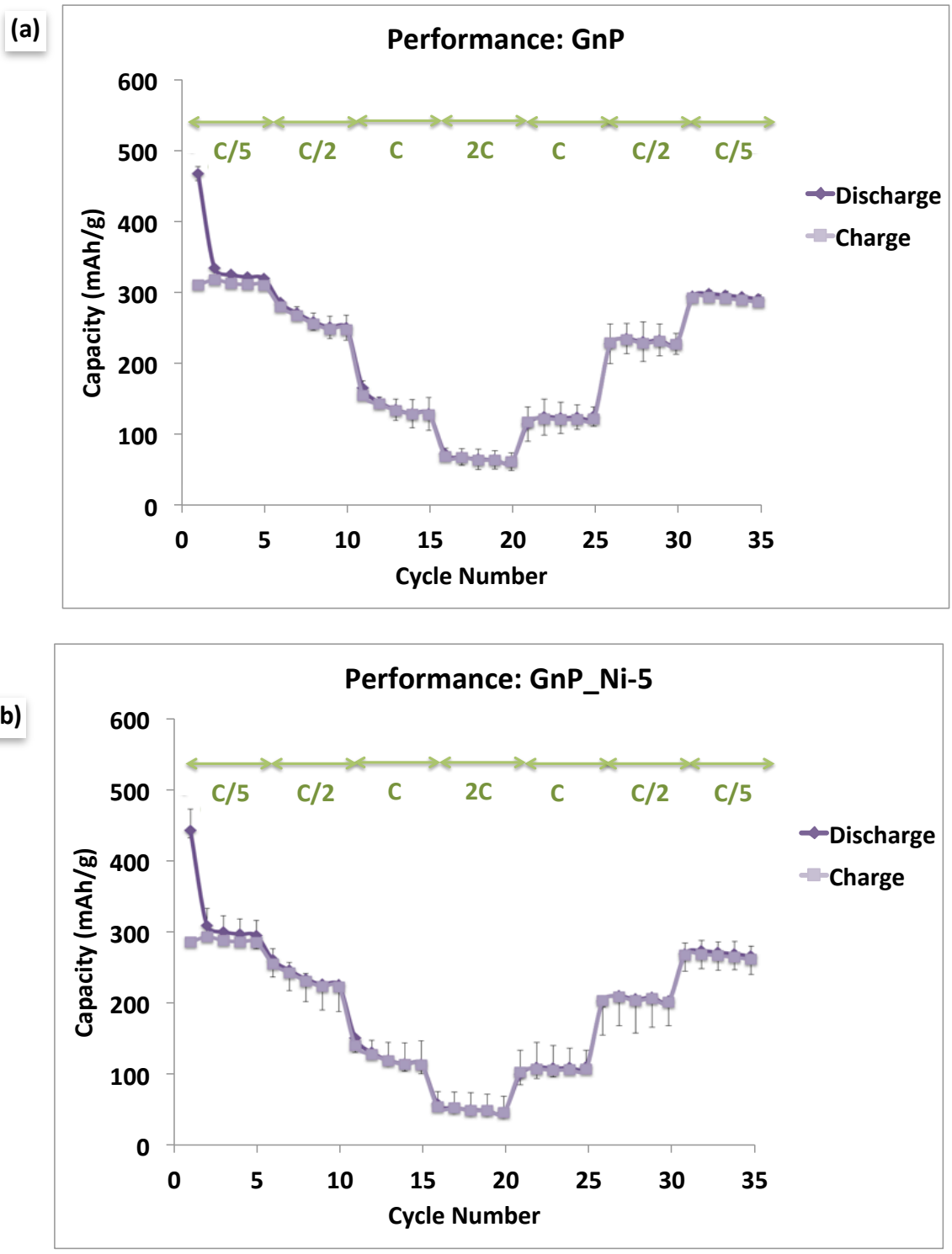

Figure 2-17: Galvanostatic performance of nickel doped materials in comparison with undoped GnP (a) Undoped GnP (b) GnP_Ni-5 (c) GnP_Ni-30c (d) GnP_Ni-60c

Figure 2-17 (cont'd)

(c)

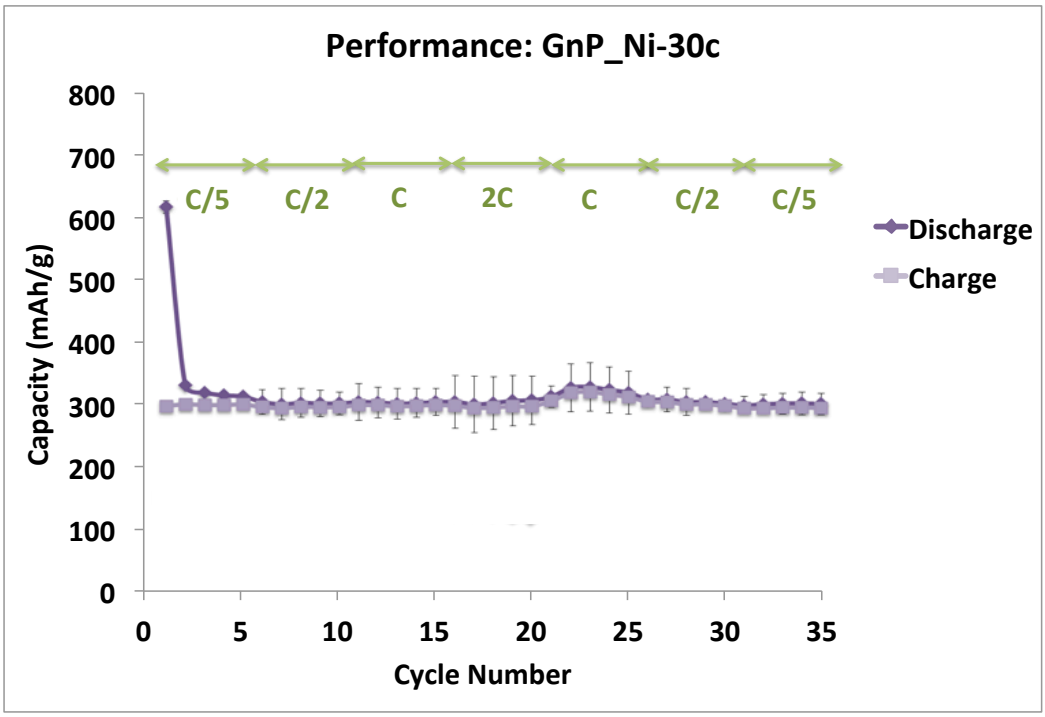

(d)

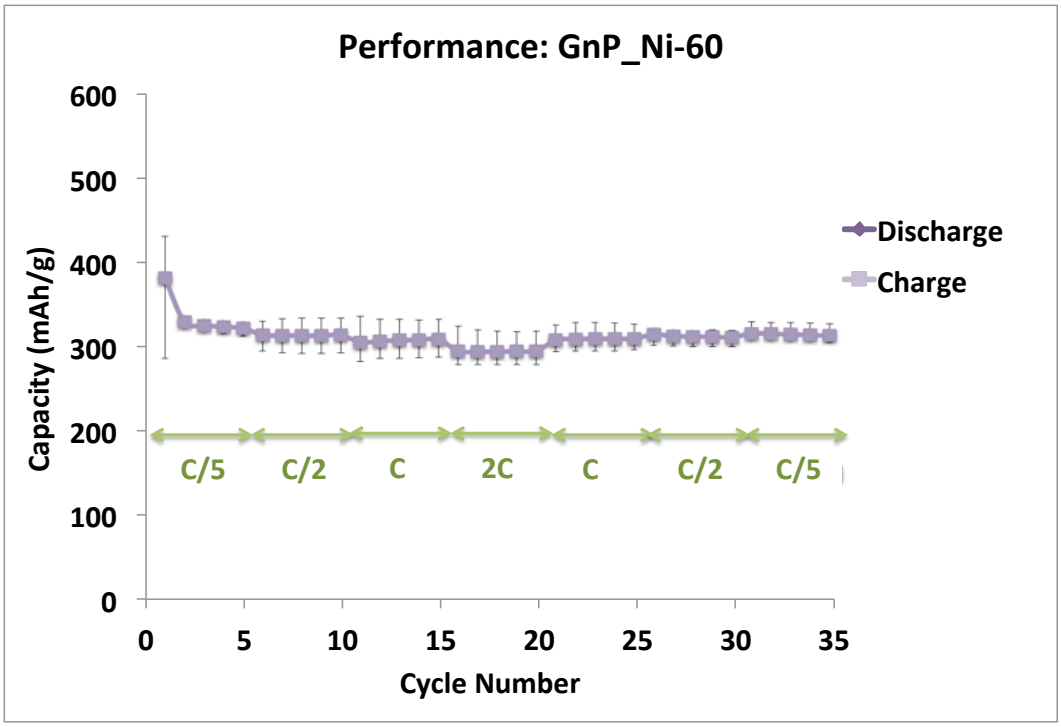

Cyclic Voltammetry

To understand the mechanism behind the improved performance at faster charge rates, cyclic voltammograms at low scan rate (0.05 mV/s) were collected to see the role of Ni in the system. Figure 2-18 shows the CV of fresh anode (without cycling), where we can identify the characteristic peaks of lithium intercalation in and out of the anode. The first cathodic peak at 0.6 V is attributed to SEI layer formation, which completely eliminated in successive sweeps. The other cathodic peaks between 0 to 0.15V represented in all sweeps are related to lithium insertion into carbon. On the anodic side, the peaks in the range 0.2-0.35V represent lithium extraction from Li_xC_6[18]. There are no peaks in the expected electrochemical region corresponding to NiO (cathodic peaks at 0.26 and 0.52 V and anodic peaks at 1.60V and 2.39 V, corresponding to electrochemical reduction and oxidation reaction respectively[9]).

From the CV profiles it was observed that intercalation peaks were relatively more enhanced for doped material relative to undoped GnP. Hence, we can infer that metal doping of >30 nm and reasonable concentration can help to keep platelets accessible for fast lithium ion diffusion. However, for GnP_Ni -30c, on disassembly of cells, a red color discoloration of electrolyte was observed, which is probably due to a side reaction between the metal nanoparticles and lithium ions or electrolyte components. The undesirable reaction products could not be identified due to hazardous nature of the material. The GnP_Ni-60 material showed the best capacity performance amongst the three materials.

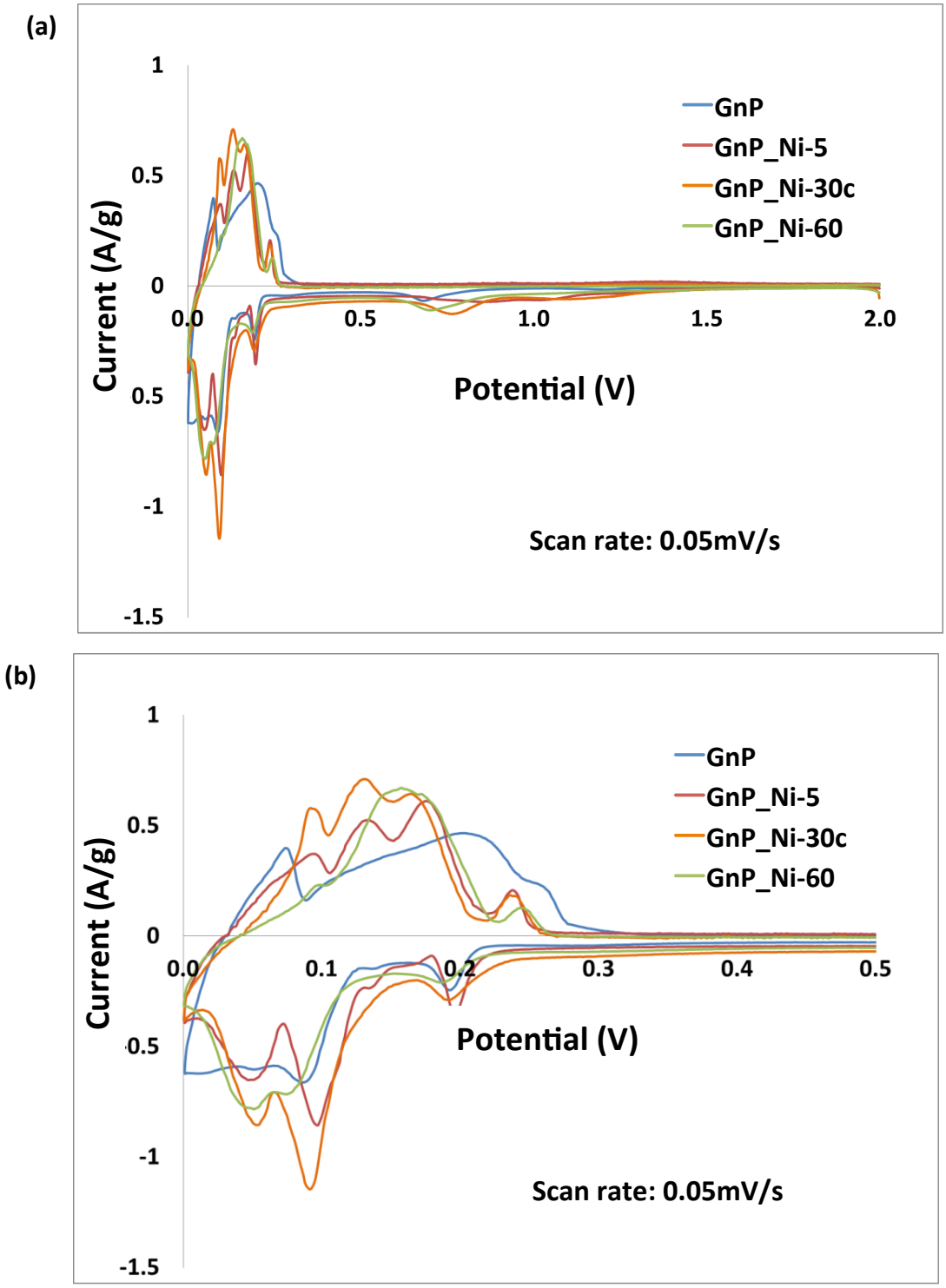

Figure 2-18: Cyclic Voltammogram of Ni doped materials

Electrochemical Impedance Spectra

Impedance spectra for the undoped GnP and GnP_Ni-60 electrode were obtained after 5 galvanostatic cycles at C/5 rate (Figure 2-19). The experimental data was further analyzed by fitting for the equivalent circuit shown in Figure 2-19 (b) with Z-view software. R_S is the bulk or solution resistance which corresponds to the intercept on the x-axis. The semi-circular loops at high and medium frequencies are attributed to the SEI film and charge transfer resistances. The inclined line is an indication of the diffusion behavior of the electrode. Based on the fitting analysis (Table 2-3), the resistance contribution due to the SEI film formation and charge transfer is lower for the GnP_Ni-60 electrode. The decreased SEI film formation is possibly due to a reduction in surface area, and hence fewer active sites for electrolyte decomposition. Also, the addition of Nickel nanoparticles might have contributed to increasing the conductivity through the electrode, thus diminishing charge transfer resistance. However, these two hypotheses need further experimentation and detailed analysis for confirmation.

Hence, from the cyclic voltammogram and capacity profiles, it was observed that the doped anodes retain the graphitic profile and do not show any significant distortions. This indicates that nickel plays an electrochemically inactive role here, and does not participate in any direct conversion reaction with lithium. The improved capacity values are probably attributable to the faster diffusion due to more open structure produced by the nickel spacers, resulting in improved performance at faster charge-discharge conditions.

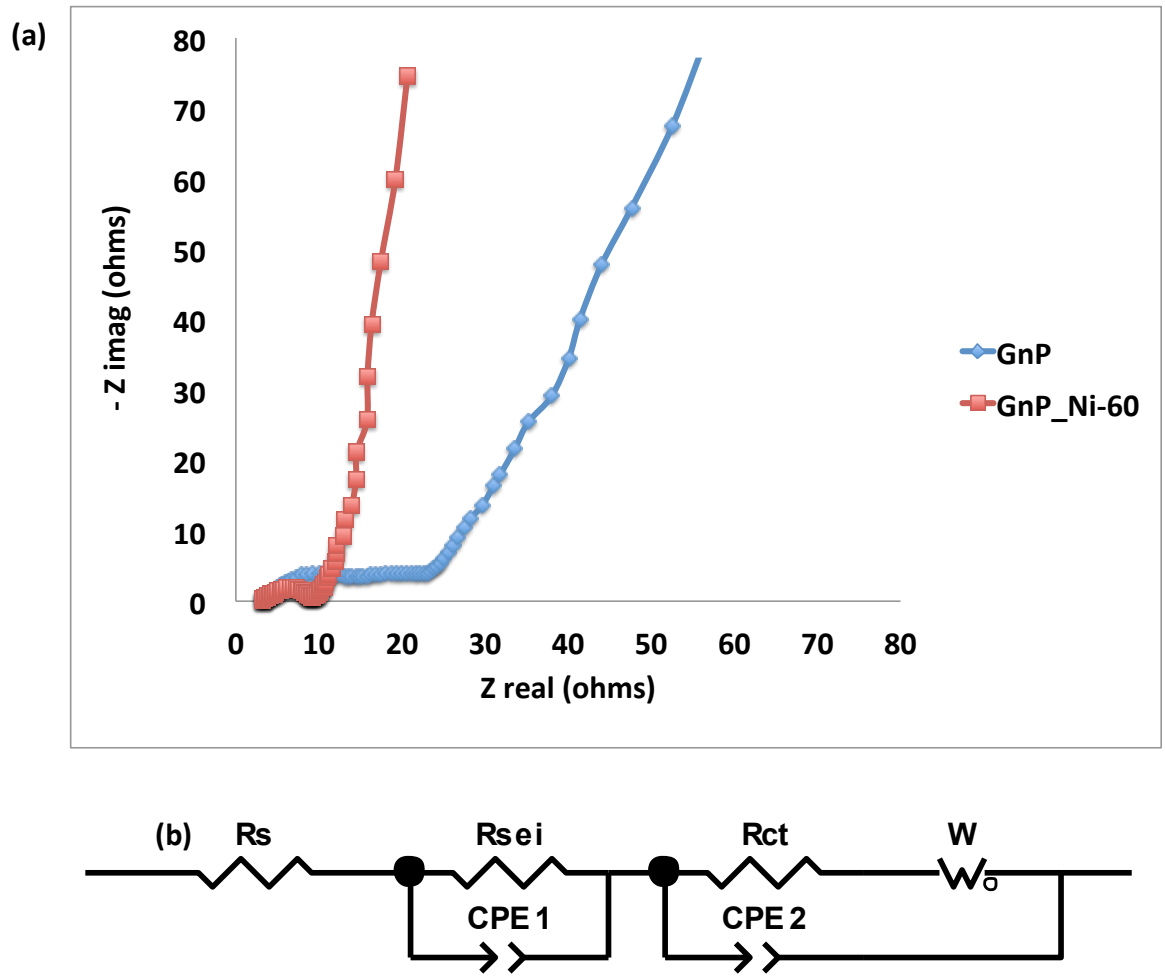

Figure 2-19: (a) Nyquist plots of undoped GnP and GnP_Ni-60 obtained after 5 cycles of charge discharge at C/5 rate. The solid lines correspond to GnP and the dotted lines correspond to GnP_Ni-60. (b) Equivalent circuit used for fitting analysis

Table 2-3: Resistance values of different components GnP and GnP_Ni electrodes obtained by impedance fitting analysis

	Rs	Rsei	Rct
Undoped GnP : 5cyc	3	14	6
GnP_Ni-60 : 5cyc	3	6	1

CONCLUSIONS

The methodology described here resulted in a multilayered 'parking garage' structure composed on parallel arrays graphene nanoplatelets, each of which were decorated with nickel metal nanoparticles which produced an open porous structure, thus allowing flexibility for easy diffusion of lithium in and out of anodes, resulting in high reversible capacity for batteries.

Although there are several publications which have demonstrated that nickel is electrochemically active and synthesizing NiO-graphene composites in a 3-D arrangement can enhance the performance of the anode [9,13], in this research, the nickel dopants seems to be passivated and has no significant contribution to the capacity of the anode material. The increase in performance at faster charge rate can be inferred as due to the effect of facile diffusion of ions.

FUTURE WORK

NI NANOPARTICLE ACTIVATION

The nickel nanoparticles produced in this research did not display the electrochemical activity expected. Heat treatment of the GnP-Ni material in selected gaseous atmospheres at high temperature or with liquid reactants can be used to remove either a nickel oxide, or a nickel organic compound that may cover the nanoparticle surface and restrict its interaction Activation by any of these means should be explored to see if the electrochemical performance would be improved.

GNP-SILICA PAPER

Preliminary work has been conducted on an electrode material nanostructured with silicon to produce a silicon-graphene self-standing electrode, with ordered porosity. The methodology is based on polyelectrolyte mediated self-assembly of an aqueous dispersion of graphene and colloidal silica. The synthesis procedure, as shown in schematic Figure 2-20, shows two separate solutions of GnP with positive and negative polyelectrolytes, combined together and filtered to obtain GnP-silica. The resulting product is a self- standing film of GnP-silica material, with an in-plane conductivity of 330 S/cm.

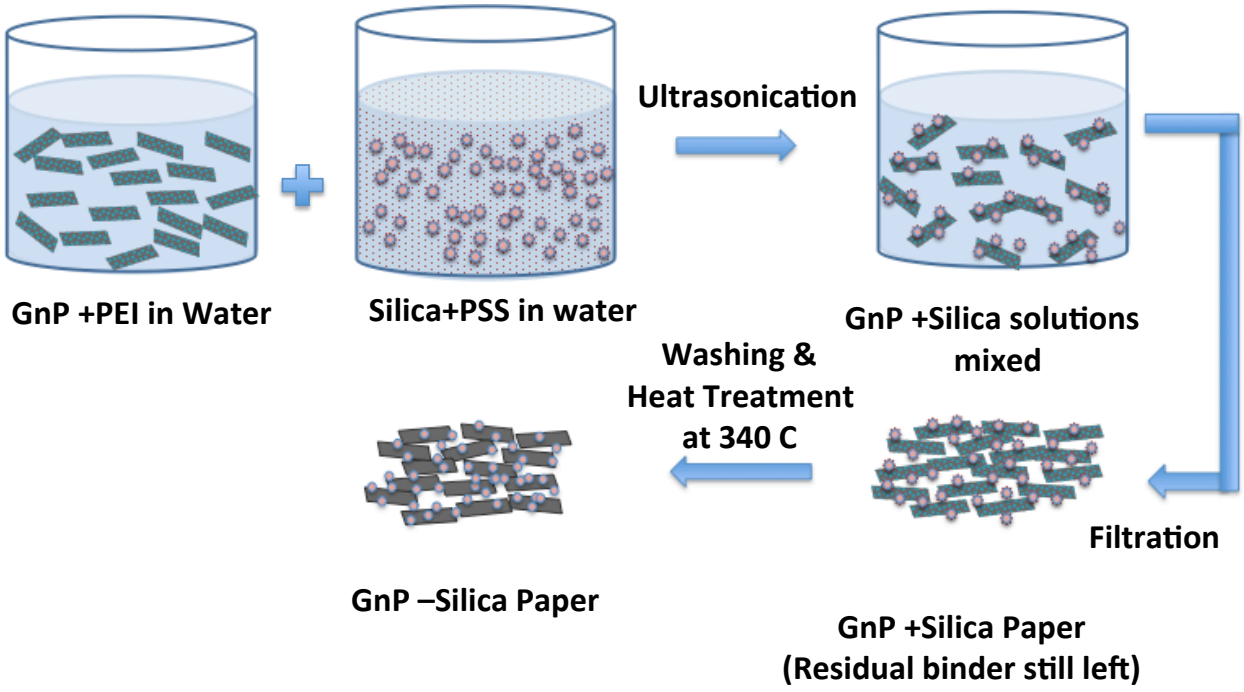

Figure 2-20: Schematic showing the synthesis procedure for GnP-Silica Nanocomposite

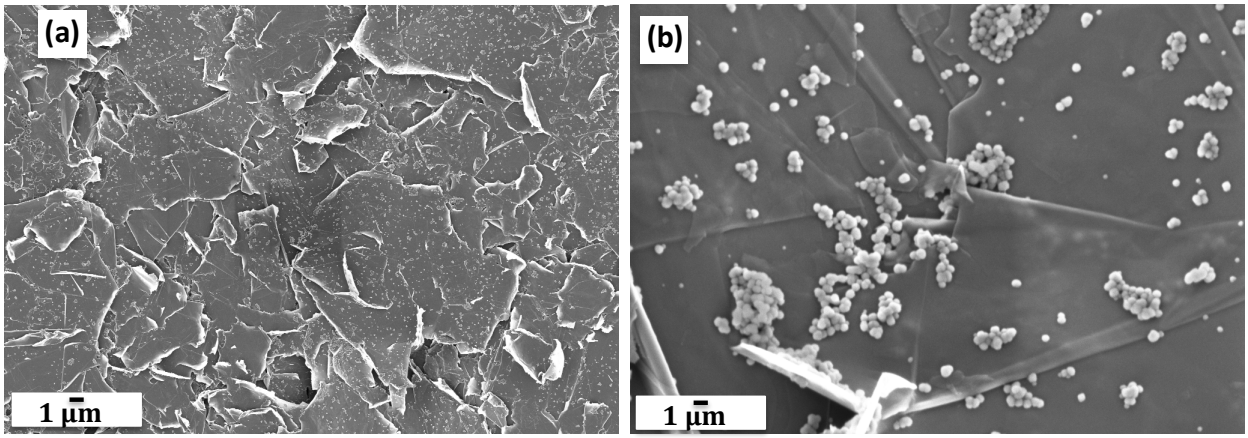

Figure 2-21: Self-Assembled silica-graphene paper: Top view

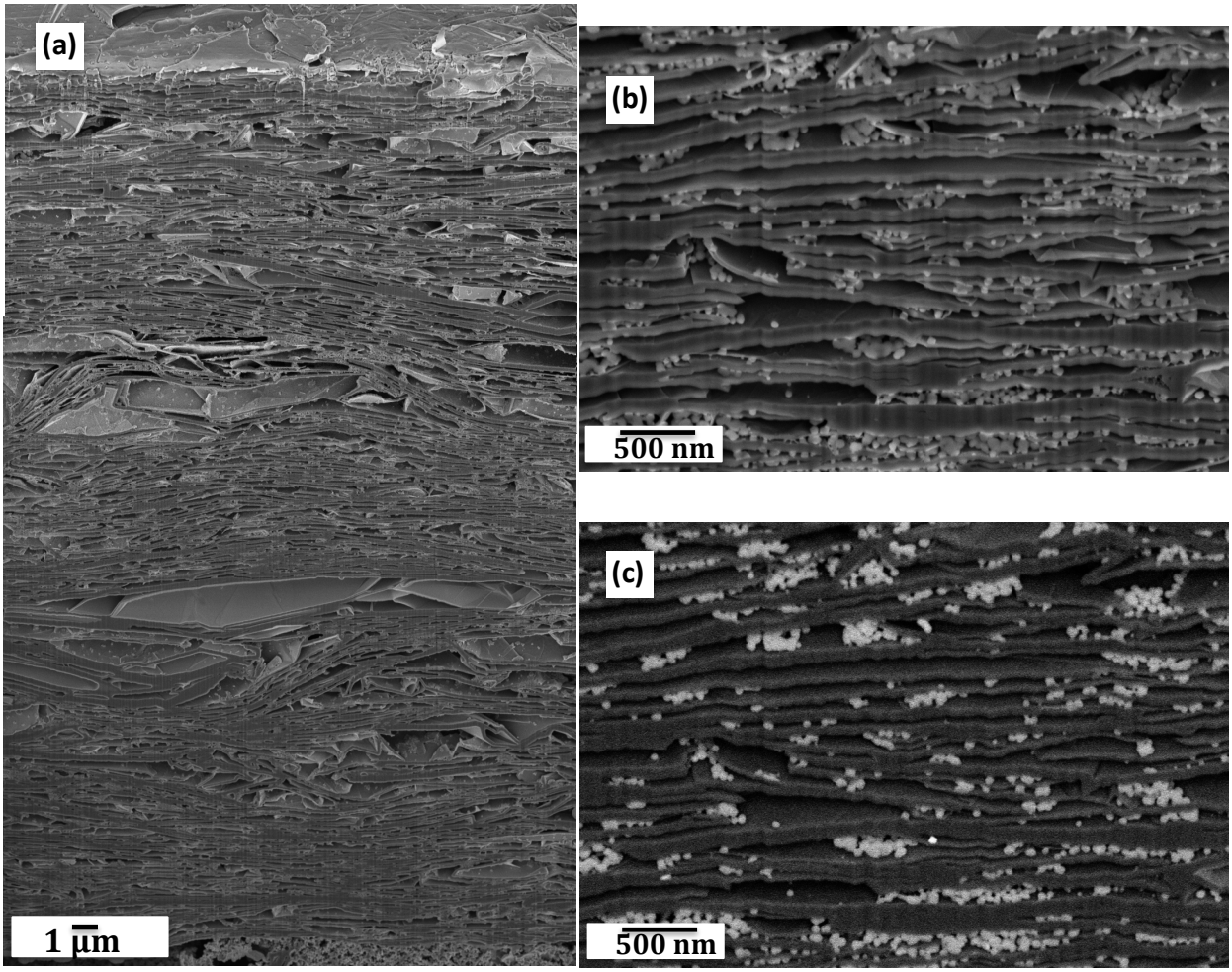

Figure 2-22: Cross-Sectional View of Self-Assembled silica-graphene paper (a) Whole electrode (b) High magnification (c) Back-scatter image of the section shown in (b)

Morphological characterization of the paper observed from top-view (Figure 2-21), shows that silica nanoparticles are distributed over the GnP platelet surface with some slight aggregation of silica nanoparticles. The cross-sectional SEM images shown in Figure 2-22 verify the highly organized electrode structure with silica nanoparticles interspersed between graphene nanoplatelets, analogous to cars parked in a parking garage. Also, shown in Figure 2-22 (b) and (c) are the secondary electron and backscatter image of the same section. In the backscatter image, we can observe that the brighter region represent the silica nanoparticles (due to higher atomic number).

Further trials are being done to reduce the silica to active silicon by heat treatment under H_2 reducing conditions. It is expected that this electrode will be able to blend the advantages of capacity of both active materials and the effect of nanostructuring the electrode.

REFERENCES

REFERENCES

1. Lian, P. *et al.* Large reversible capacity of high quality graphene sheets as an anode material for lithium-ion batteries. *Electrochimica Acta* **55**, 3909–3914 (2010).

2. Yang, S., Feng, X., Ivanovici, S. & Müllen, K. Fabrication of graphene-encapsulated oxide nanoparticles: towards high-performance anode materials for lithium storage. *Angewandte Chemie* **49**, 8408–11 (2010).

3. Wang, D. *et al.* Ternary self-assembly of ordered metal oxide-graphene nanocomposites for electrochemical energy storage. *ACS nano* **4**, 1587–95 (2010).

4. Li, X. *et al.* Functionalized graphene sheets as molecular templates for controlled nucleation and self-assembly of metal oxide-graphene nanocomposites. *Advanced materials* **24**, 5136–41 (2012).

5. Guo, Y.-G., Hu, J.-S. & Wan, L.-J. Nanostructured Materials for Electrochemical Energy Conversion and Storage Devices. *Advanced Materials* **20**, 2878–2887 (2008).

6. Sun, Y., Wu, Q. & Shi, G. Graphene based new energy materials. *Energy & Environmental Science* **4**, 1113–1132 (2011).

7. Wu, Z.-S., Ren, W., Xu, L., Li, F. & Cheng, H.-M. Doped graphene sheets as anode materials with superhigh rate and large capacity for lithium ion batteries. *ACS nano* **5**, 5463–71 (2011).

8. Zhou, X., Yin, Y.-X., Wan, L.-J. & Guo, Y.-G. Facile synthesis of silicon nanoparticles inserted into graphene sheets as improved anode materials for lithium-ion batteries. *Chemical communications* **48**, 2198–200 (2012).

9. Tao, L. *et al.* 3D-hierarchical NiO–graphene nanosheet composites as anodes for lithium ion batteries with improved reversible capacity and cycle stability. *RSC Advances* **2**, 3410–3415 (2012).

10. Fukushima, H. Graphite Nanoreinforcements in Polymer Nanocomposites. Chemical Engineering & Materials Science Department, Michigan State University, East Lansing (2003).

11. Lin, Y. *et al.* Rapid, solventless, bulk preparation of metal nanoparticle-decorated carbon nanotubes. *ACS nano* **3**, 871–84 (2009).

12. Fu, J. & Joshi, S. Optimization Based Geometric Modeling of Nano/Micro Scale Ion Milling of Organic Materials for Multidimensional Bioimaging. *Journal of Nanotechnology in Engineering and Medicine* **1**, 031003 (2010).

13. Mai, Y. J., Tu, J. P., Gu, C. D. & Wang, X. L. Graphene anchored with nickel nanoparticles as a high-performance anode material for lithium ion batteries. *Journal of Power Sources* **209**, 1–6 (2012).

14. Kottegoda, I. R. M., Idris, N. H., Lu, L., Wang, J.-Z. & Liu, H.-K. Synthesis and characterization of graphene–nickel oxide nanostructures for fast charge–discharge application. *Electrochimica Acta* **56**, 5815–5822 (2011).

15. Ferrari, a. C. *et al.* Raman Spectrum of Graphene and Graphene Layers. *Physical Review Letters* **97**, 187401 (2006).

16. Dresselhaus, M. S., Jorio, A., Hofmann, M., Dresselhaus, G. & Saito, R. Perspectives on carbon nanotubes and graphene Raman spectroscopy. *Nano letters* **10**, 751–8 (2010).

17. Terrones, M., Filho, A. G. S. & Rao, A. M. *Doped Carbon Nanotubes : Synthesis , Characterization and Applications*. **566**, 531–566 (2008).

18. Levi, M. D. & Aurbach, D. Simultaneous Measurements and Modeling of the Electrochemical Impedance and the Cyclic Voltammetric Characteristics of Graphite Electrodes Doped with Lithium. *Journal of Physical Chem. B* **5647**, 4630–4640 (1997).

3 GRAPHITE NANOPLATELETS AS A CONDUCTING ADDITIVE FOR LITHIUM TITANATE ELECTRODES

BACKGROUND

Lithium titanate (LTO) is one of the prominent materials being considered for lithium ion batteries anodes, with a theoretical lithium storage capacity of 175 mAh/g. Despite of its significantly lower storage capacity in comparison to other anode materials such as Graphite (375 mAh/g), SnO_2 (990 mAh/g) and Silicon (4200 mAh/g), LTO has attracted interest due to its high rate performance, cyclic stability, reversibility and no volume change during the charge-discharge process[1,2]. In addition, since the operating voltage of LTO is higher than that for deposition of metallic lithium, this material is not prone to problems of dendritic growth and hence, is safer than other anode materials[2].

Lithium titanate can be combined with a variety of cathode materials such as $LiCoO_2$, $LiFePO_4$ and $LiMn_2O_4$ to form a Li ion battery setup capable of delivering 2.5 V (schematic shown in Figure 3-1).

Spinel lithium titanate structure acts as an intercalation host, allowing reduction of 3 Ti^{4+}, and changing to a stable $Li_7Ti_5O_{12}$ rock salt structure (Figure 3-2). The insertion process allows inclusion of 3 Li atoms per formula unit with minimal change in cubic unit cell[3,4]. This

zero-strain feature of LTO helps to maintain electrode structure over cycle life, thus making it an attractive anode material.

$$Li_4Ti_5O_{12} + 3\,Li^+ + 3\,e^- \rightleftharpoons Li_7Ti_5O_{12}$$

However, lithium titanate suffers from the problem of low conductivity and thus offers high resistance to electron and Li^+ transport, resulting in low power density of the batteries. The conductivity problem of lithium titanate electrodes is addressed by two different approaches. One methodology is to develop nanoscale or nanostructured particles, which will have shorter lithium diffusion paths and hence will allow better ionic conductivity[5,6]. Electrical conductivity can be improved by doping and conductive coatings of active materials[7] or by the addition of conducting materials to the electrode[2,6].

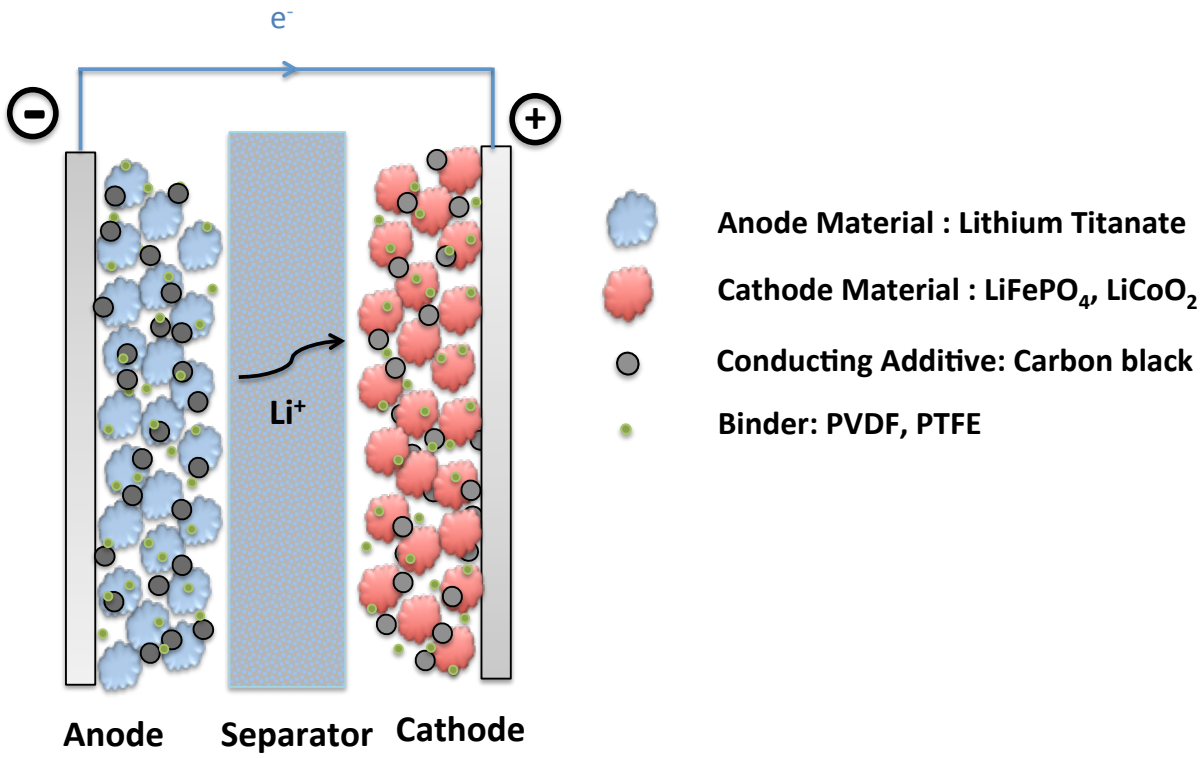

Figure 3-1: Schematic showing battery setup with lithium titanate as anode

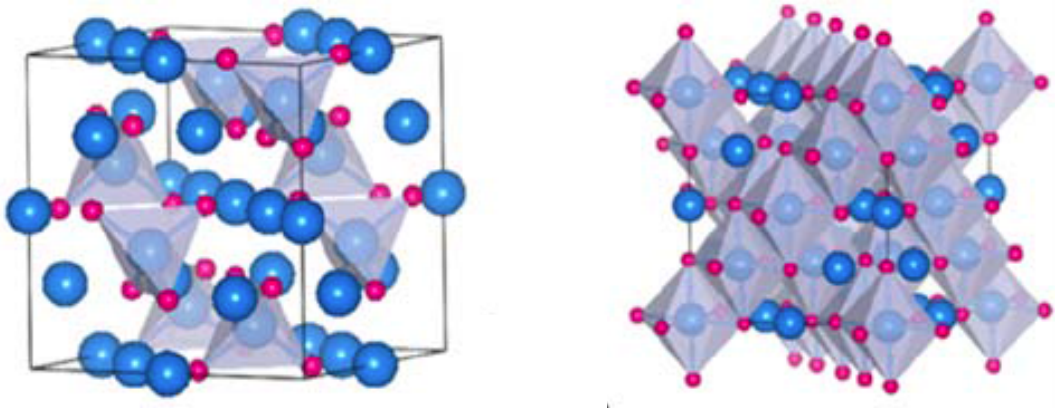

Figure 3-2: Crystal structure of (a) Spinel $Li_4Ti_5O_{12}$ and (b) Rock-salt $Li_7Ti_5O_{12}$ [4]

SIGNIFICANCE

Conductivity is one of the major concerns associated with the performance of lithium titanate and several other cathode materials ($LiCoO_2$, $LiMnO_2$, $LiFePO_4$). The ionic conductivity is tackled by making the size of active material smaller which will reduce the diffusion distance for lithium ion. For electrical conductivity, suitable modifications are done by addition of conductive coatings, conductive templates or by addition of conductive materials such as metal fibers[7,8] and carbon materials[6,9,10] in the electrode structure.

Carbon black is the preferred choice of conducting additive for such electrodes, which is primarily due to good conductivity, good cycle life and low cost. However, to achieve percolation, high concentration 10-20% of carbon black is needed. Such high concentration of additives can have negative impacts such as lower gravimetric performance and increased side reactions. Hence, there have been attempts to reduce the amount of inactive materials in the electrode to increase its gravimetric capacity/energy density.

High aspect ratio carbon nanomaterials, such as CNTs[11], CFs[12] and graphene sheets[1,2,13,14] have been investigated as potential additive materials. Graphene, It has been observed that electrical percolation can be obtained at lower concentrations of 5 % or less[2,14]. In addition some results have also shown that using high aspect ratio graphene sheets also reduces polarization[7,15]. The combination of carbon black with conductive high aspect ratio materials has been used to improve the performance of the electrode materials[12,16].

APPROACH

Graphene nanoplatelets (GnP) are two-dimensional, high aspect ratio nanoplatelets, which can be synthesized at a low cost of ~$20/lb., by a simple intercalation-exfoliation procedure. These platelets, which are a stack of few graphene sheets, have the advantage of high aspect ratio, nanoscale thickness dimension, and can percolate to form an interconnected network at low concentrations. High chemical tolerance, good thermal stability and good mechanical strength are additional benefits, which can help maintain electrode integrity and good cycle life. In this section, we have investigated the effect of the addition of different sizes of GnP on the lithium storage capacity of LTO and have investigated the effect of reducing the concentration of conducting additive on the impedance and cycling performance.

EXPERIMENTAL SECTION

MATERIALS

Spinel lithium titanate nanopowder (<100nm nanopowders), polyvinylidene fluoride (PVDF) and N-methyl pyrrolidone were obtained from Sigma-Aldrich. Lithium foil used as the counter electrode was obtained from Alfa-Aesar. Different grades of graphene nanoplatelets viz. GnP-1, GnP-5 and GnP-25 were obtained from XG Sciences®. Commercial conducting additive Super P was obtained from Timcal. Aluminum foil of 15μm thickness, obtained from MTI Corporation was used as the current collector for casting electrodes.

ELECTRODE PREPARATION

The electrode slurry is prepared by ball milling the appropriate amounts of lithium titanate powder, conducting additive (varies from 2-10%), and 10% binder PVDF, with desired amount of N-methyl pyrrolidone. The well-dispersed viscous slurry is cast on the aluminum foil current collector using the adjustable film applicator on the MTI automatic film coater. The electrodes were dried under ambient condition for 12 hours, and then heated in a vacuum oven at a temperature of around 120°C for 8 hours. Finally the electrodes were pressed in a Carver press at a pressure of 0.1 MPa to ensure good electrical contact, inter-particle contact and lower volumetric density.

MORPHOLOGY CHARACTERIZATION

The morphology of the LTO, different carbon materials, electrode top view and electrode cross-section was observed using the Carl Zeiss Auriga® CrossBeam scanning electron microscope. The sample preparation for observing electrode cross-section was done by epoxy embedding and polishing method, as described previously.

ELECTROCHEMICAL CHARACTERIZATION

The electrochemical performance of LTO-GnP Electrodes were evaluated in a two electrode coin cell configuration with lithium foil as the counter electrode and 1M solution of $LiPF_6$ in 1:1 (v/v) EC/DMC solution, as the electrolyte. Figure 3-3 shows the schematic and pictures of the 2-electrode coin cell setup. The CR-2032 coin cells were assembled in argon filled glove box (<1 ppm H_2O, <1 ppm O_2), and were tested using an Arbin Instruments BT 2000 Battery Testing System. The electrodes were galvanostatically cycled between 1 V and 2.5 V at

different charge rates of C/5, C/2, C and 2C. The C-rates are calculated based on the mass of LTO in the electrode. Electrochemical Impedance Spectroscopy was done using a VersaSTAT MC Instrument in the frequency range of 1 Hz to 1 MHz at amplitude of 5mV.

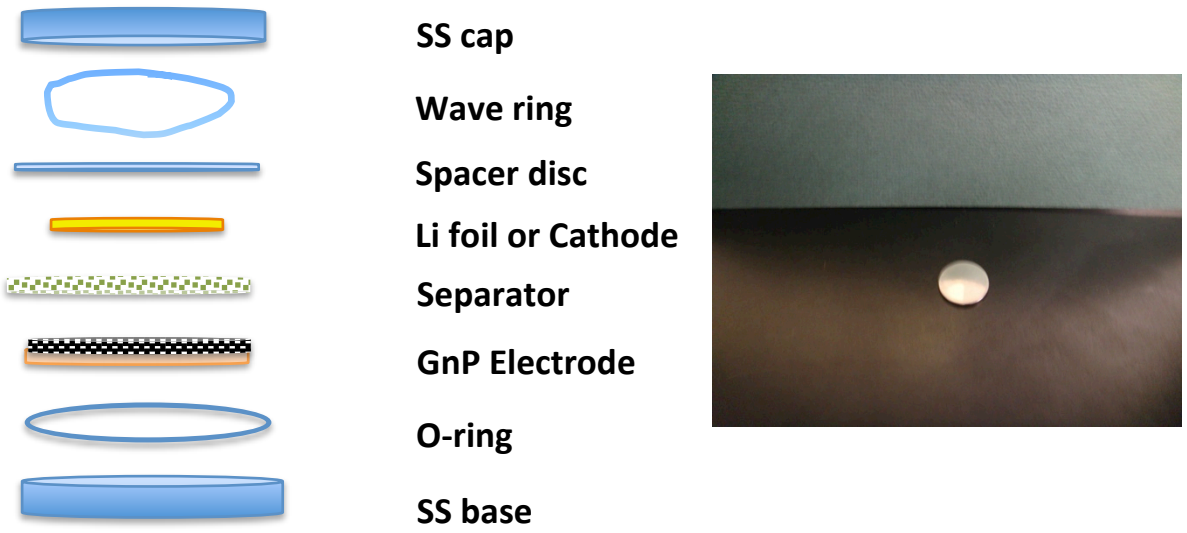

Figure 3-3: Schematic and pictures of Two-electrode Coin cell

RESULTS & DISCUSSION

MORPHOLOGICAL OBSERVATION

The morphology of Lithium titanate nanopowder (Figure 3-4(e)) and the conducting additives were analyzed by SEM. Figure 3-4 (a), (b) & (c) shows SEM images of three different GnP materials being used for this study. These platelets are represented by GnP-*x* nomenclature, where *x* represents the average diameters of these platelets. Figure 3-4 (d) is the SEM image of Super P particles, which are spherical in shape and are of nano-dimension. The properties of different carbon materials are summarized below in Table 3-1.

Table 3-1: Different carbon materials with their physical properties

Material	Particle size Dia (µm)	Thickness (µm)	Surface Area (m^2/g)	Aspect Ratio
GnP-1	1	<0.01	100	<100
GnP-5	5	<0.01	100	~500
GnP-25	25	<0.01	120	~2500
Super P	<0.1	<0.1	62	1

The top view and cross-sectional view of all the electrodes SEM images are shown in Figure 3-5 and Figure 3-6. The SEM images illustrate uniform distribution of the conducting additives through the electrode matrix however their interaction with LTO are significantly different, which is discussed in detail in later section. From the cross-sectional images of GnP electrodes, we can observe that the GnP platelets are dispersed in the electrode forming an interconnected network. The platelets are flexible and bend out-of-plane providing contact with the LTO particles. There is overlapping of platelets in the in-plane and through-plane direction, which ensures a continuous electrical pathway, resulting in good electrical conductivity. Also, the large dimension of platelets can provide good mechanical integrity to the electrode made of LTO nanopowders.

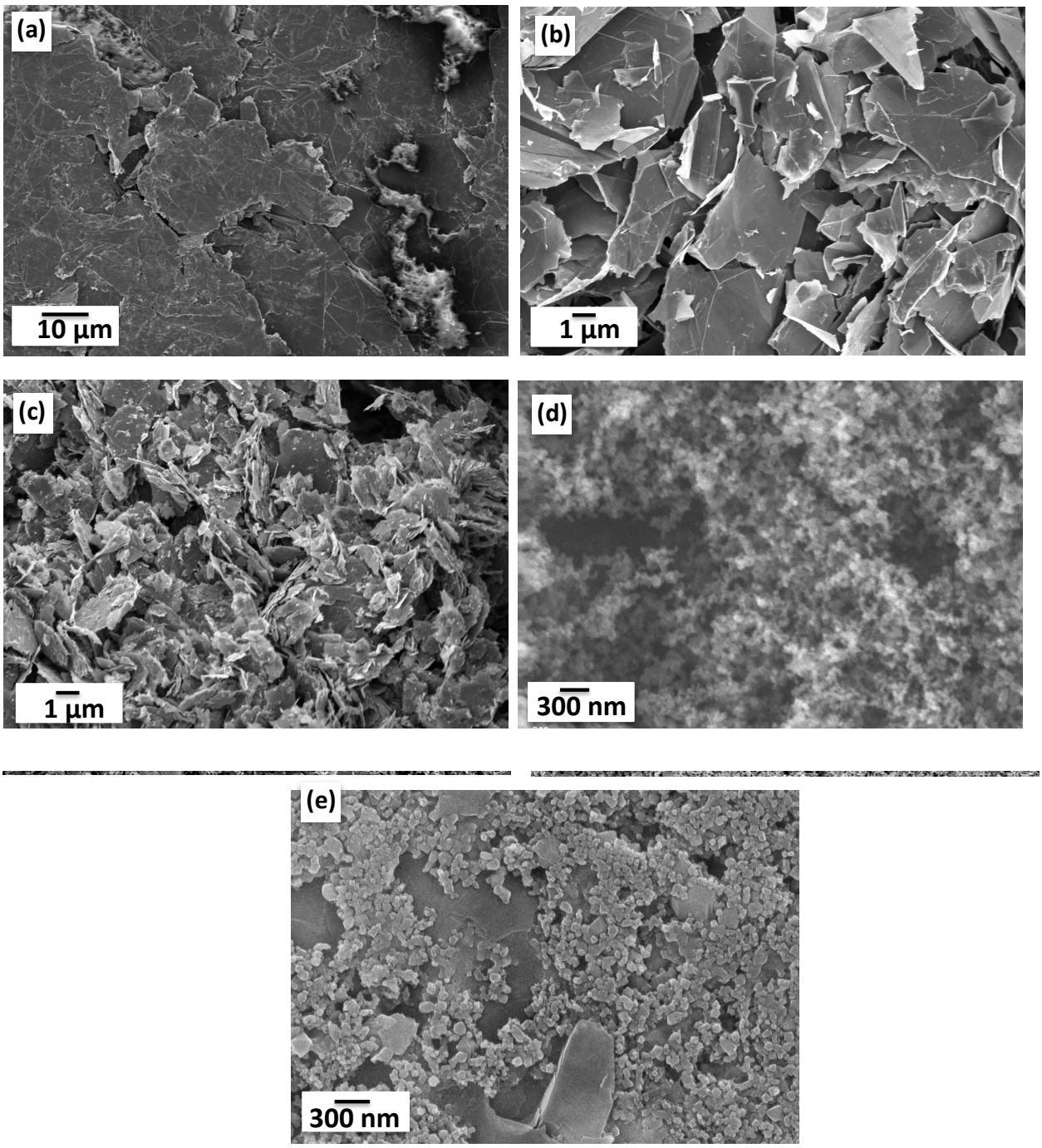

Figure 3-4: SEM Images of (a) GnP-25, (b) GnP-5, (c) GnP-1 , (d) Super P, (e) LTO (Scale bar- (a): 10 µm; (b),(c): 1 µm; (d),(e): 300 nm).The image of LTO is taken from LTO+GnP electrode, because of difficulty in doing SEM of pure LTO powder due to its poor conductivity

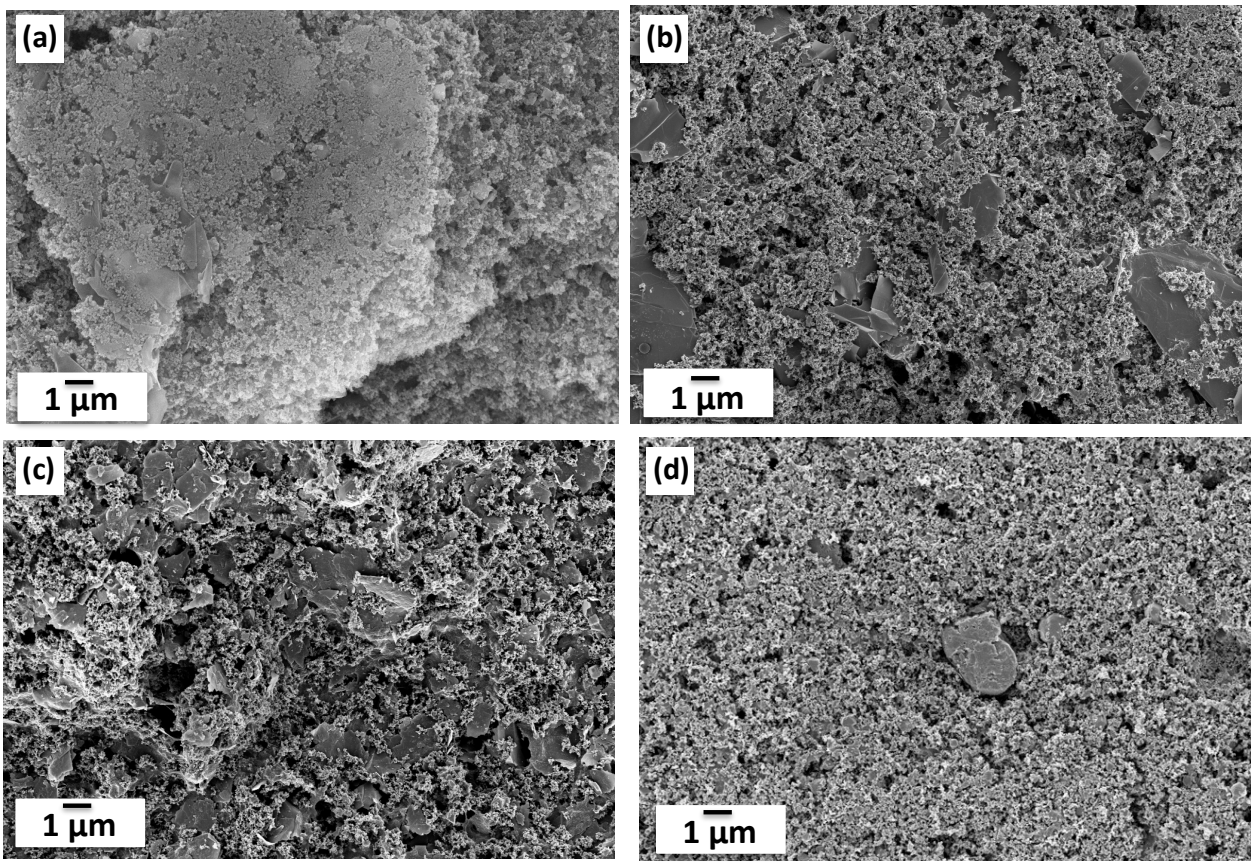

Figure 3-5: SEM Images of top view of various LTO electrodes (a) LTO+GnP-25, (b) LTO +GnP-5, (c) LTO +GnP-1, (d) LTO+Super P electrodes.
In all these electrodes, the concentration of carbon additive material is 10% by weight.

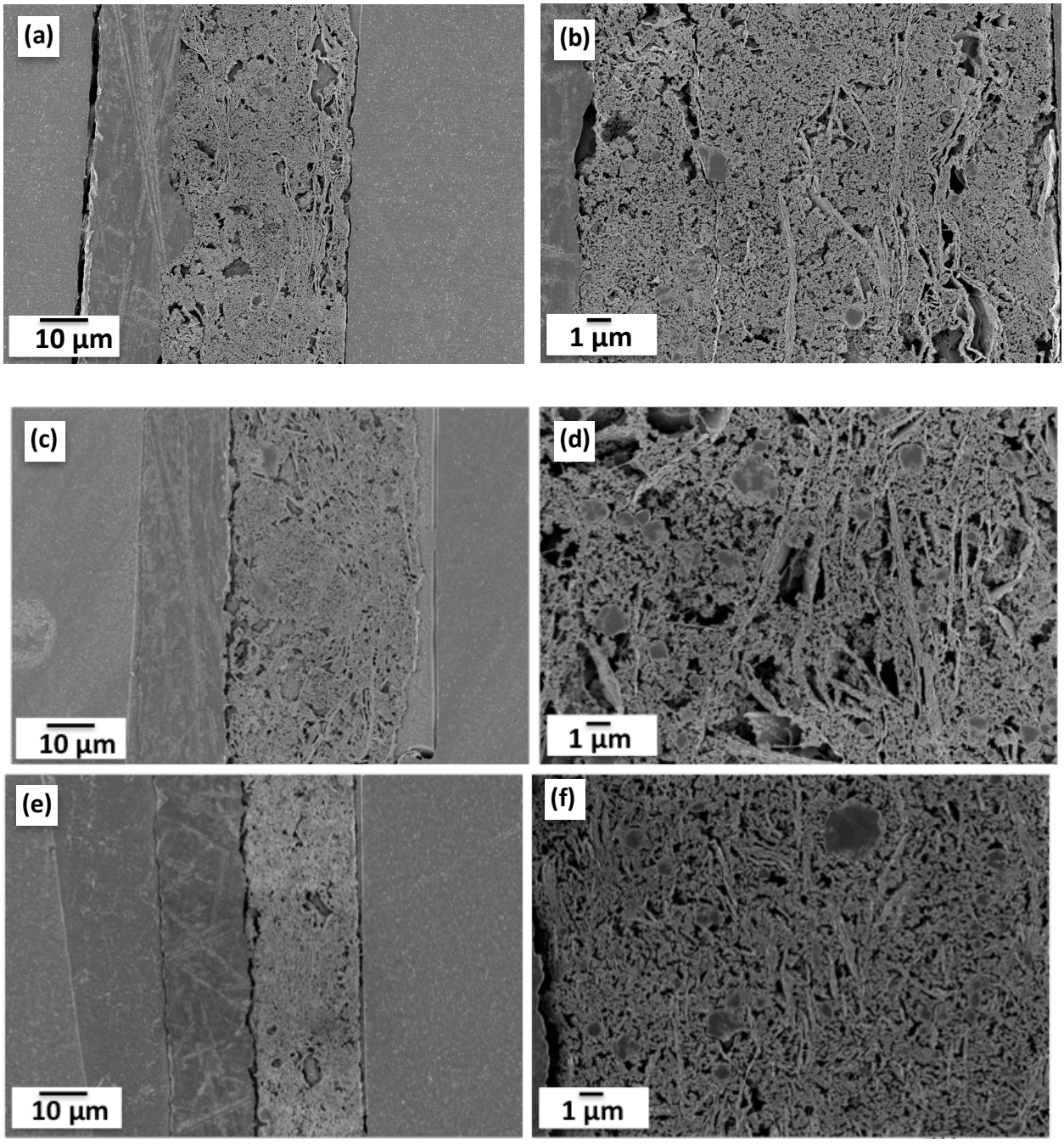

Figure 3-6: Low magnification (Left) and corresponding High-magnification (Right) SEM Images of the cross-sectional views of the following electrodes (a), (b) LTO+GnP-25; (c),(d) LTO +GnP-5; (e),(f) LTO +GnP-1; (g),(h) LTO+ Super P. In all these electrodes, the concentration of carbon additive material is 10% by weight.

Figure 3-6 (cont'd)

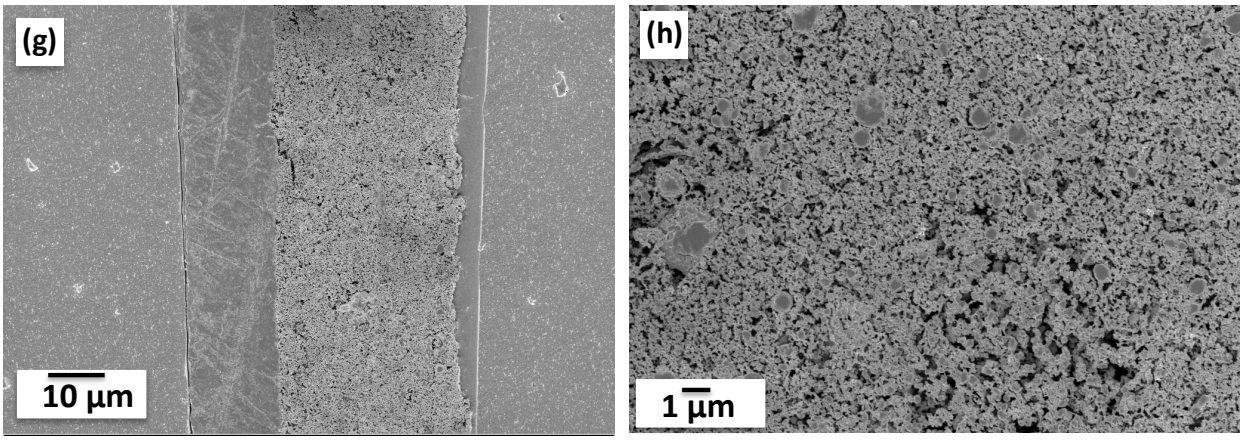

ELECTROCHEMICAL CHARACTERIZATION

The performances of the different LTO electrodes were investigated in a coin cell setup with lithium foil as counter electrode. The electrodes were galvanostatically cycled at different charge rates, for 5 cycles each. The performances, shown in Figure 3-7and Figure 3-9 represent the mean value of the capacities obtained, with the error bars representing the range of data. We observe from Figure 3-7, which shows both charge and discharge capacity of all the electrodes that the capacity values of these electrodes, is very repeatable, with low error margin and high coulombic efficiency. The capacity profiles of LTO+GnP electrodes were plotted at different charge rates (Figure 3-8), which shows typical plateaus corresponding to charge-discharge. We observe relatively flat plateau for C/5 and C/2 charge rates, however for faster charge rate of C and 2C, the profiles start having a slope shape, which is indicative of increased polarization[15].

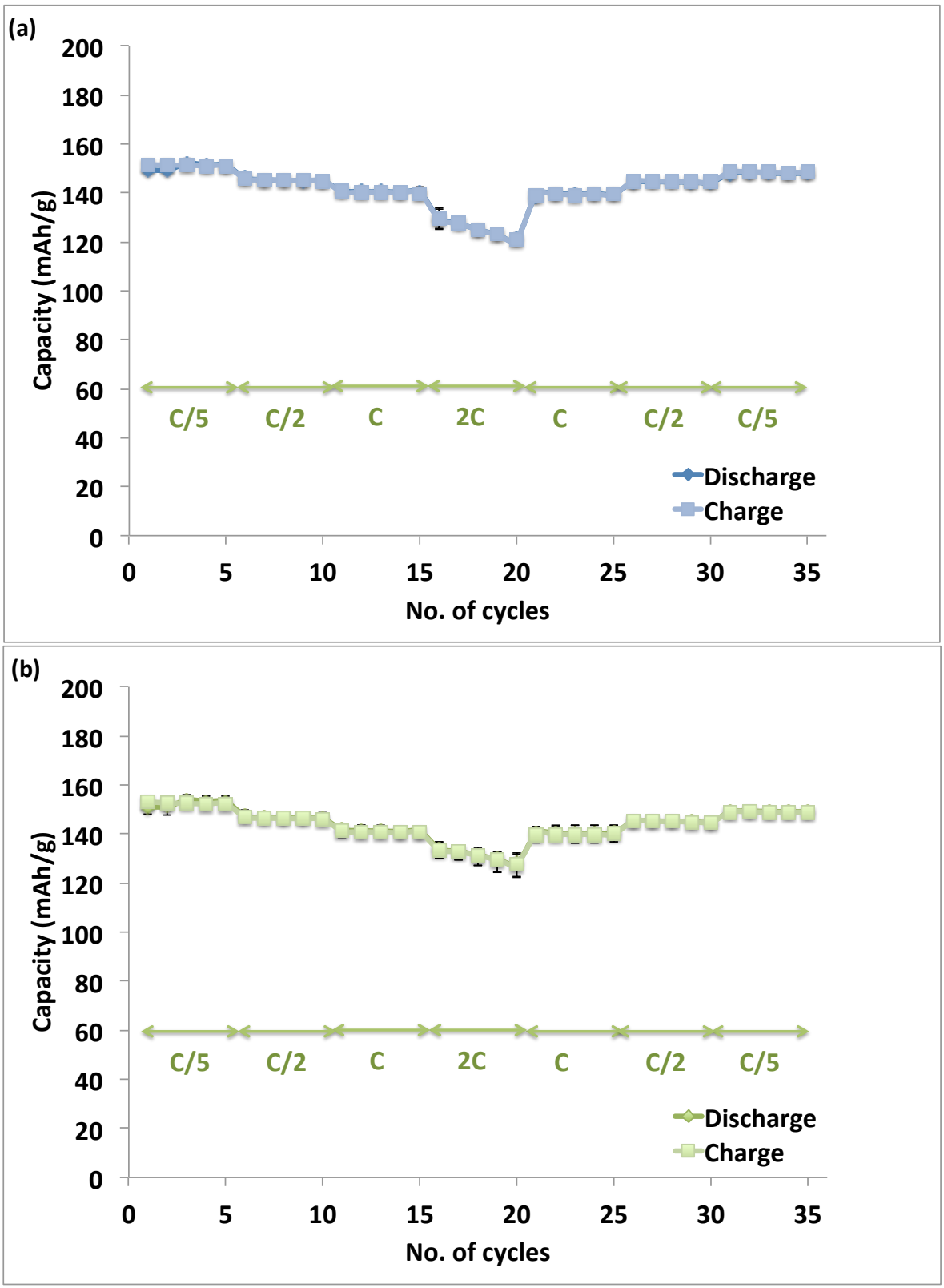

Figure 3-7: Galvanostatic performance of at different charge rates (C/5,C/2,C and 2C) of (a) LTO+GnP-25, (b) LTO+GnP-5, (c) LTO+GnP-1, (d) LTO+Super-P

Figure 3-7 (cont'd)

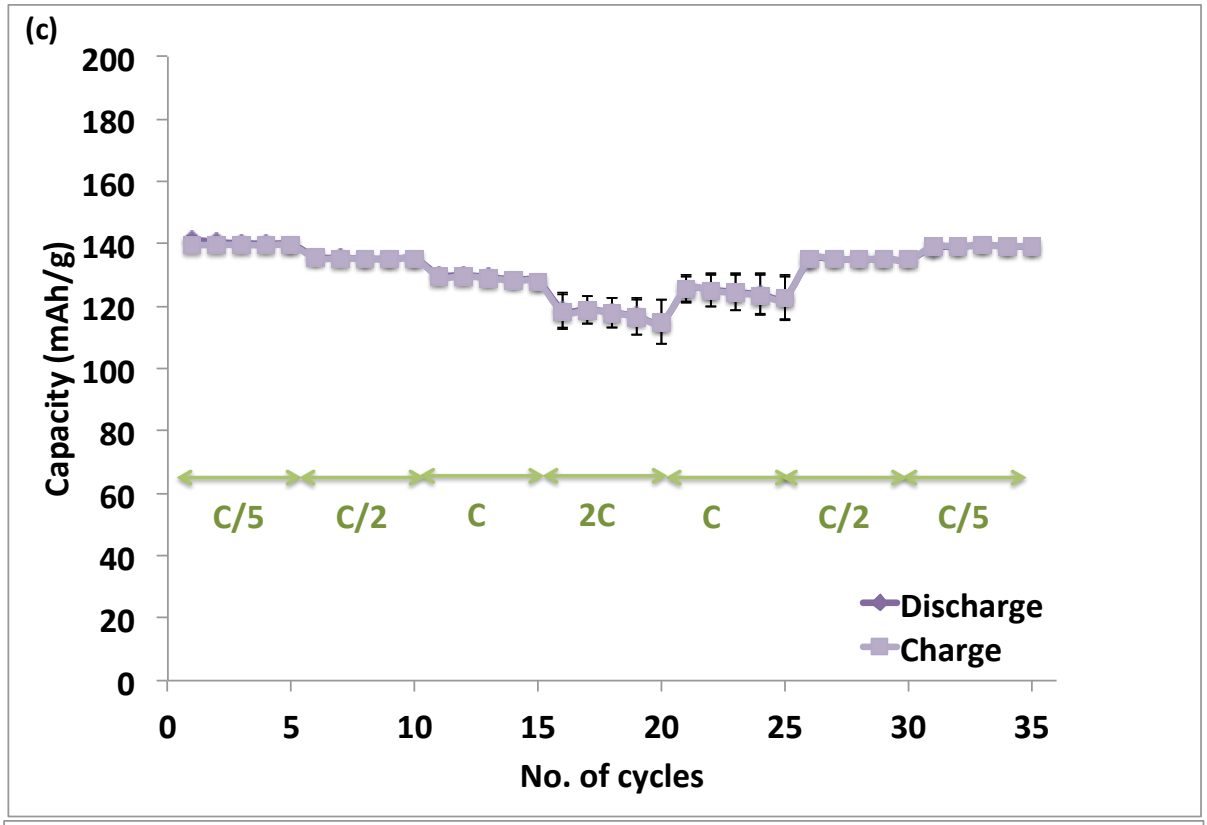

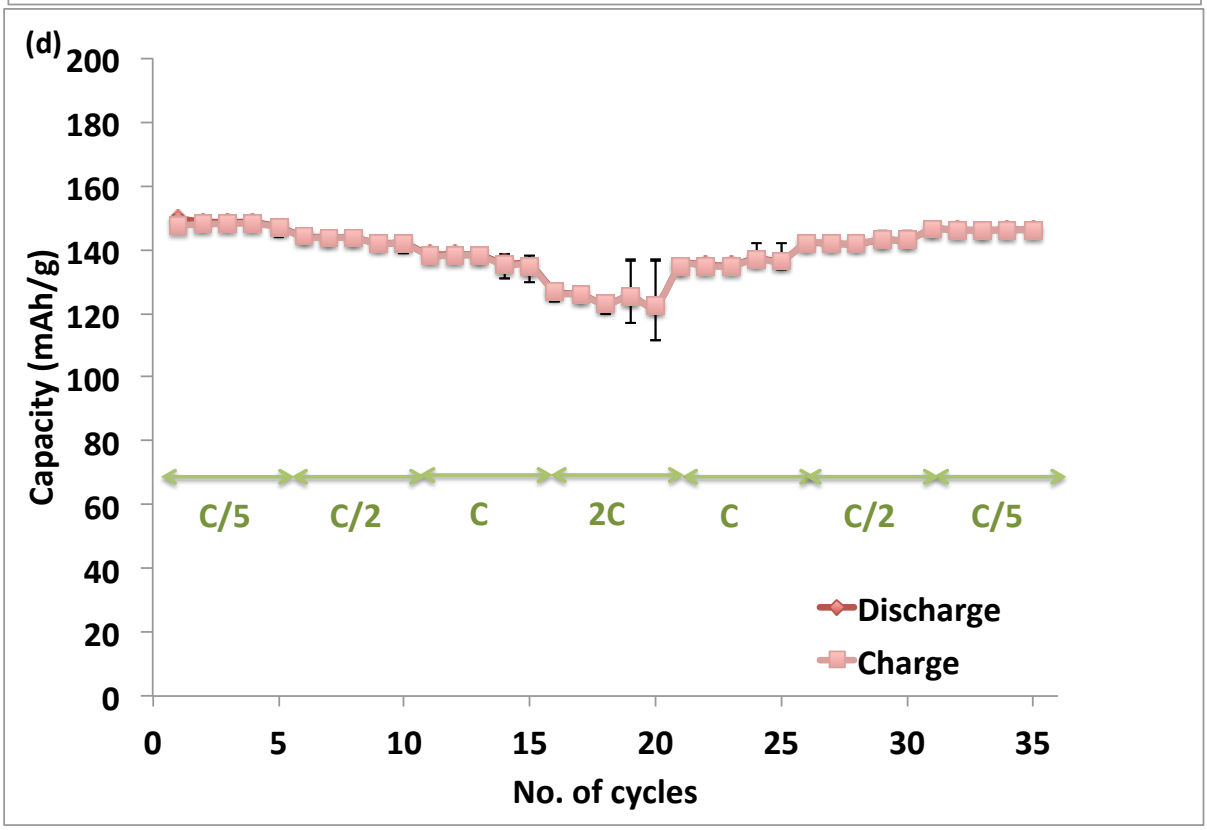

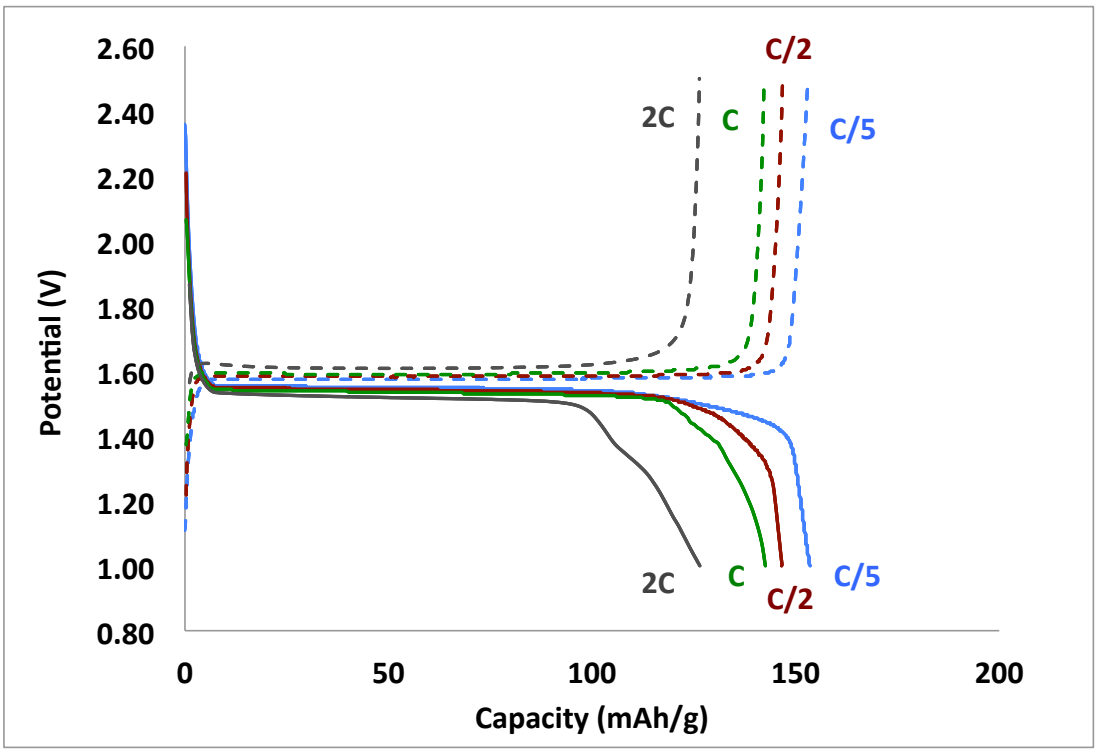

Figure 3-8: Capacity profiles of LTO+GnP-25 Electrode at different charge rates

Influence of different GnP materials

The comparison of capacity values of different sizes of GnP material as conducting additive was evaluated. Figure 3-9 shows the performance of LTO electrodes with a 10 weight % addition of different conducting additives. It was observed that the capacity values of LTO electrodes with GnP-25 and GnP-5 are slightly larger than the one with Super P as the conducting material. However, the performance of LTO+GnP-1 was found to be lower than these electrodes. These results were in accordance with the trends observed in the EIS data. Figure 3-10 below shows the Nyquist plots of the electrodes, obtained after 5 complete galvanostatic cycles at a rate of C/5. The intercept on x-axis corresponds to the electrolyte solution resistance. The depressed semi-circle at high frequencies comes from two overlapping semi-circles associated with surface film resistance and charge transfer resistance. The line at

low frequencies is indicative of diffusion behavior. The impedance curves were fitted to the equivalent circuit[1,2] (shown in Figure 3-13 (b)) using Z-view software. Figure 3-13 (c) shows the comparison of experimental and fitted data, which indicates a good fit with very small error percentage. Based on the fitting, the values of resistance parameters are summarized in the Table 3-2. The electrolyte solution resistance was found to be the same for all the electrodes. There is an increase in resistance due to the surface film with reduced size of GnP particles, which can be possibly translated to increased edges, which acts as active sites for electrolyte decomposition and surface film formation. However, the variation of SEI for different GnP materials is not completely understood and needs further experimental verification. The charge transfer resistance values of the electrodes show the following trend GnP-5 < GnP-25 < Super P <GnP-1. The good conductivity of GnP-25 and GnP-5 electrodes can be directly translated to their enhanced capacity performance. The enhanced conductivity and performance can be attributed to the high aspect ratio of GnP particles, which forms an interconnected network throughout the electrode.

The decrease in performance of LTO+GnP-1 electrodes is not well understood, but the increase in impedance can be possibly associated with breaks in the network due to aggregation or inhomogeneous dispersion. Also, because of the large number of particles forming a close packed network, the accessibility of the ions to the electrode in through-plane direction may be restricted. The reduced conductivity and hindered lithium ion transport, results in degradation in the performance. The cross-section images obtained by epoxy

mounting method can show artifacts due to polishing methodology and hence, more detailed analysis such as FIB milling can be helpful to give an insight about the observed results.

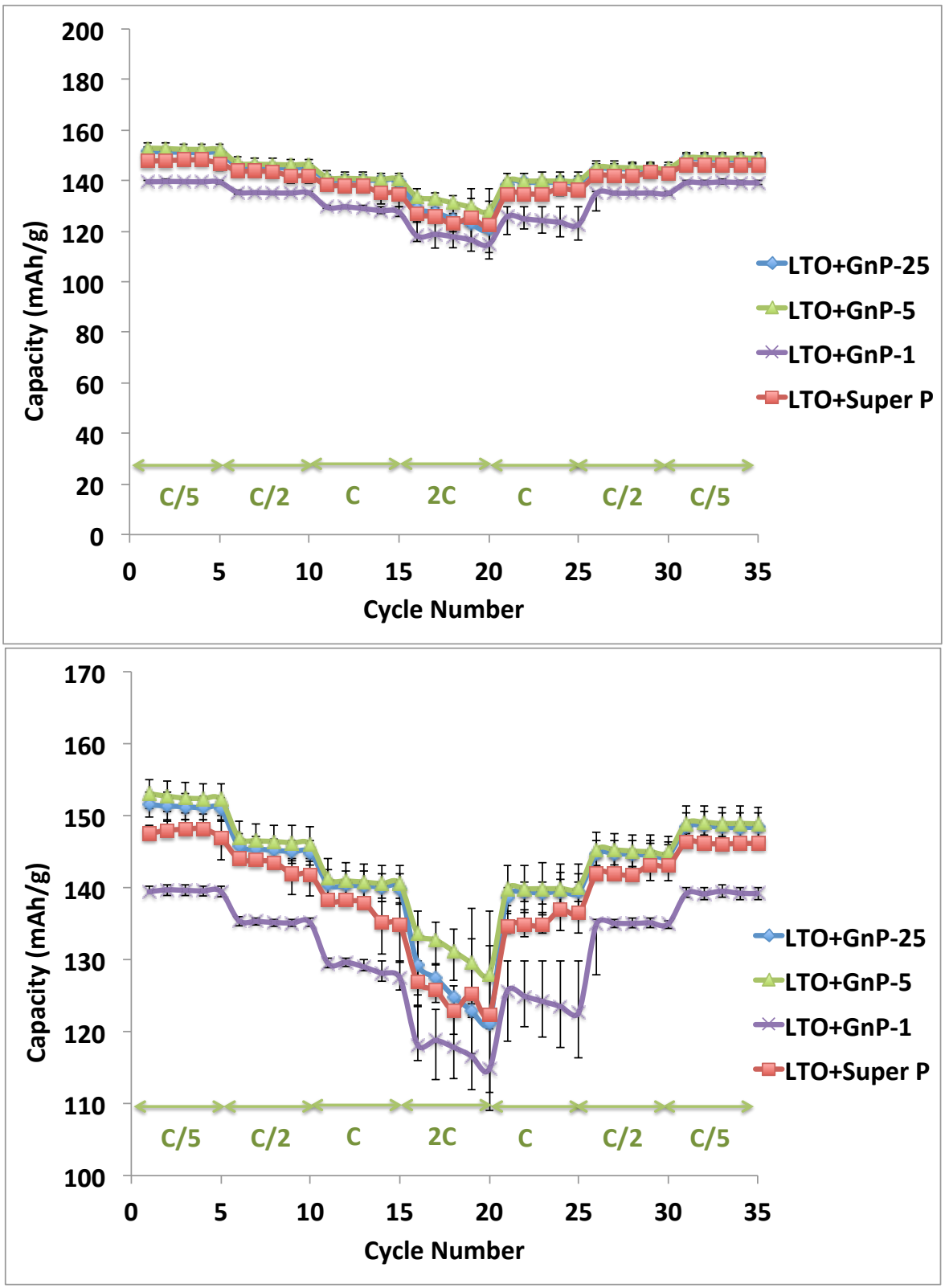

Figure 3-9: Comparison of charge-discharge performance of different LTO electrodes, with 10 wt% conducting additive on different scales

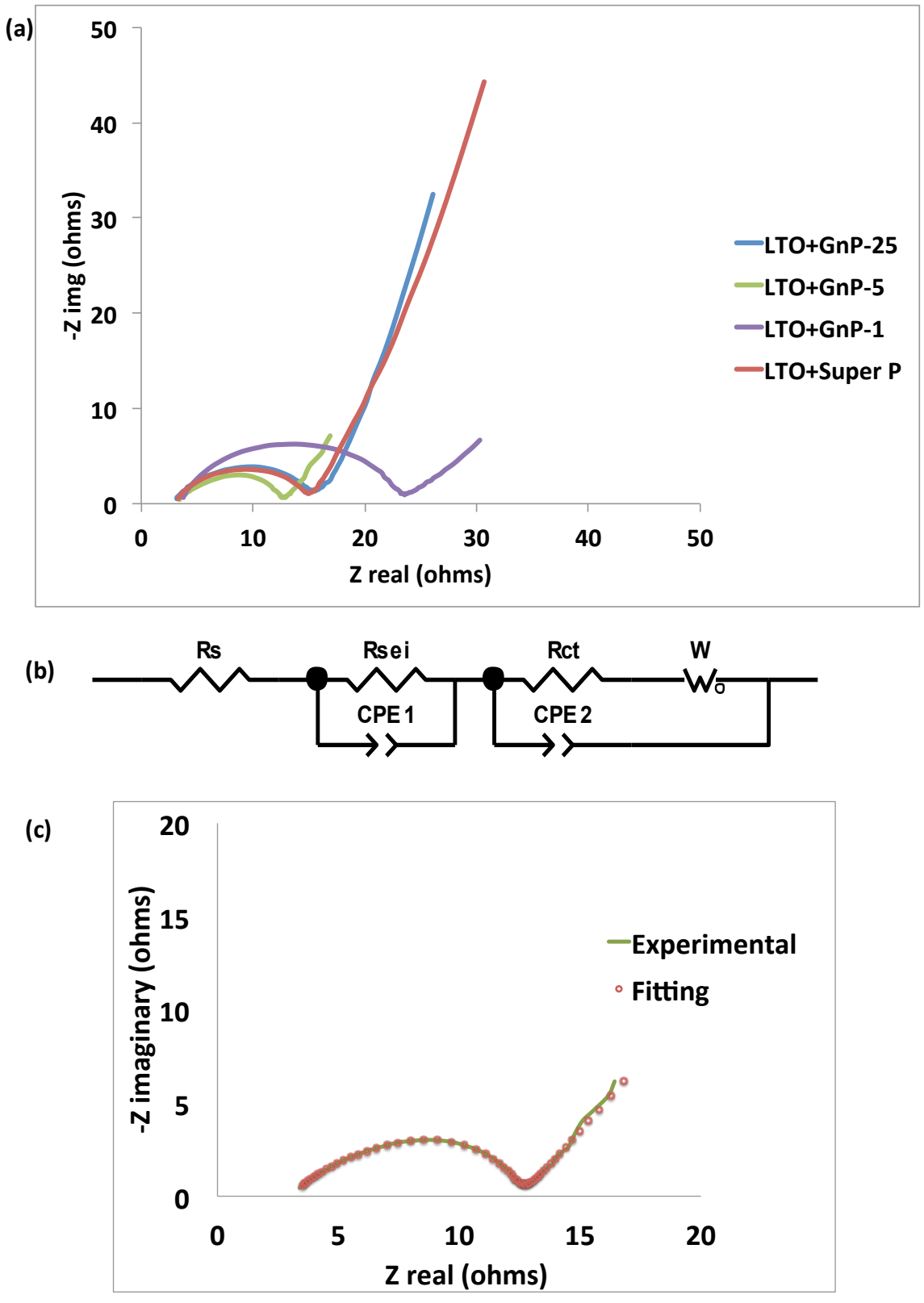

Figure 3-10: (a) Nyquist plots of different electrodes, obtained after 5 cycles at C/5 charge rate (b) Equivalent circuit used for fitting (c) Experimental vs. fitting data for LTO+GnP-5

Table 3-2: Resistance values obtained by fitting experimental impedance data to the equivalent circuit

Electrode Specifications	Rs	Rsei	Rct
LTO + GnP-25	2.8	1.1	13.2
LTO + GnP-5	3.1	3.3	6.3
LTO + GnP-1	3.2	6.1	15.7
LTO + Super P	2.8	2.2	12.7

Influence of concentration of additive

The effect of the concentration of the conducting additive on the performance of the LTO electrodes was studied. LTO electrodes with GnP-25 as the conducting additive were prepared with three different weight concentrations , viz., 2% , 5% and 10% GnP-25 in the composite electrode. The composition of binder(PVDF) was kept the same at 10 wt%. The galvanostatic performance, shown in Figure 3-12, indicates a decrease in capacity with reduced conducting additives. This phenomenon is pronounced at faster charge rates, indicating incomplete accesibility of LTO particles during cycling. The capacity data is in accordance with the imepdance behavior (Figure 3-13), which confirms the decrease in conductivity with reduced concentration of conducting additive. The resistance increases significantly with a decrease in concentration of the GnP additive. The results obtained can possibly be due to insufficient number of GnP particles dispersed through the LTO matrix, as depicted by the cross-sectional images shown in Figure 3-11.

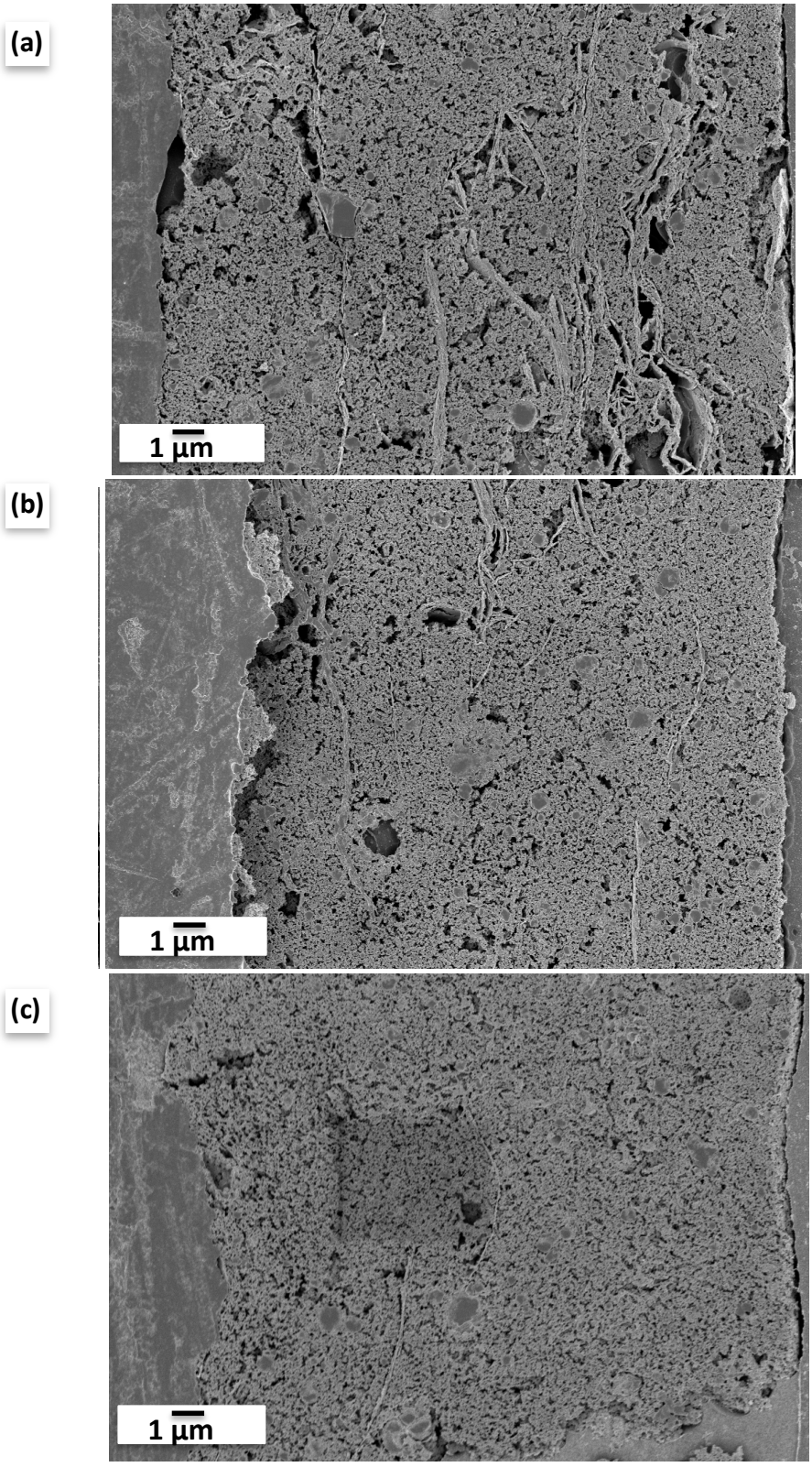

Figure 3-11: Cross-sectional images of LTO-GnP-25 electrodes, with GnP concentration (a) 10wt%, (b) 5 wt%, (c) 2 wt%

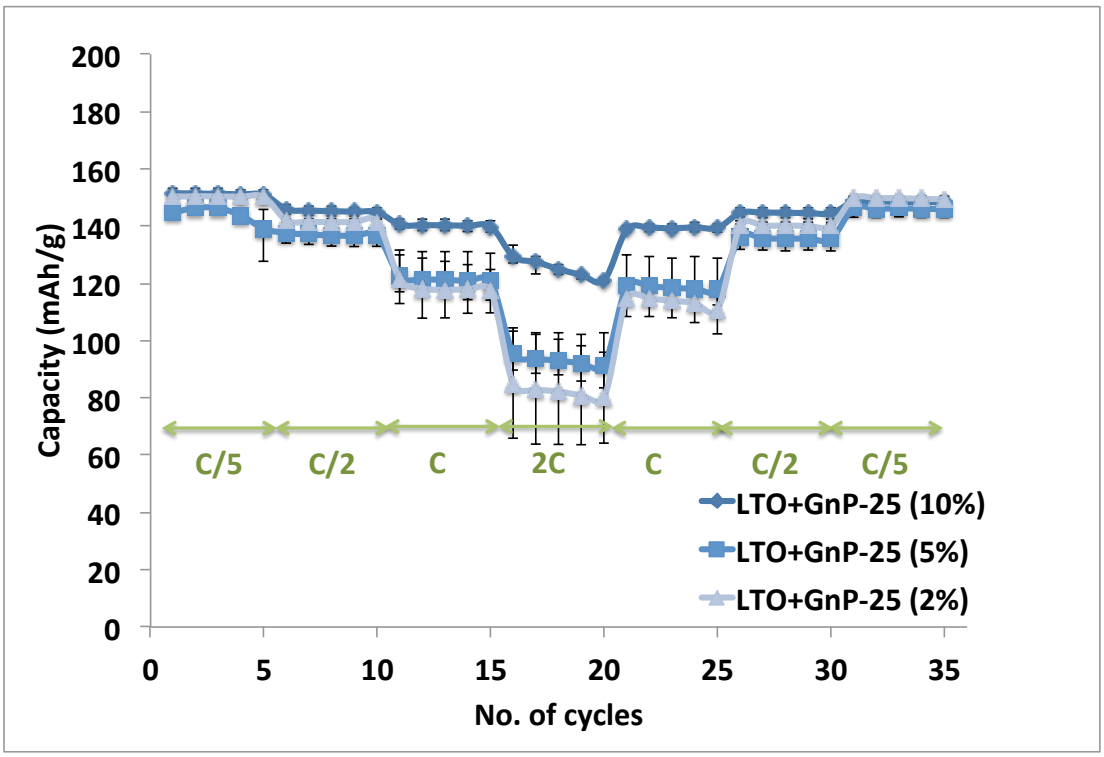

Figure 3-12:Galvanostatic performance of LTO+GnP-25 electrodes for different concentration of GnP-25 in the electrodes

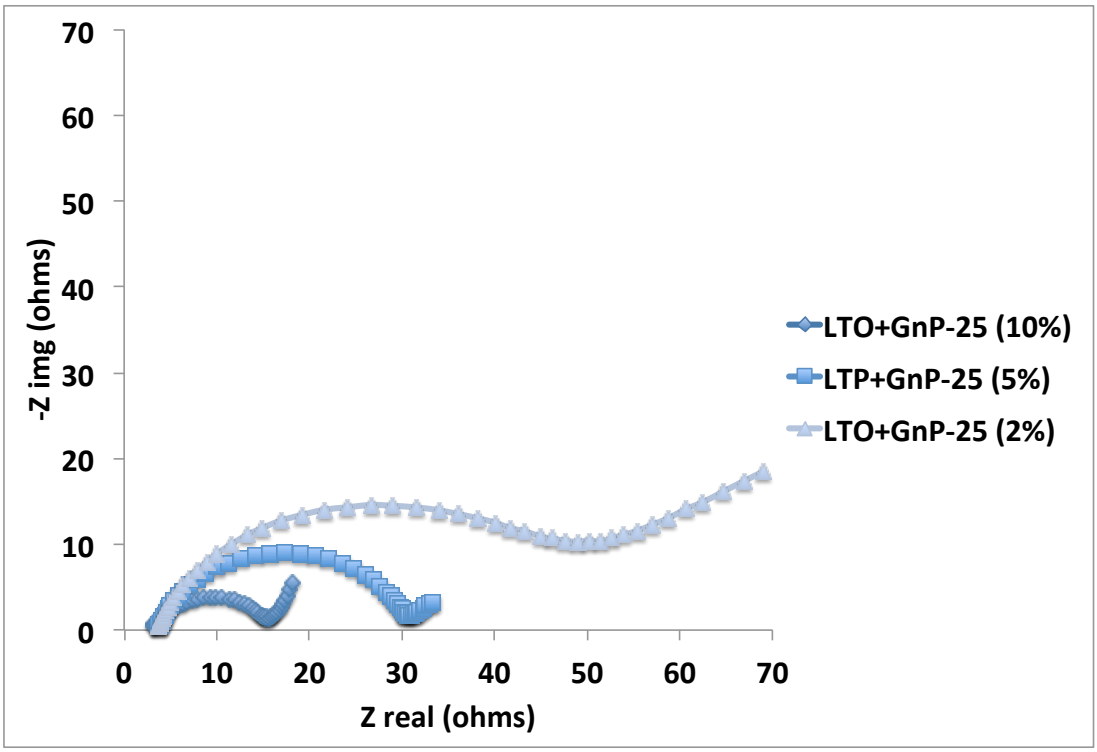

Figure 3-13: Nyquist plots of LTO electrodes with varying concentration of GnP-25

CONDUCTION MECHANISM

The morphology characteristics of the Super P and GnP are considerably different due to a huge difference in their aspect ratios, which results in obvious difference in their conduction mechanism. Su et. al [13,14] have studied the conduction models associated with Super P and graphene based conducting additives for $LiFePO_4$ (LFP) electrodes. The interaction of zero dimension Super P particles with small spherical type LFP particles results in "Point to point" contact mode of Super P-LFP electrodes. Whereas, in case of high aspect ratio, thin, and flexible graphene nanosheets as conducting additive, a 'plane to point' contact mode is proposed. The basis of their proposed mechanism is based on the top view of the electrode (top view)[14] and a 2-D simulation is done to predict the ion transport[13]. Based on the simulation results, it has been inferred that a higher concentration of graphene nanosheets can block the shortest ionic conduction path, and can thus negatively influence the rate performance[13].

A similar phenomenon is expected in the case of our LTO electrodes. The LTO material has more or less spherical particles of nano-dimensions and Super P has a spherical morphology, corresponding to aspect ratio of nearly 1, thus exhibiting 'point to point' contact interaction. However, GnP has a two-dimensional planar morphology with significantly larger aspect ratio (>100), hence interacts with LTO particles via a 'plane to point contact' mechanism. This phenomenon is demonstrated in the SEM images of the electrode morphologies shown in Figure 3-5 and Figure 3-6.

To verify and demonstrate the behavior of these materials throughout the electrode thickness, cross-sections of the electrodes was obtained by FIB sectioning. FIB milling gives us an advantage over the epoxy embedding and polishing method, since it allows us to view the sections using the backscatter electron detector (BSD), (in addition to the usual secondary electron images), thus giving meaningful information about the interaction of the two phases. The BSD images show brighter spots of LTO particles in comparison to carbon particles, because of their higher atomic number elements. These images (shown in Figure 3-14) distinctly highlight the 'point to point' and 'plane to point' contact of LTO-Super P, and LTO-GnP, respectively.

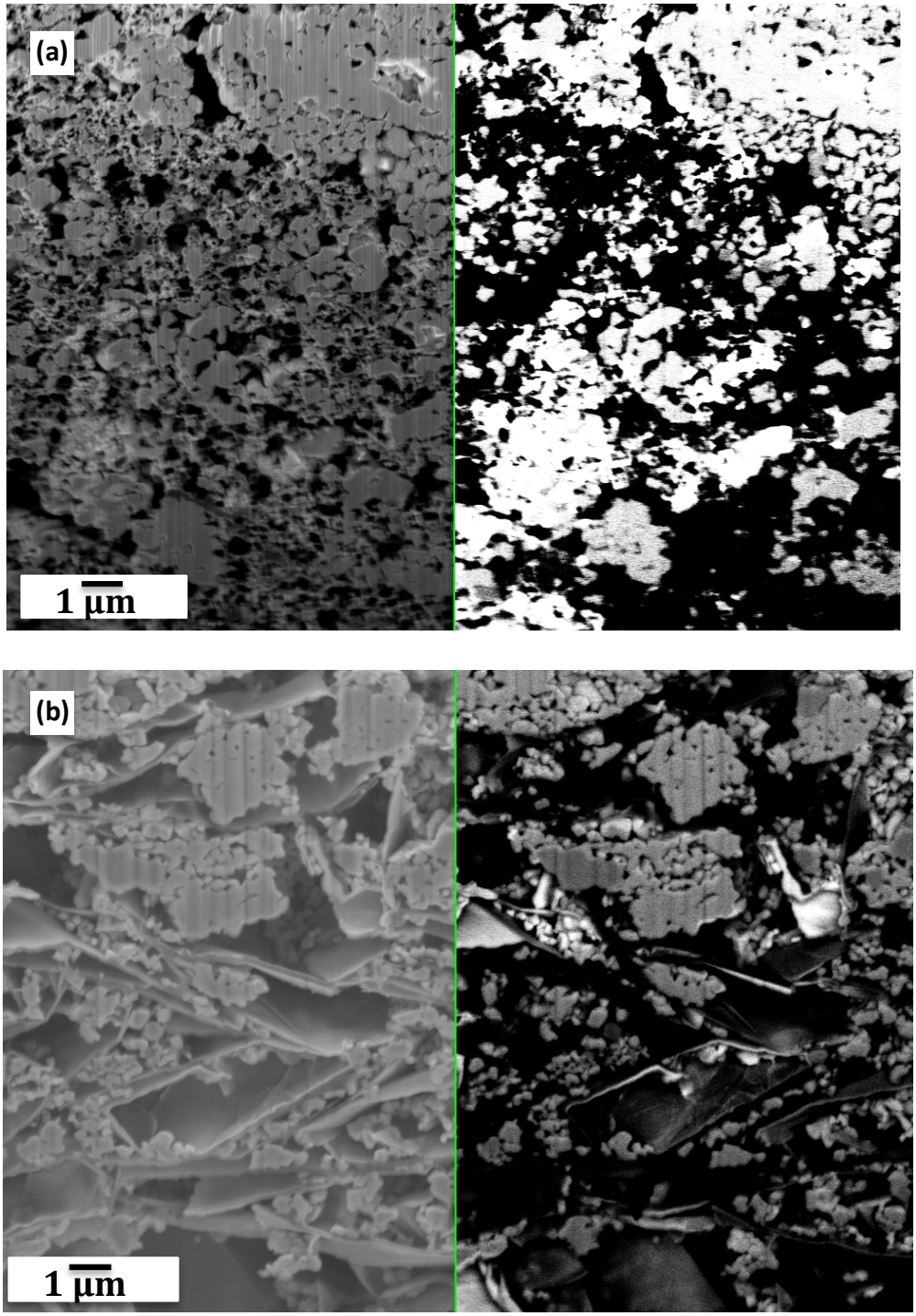

Figure 3-14: Secondary electron and back scatter electron images of (a) LTO + Super P electrodes (b) LTO + GnP electrodes

CONCLUSIONS

In summary, we have demonstrated the potential of GnP platelets as a conducting additive for low conductivity electrode materials such as transition metal compounds. The large size GnP materials such as GnP-25 and GnP-5 have shown better performance in comparison to the commercial Super P material. However, for small size GnP platelets (GnP-1), a reduction in capacity was observed which could be a result of aggregation, inhomogeneous distribution or higher particle contact resistance.

FUTURE WORK

Future work should explore improving the gravimetric performance by reducing the percentage of conducting additive used. The following approaches are suggested to achieve electrical percolation at lower weight percentage of carbon additives:

- The dispersion of GnP platelets can be improved by a pre-mixing step involving sonication of GnP in the solvent, before addition of LTO material.
- Developing hybrid electrodes with the combination of small size carbon materials (with low aspect ratio) and high aspect ratio platelets, can lead to improved capacity at certain additive concentration. The high surface area small platelets can provide good interaction contact with LTO particles, and the high aspect ratio platelets can provide overall external conductivity to the electrode. The synergistic effect of the two types of GnP platelets can be carefully optimized to obtain improved performance.

REFERENCES

REFERENCES

1. Zhu, N. *et al.* Graphene as a conductive additive to enhance the high-rate capabilities of electrospun Li4Ti5O12 for lithium-ion batteries. *Electrochemica Acta* **55**, 5813–5818 (2010).

2. Zhang, B. *et al.* Percolation threshold of graphene nanosheets as conductive additive in Li4Ti5O12 anodes of Li-ion batteries. *Nanoscale* (2010).doi:10.1039/b000000x

3. Pralong, V. Lithium intercalation into transition metal oxides: A route to generate new ordered rock salt type structure. *Progress in Solid State Chemistry* **37**, 262–277 (2009).

4. Park, J., Lee, S., Kim, S. & Kim, J. Effect of Conductive Additives on the Structural and Electrochemical Properties of Li 4 Ti 5 O 12 Spinel. *Bull. Korean Chem. Soc.* **33**, 4059–4062 (2012).

5. Bruce, P. G., Scrosati, B. & Tarascon, J.-M. Nanomaterials for rechargeable lithium batteries. *Angewandte Chemie (International ed. in English)* **47**, 2930–46 (2008).

6. Rev, A. *et al.* Materials for Rechargeable Lithium-Ion Batteries. *Annu. Rev. Chem. Biomol. Eng.* **3**, 445–471 (2012).

7. Cheng, L. *et al.* Carbon-Coated Li4Ti5O12 as a High Rate Electrode Material for Li-Ion Intercalation. *Journal of The Electrochemical Society* **154**, A692 (2007).

8. Ahn, S. High Capacity, High Rate Lithium-Ion Battery Electrodes Utilizing Fibrous Conductive Additives. *Electrochemical and Solid-State Letters* **1**, 111 (1999).

9. Guo, Y.-G., Hu, J.-S. & Wan, L.-J. Nanostructured Materials for Electrochemical Energy Conversion and Storage Devices. *Advanced Materials* **20**, 2878–2887 (2008).

10. Choi, N. *et al.* Challenges Facing Lithium Batteries and Electrical Double-Layer Capacitors. *Angewandte Chemie (International ed. in English)* **51**, 9994–10024 (2012).

11. Landi, B. J., Ganter, M. J., Cress, C. D., DiLeo, R. a. & Raffaelle, R. P. Carbon nanotubes for lithium ion batteries. *Energy & Environmental Science* **2**, 638 (2009).

12. Kang, X. *et al.* Effect of Conductive Additives and Surface Fluorination on the Electrochemical Properties of Lithium Titanate (Li4/3Ti5/3O4). *Journal of The Electrochemical Society* **157**, A437 (2010).

13. Su, F.-Y. *et al.* Could graphene construct an effective conducting network in a high-power lithium ion battery. *Nano Energy* **1**, 429–439 (2012).

14. Su, F.-Y. *et al.* Flexible and planar graphene conductive additives for lithium-ion batteries. *Journal of Materials Chemistry* **20**, 9644 (2010).

15. Shi, Y., Wen, L., Li, F. & Cheng, H.-M. Nanosized Li4Ti5O12/graphene hybrid materials with low polarization for high rate lithium ion batteries. *Journal of Power Sources* **196**, 8610–8617 (2011).

16. Wang, Q., Su, F., Tang, Z., Ling, G. & Yang, Q. Synergetic effect of conductive additives on the performance of high power lithium ion batteries. *New Carbon Materials* **27**, 427–432 (2012).

4 GRAPHENE NANOPLATELET PAPER AS CURRENT COLLECTOR

SIGNIFICANCE

For lithium ion batteries, copper is used as current collector for anode materials. This copper film, which is around 10 μm in thickness, contributes to 12% of the total weight and 5% of total cost of a high power battery (Figure 4-1)[1]. For high performance compact batteries, improvements in all components are being sought, and this need motivates the exploration of alternate current collectors, which adds less weight to the battery setup without increasing any cost.

To increase the energy density and reduce the cost contribution of the current collector, various alternatives are being explored. The approach used is generally to make self-supporting films of the anode material [2], so that there is no need for a current collector. But such technologies are restricted by the morphology and properties of the active electrode materials. It's either limited to certain kinds of materials or requires addition of conductive matrix, fillers and binders [3–5].

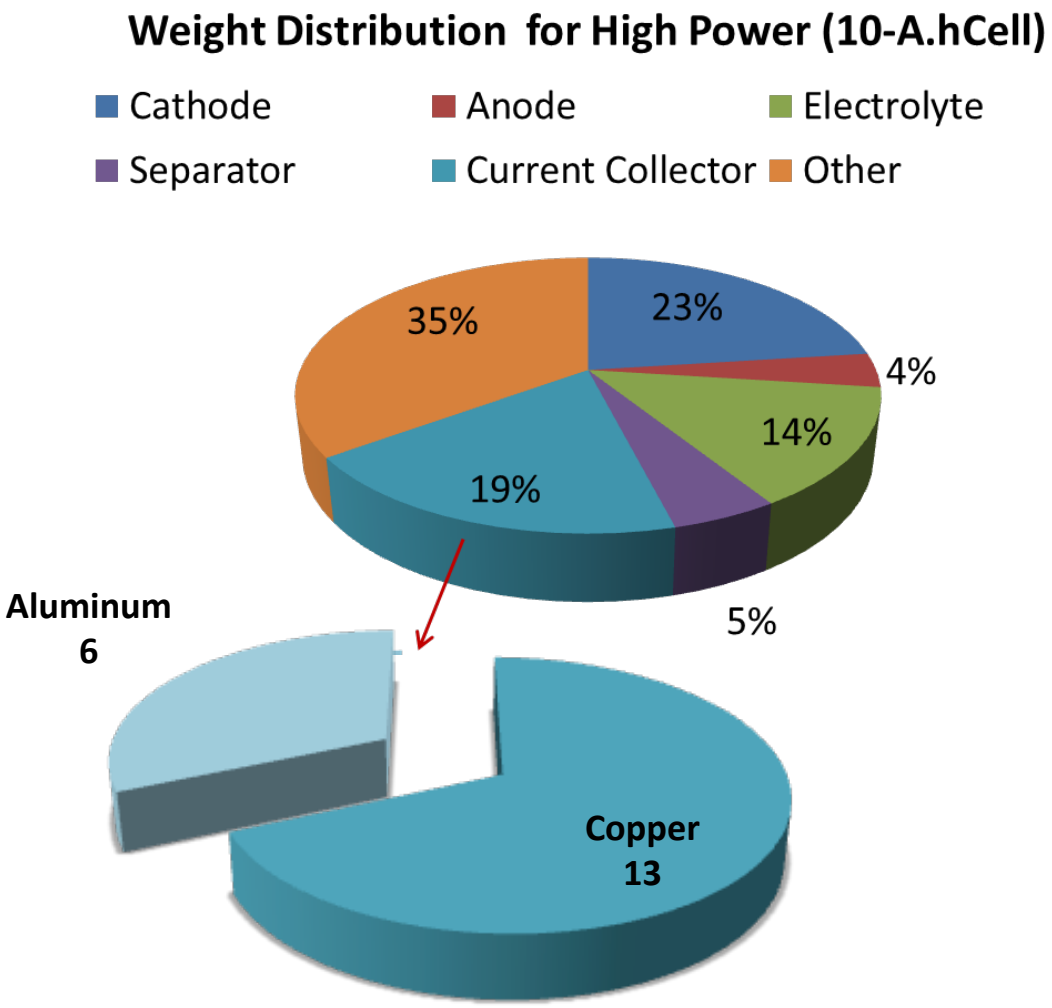

Figure 4-1 : Weight and cost distribution of different battery components for High Power Cell (based on data from Gaines et. al [1])

Figure 4-1 (cont'd)

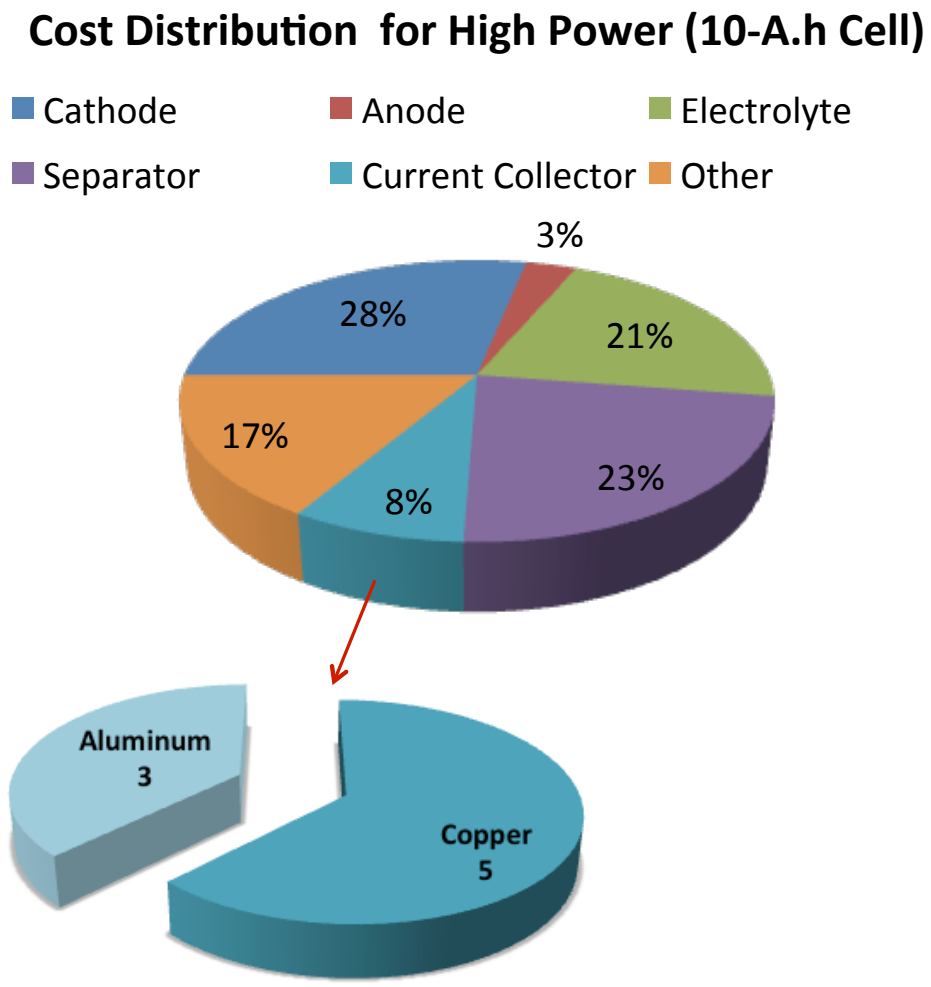

Conductive graphitic films because of their low density, low price, high electrical and thermal conduction, good chemical and thermal stability, conformability and flexibility, find its use in numerous electrochemical applications such as supercapacitors[2,6,7], fuel cells[8], sensors[5], lead acid cells and DSSC counter electrodes[9]. For lithium ion batteries, conducting graphitic films have enormous potential for its use as current collector owing to its excellent electronic transport, good adhesion to active materials, and conformability. Copper has a

density of 9 g/cc while graphene has a density of ~2 g/cc. In addition to being lightweight and flexible, graphitic films are known to have comparable thermal conductivity to copper, which will ensure fast heat dissipation avoiding thermal build up during high charging conditions.

Graphitic current collectors are a perfect choice of current collector for anode materials, due to inherent lithium storage capability of carbon, in addition to the other properties mentioned above. With this concept in mind, the potential of commercial Grafoil flexible graphite sheet has already been explored as anode material and current collector[10]. Carbon nanotube films (Bucky paper and others) are a popular choice for self-standing electrodes, composite films [11] and current collector supports[7,12,13]. CNT films are low density and have good properties and have found widespread use in capacitors[7], lithium ion batteries[7,11,13–15]. However the complex synthesis and high cost associated of CNTs can restrict their commercial viability and utilization. Also, there have been literature evidence showing that carbon fiber based papers have advantages over copper current collectors, particularly for tin based and silicon based anode systems[4]. These systems, specifically the ones involving heat treatment on cast electrodes, face a problem of flaking material off of copper electrodes due to a significant difference in coefficient of thermal expansion between copper and the coated material. Using carbon or graphitic current collectors has resolved this problem by capitalizing on the similar coefficient of thermal expansion of the electrode material with carbon papers. Use of carbon fiber mats (by Toray and Pyrograf CFs) as current collector[16,17] owing to enhanced electronic transport, thermal management and better adhesion has been shown.

APPROACH

Our approach involves the use of GnP Paper synthesized by a simple method involving filtration of an aqueous GnP suspension[18]. This self-standing film of nanostructured graphene nanoplatelets (GnP) is known to have low density, reasonable mechanical strength[18] and good electrical[18] and thermal conductivity[18,19] , thus making it a promising candidate for the role of current collector. In comparison to copper, it's a lightweight material, less expensive and has good adhesion to most common anode materials (carbon based). Furthermore, the technology proposed here offers more versatility and has several advantages as listed below:

- GnP paper is a self- sustaining current collector which has the desired electrical conductivity with significantly less areal density
- GnP paper has inherent lithium storage capability and hence contributes to energy density, thus reducing the dead weight
- This paper can also be used as current collector for other electrode materials and other electrochemical systems

EXPERIMENTAL SECTION

GNP PAPER SYNTHESIS

The self standing flexible GnP paper is prepared by a simple filtration process starting with an aqueous suspension of GnP as shown in Figure 4-2 [18]. GnP was dispersed in an aqueous solution with the aid of Polyethyleneimine (PEI) as a dispersing aid in the weight ratio of GnP:PEI:Water=1:1:1000. Then the dispersed solution is filtered using a Durapore 0.65 μm

filter paper, and washed with deionized water to remove excess PEI. After filtration, the paper is dried under ambient condition, peeled off from the filter paper and then annealing at 340 °C to eliminate residual PEI from the paper. The GnP paper can be compressed to any level to control porosity and thickness.

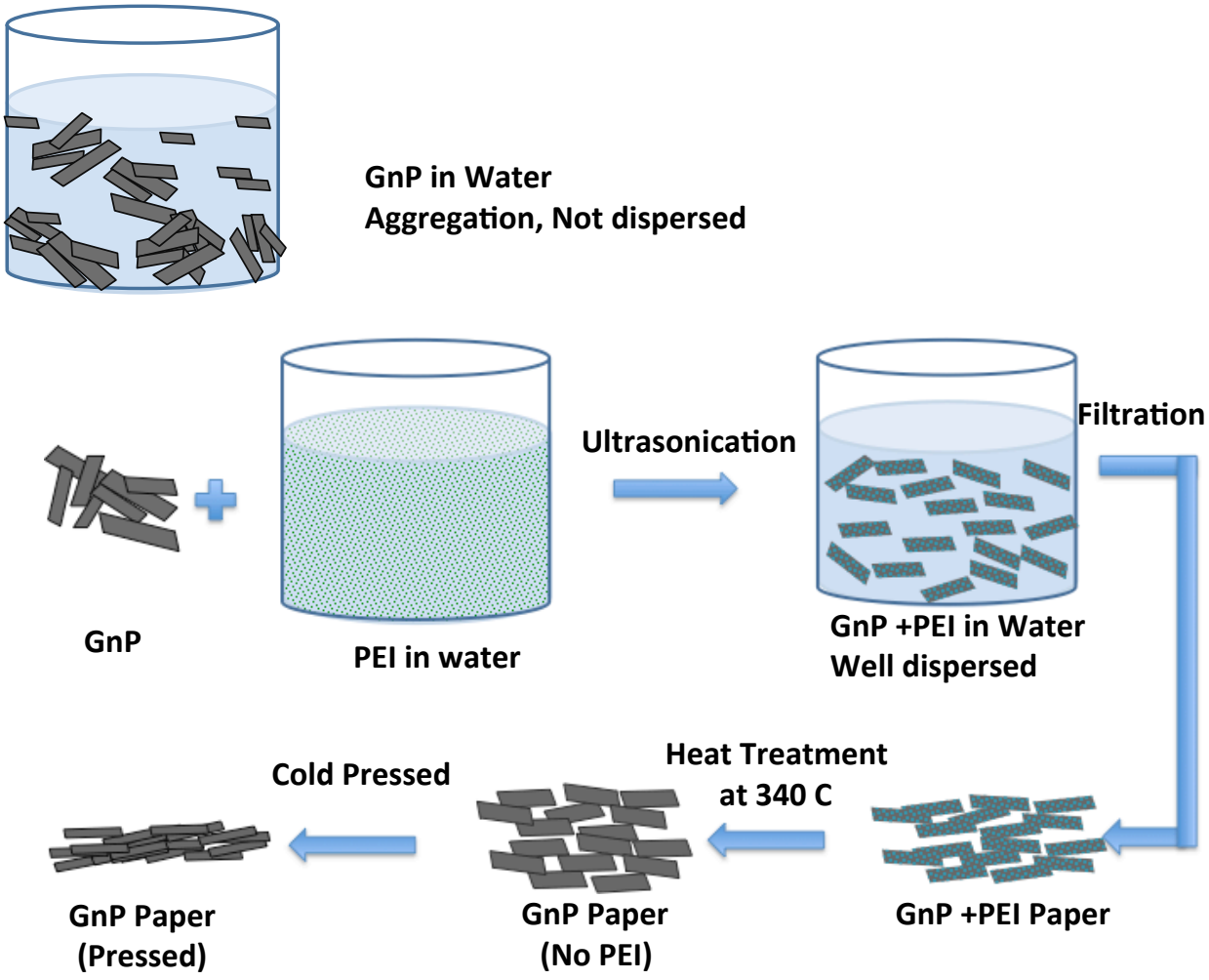

Figure 4-2: Schematic illustrating the synthesis of GnP Paper

ELECTRODE PREPARATION

For evaluating the performance of GnP paper as current collector, electrodes of different active materials viz. GnP-15 and Lithium Titanate (LTO) were investigated. The electrodes were prepared by coating the slurry of active anode material with N-Methyl-2-pyrrolidone and 10 % PVDF as the binder, using a microfilm applicator on an automatic electrode coating instrument. The electrodes were cast on two different current collectors, viz. the Cu foil and GnP Paper. For LTO Electrodes, Super P was used as a conducting additive in the proportion of 10 wt %.

MORPHOLOGY OBSERVATION

To understand the interaction of electrode materials with the current collector and to evaluate the quality of electrodes, an assessment of electrode morphology was done by observing the material distribution in both the top-view and cross-sectional view. The GnP paper and GnP electrode samples for cross- section observation were prepared by an epoxy mounting and polishing procedure (described before). The LTO samples were prepared by FIB milling procedure using Carl Zeiss Auriga® CrossBeam) instrument.

PROPERTIES

The electrical conductivity of GnP paper was measured with a 4-probe conductivity method, using the Keithley 2400 Source Meter. GnP paper was cut into thin strips of 4 cm X 1 cm and 4 probes having 1 cm spacing were pressed into the surface of the paper to make the resistance measurement.

The tensile strength of the paper was measured at 0.1 % min^{-1} strain rate using TA Instruments Dynamic Mechanical Analyzer (DMA Q 800) with the film tension clamp.

ELECTROCHEMICAL CHARACTERIZATION

The anode material was tested in a three-electrode half-cell Swagelok setup (for GnP electrodes) or Coin cell setup (for LTO) with ethylene carbonate-dimethyl carbonate-lithium hexafluorophosphate as electrolyte and lithium foil as counter and reference electrodes. The relative loading of active material on the electrode was kept around 4-5 mg/cm2. Fundamental performance characterization at different charge rates was done to assess the response of this electrode. The protocol adopted to evaluate the performance at different charge rates is the same as explained in Section 2.3.3. The galvanostatic cycling was done at different rates every 5 cycles, keeping the rate same for both charge and discharge. Charge rate C corresponds to a charge or discharge rate equal to the theoretical capacity of a battery in one hour.

Electrochemical Impedance measurements were also done on the GnP electrode on different substrates viz., GnP paper and copper as current collectors. For EIS studies, coin cells with lithium foil as counter electrode were used. This setup was preferred over three electrode Swagelok T-cell setup to avoid any manual errors. AC impedance spectroscopy was obtained by applying a sine wave of 5mV amplitude over a frequency range of 100 KHz to 0.01 Hz.

RESULTS & DISCUSSIONS

GNP PAPER

GnP paper is a binder-free self-standing, flexible and porous paper prepared by a simple filtration process using aqueous suspension of GnP [18]. This paper can be made in controlled porosities (ranging from 30-90 %) and thickness (ranging from 3 microns to several hundred microns) using different sizes of GnP materials. This GnP paper has very good electrical conductivity, which ranges from 500-2000 S/cm depending on the size of platelets, porosity and thickness of paper. Figure 4-3 below shows the cross-sectional morphology of GnP paper at different magnifications. As can be seen from the high magnification images, the paper is a very ordered network of GnP platelets having a high degree of in-plane alignment with GnP particles connected together to produce good electrical conductivity.

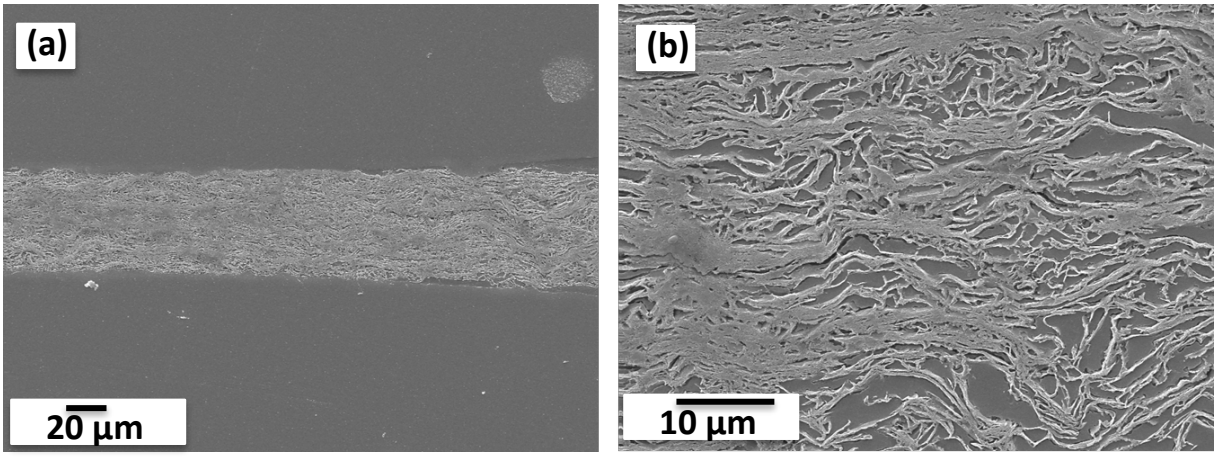

Figure 4-3: SEM Images of the GnP paper (as made) at different magnifications

GNP ELECTRODE ON GNP PAPER

Figure 4-4 below shows the SEM images, at different locations and magnifications, of the cross-section of electrodes of graphene nanoplatelets of 15 µm diameter on GnP Paper as current collector by the procedure described above.

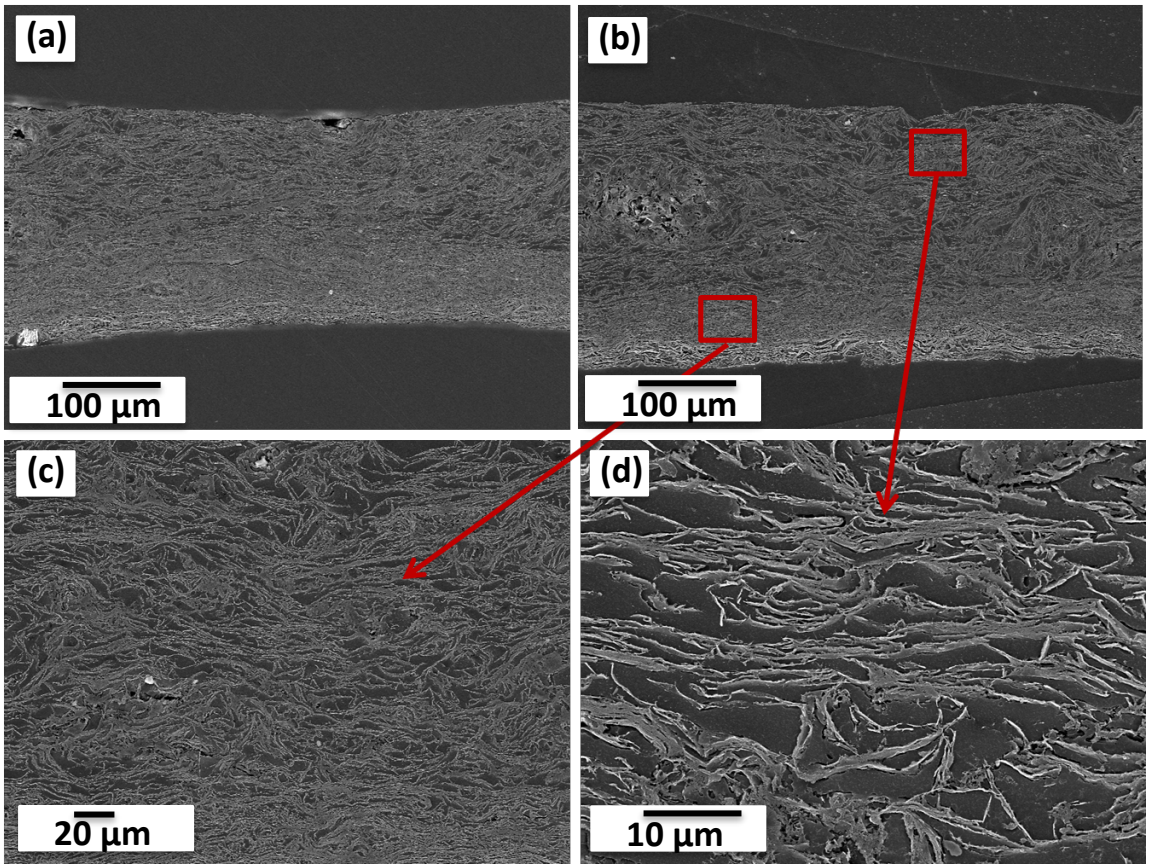

Figure 4-4: Cross-sectional SEM Images of the electrode at different magnifications (a) & (b), followed by high mag images of (c) GnP paper (d) active material region

From the cross-sectional SEM images, we can see that there is good adhesion between the GnP paper and the electrode material coated on top of it. The actual junction between the GNP current collector and the anode is not easily differentiated indicating the high degree of compatibility between the two components. The high-resolution images shown in Figure 3(c) and (d) show that the morphology of both the paper and electrode active material indicating a

highly porous well-arranged network, although the GnP paper is more compacted dense than the electrode coated above it, which is the result of the preparation procedure.

For electrochemical testing, the electrodes were pressed at 0.1 MPa to produce the controlled porosity. SEM images in Figure 4-5 below show the changes that the GNP paper morphology undergoes in the process of electrode coating, and battery anode fabrication.

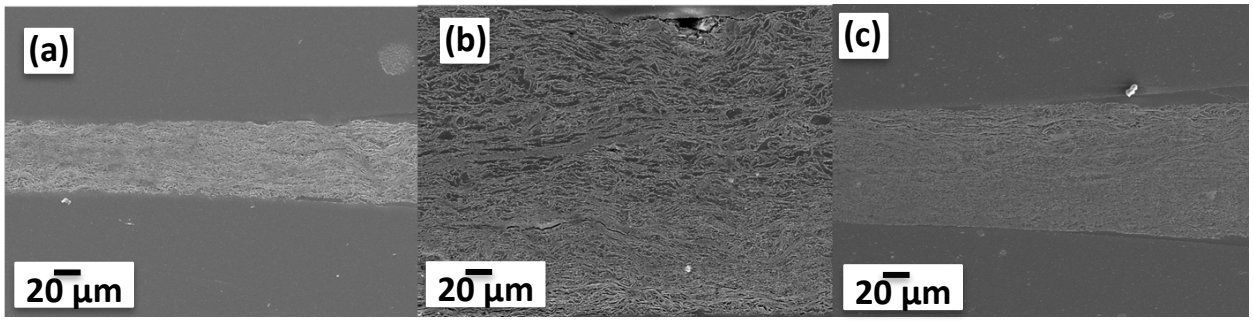

Figure 4-5: SEM images of X-sectional view of (a) current collector GnP paper, GnP electrode on GnP current collector (b) the unpressed and (c) pressed electrode

COMPARISON OF GNP PAPER AND COPPER AS CURRENT COLLECTORS

Figure 4-6 below shows the comparison of electrode made by GnP-15 as active material on two different substrates, viz. copper and GnP Paper. We can clearly observe that the adhesion of electrode material is better to the GnP paper in comparison to the copper foil.

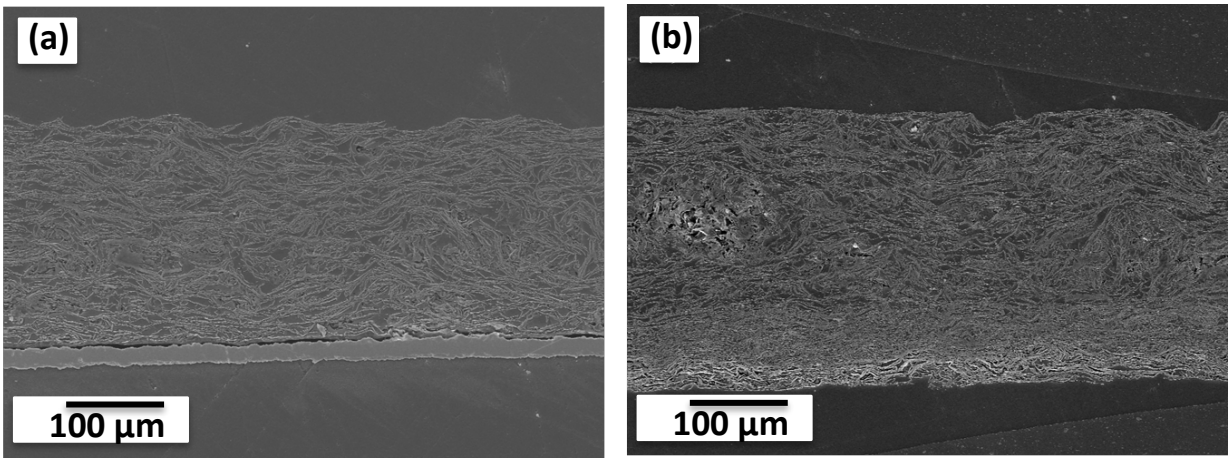

Figure 4-6: SEM images showing cross-sectional view of GnP-15 electrode on different current collectors: (a) Copper (b) GnP paper

Figure 4-7 shows the performance of GnP electrode casted on Cu foil at different charge rates. The results of the electrochemical performance for the GnP electrode on GnP paper as current collector are shown below in Figure 4-8, calculated based on the weight of just the active material coated on GnP paper (Figure 4-8(a)) and also using the complete weight including that of GnP paper (Figure 4-8 (b)). As expected, GnP paper itself contributes towards lithium storage; hence calculations based on weight of active material indicate exceptional performance. However, in a real system, considering the weight of GnP paper as a contribution to electrode weight, the storage capability is similar to GnP electrode on Cu foil. However, over long cycling, the lithium storage capacity of the material is not completely utilized. This can be attributed to incomplete access of material at very high loading 7-8 mg/cm2. Also, there is a higher irreversible capacity loss in the first cycle for electrodes with GnP paper as current collector. This can be a consequence of increased SEI layer formation due to higher surface area available. The performance at faster charge rates is relatively slower due to restricted ion diffusion.

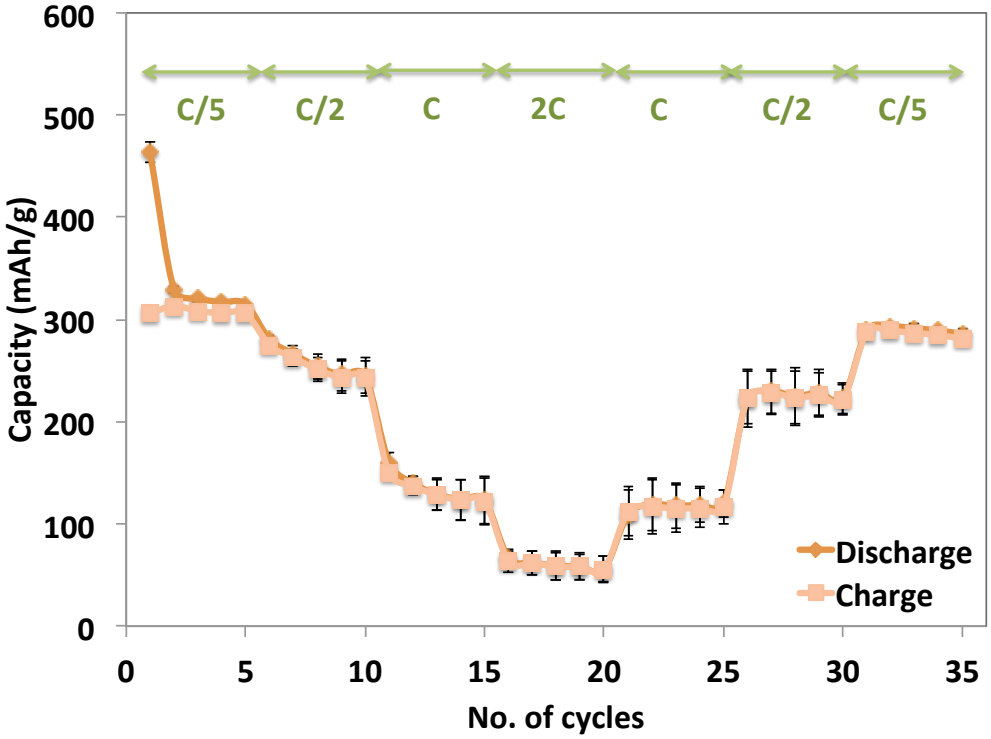

Figure 4-7: Galvanostatic Performance of GnP-15 electrode on Copper current collector

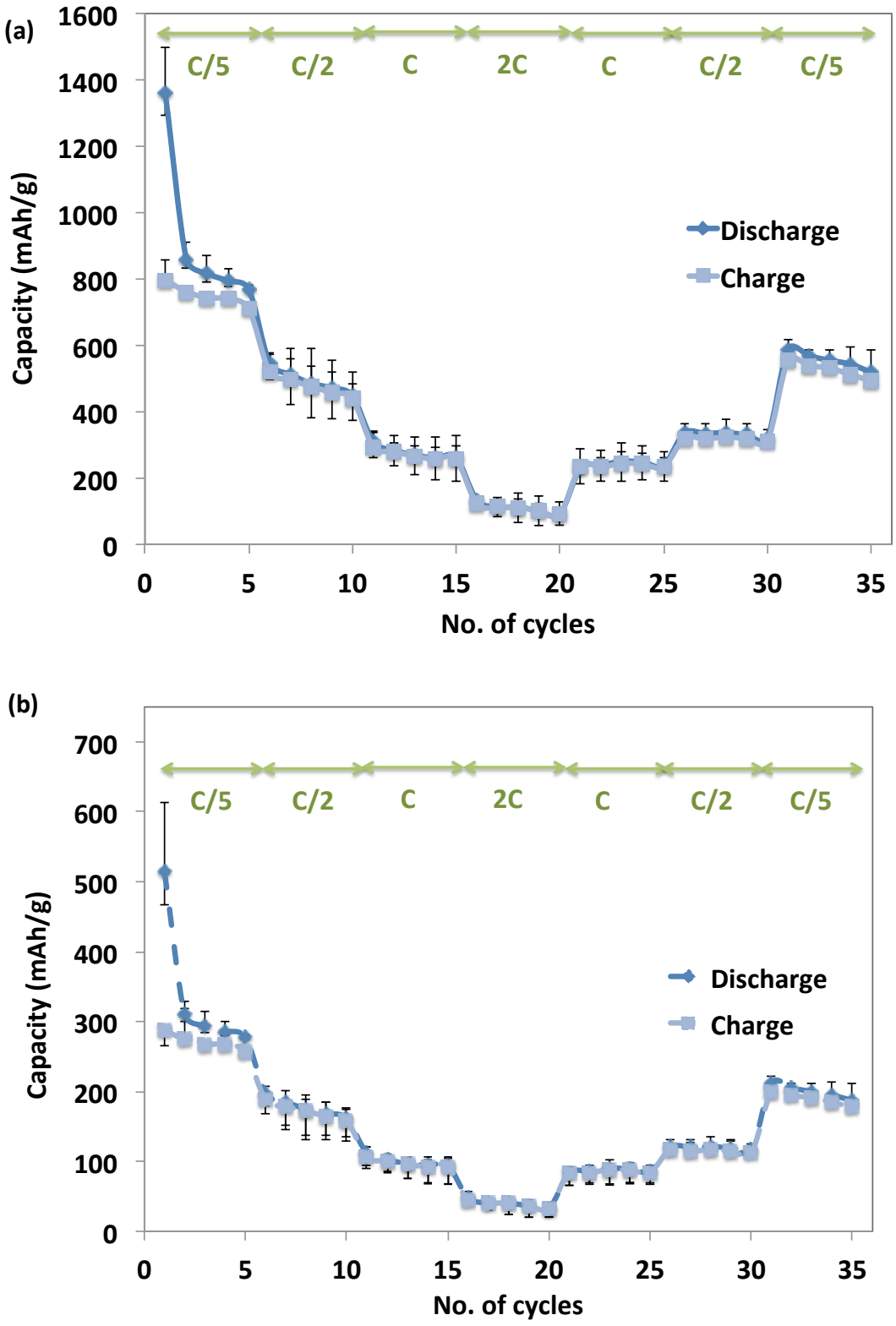

Figure 4-8: Galvanostatic Performance of GnP-15 electrode on GnP paper current collector (a) Active material (b) Total weight including the substrate weight of GnP paper

Electrochemical Impedance Spectra

Electrochemical impedance spectroscopy (EIS) was done to evaluate the resistances involved in the system. Figure 4-9 shows the EIS data of the GnP electrodes made on Copper and GnP paper as current collector after 10 complete charge discharge cycles. The bulk resistance (R_s), corresponding to the intercept on the x-axis, is a combination of electrolyte ionic resistance, intrinsic resistance of electrode materials and the contact resistance of the active material and current collector[20]. The two depressed semi-circles at high and medium frequencies are associated with the resistances due to SEI layer formation (R_{sei}) and charge transfer (R_{ct}). The inclined line at low frequencies is attributed to the diffusion of lithium ions in the electrodes.

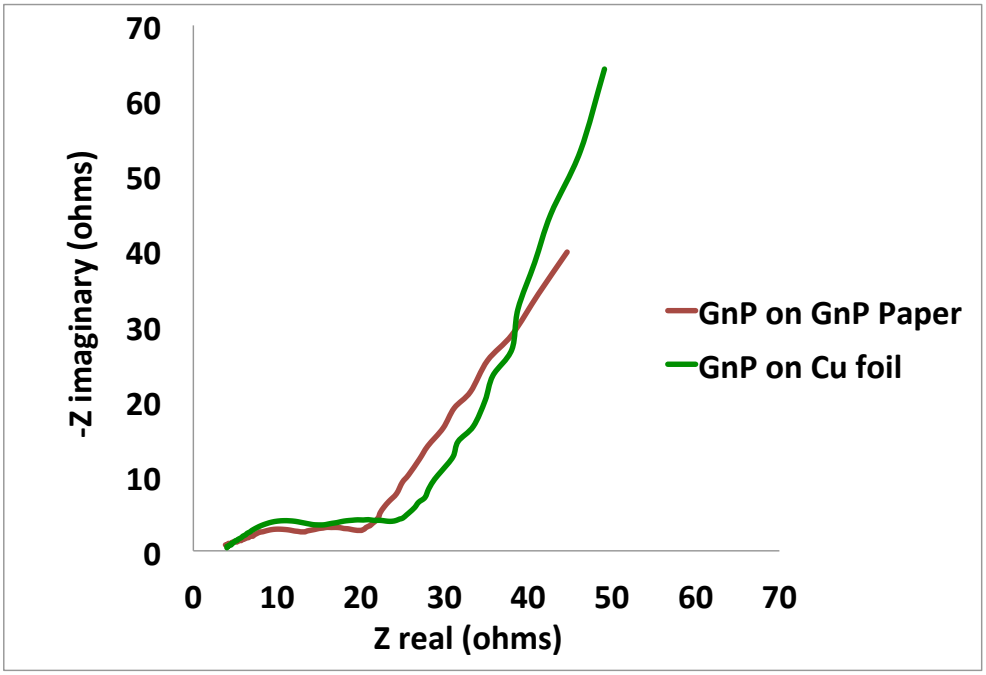

Figure 4-9: Nyquist plots of GnP electrode on different current collectors: Copper foil and GnP Paper, after 10 complete charge discharge cycles

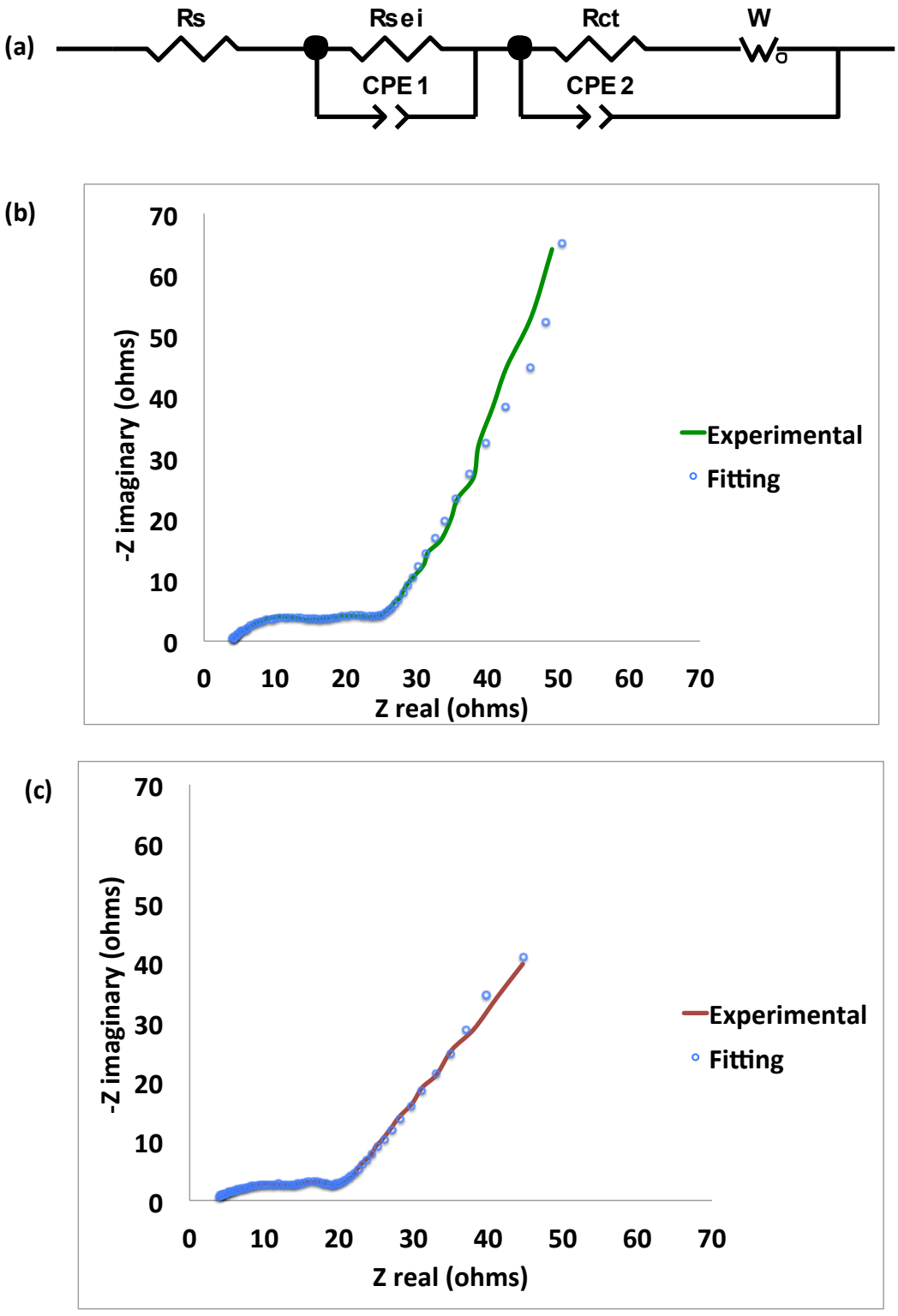

Figure 4-10: (a) Equivalent circuit for fitting of impedance data; Comparison of experimental and fitted data for (a) GnP electrode on Cu foil after 10 cycles (c) GnP electrode on GnP Paper after 10 cycles

Table 4-1: Resistance values obtained by parametric fitting of impedance data

	Rs	Rsei	Rct
GnP on Cu foil-10cyc	3	14	8
GnP on GnP Paper-10cyc	3	15	6

The experimental impedance data was fitted with the Z view software using the equivalent circuit shown in Figure 4-10 (a). The–data calculated with the equivalent circuit model fits the experimental data well as can be observed in Figure 4-10 (b) and (c). The estimated resistance parameters obtained from this analysis are summarized in Table 4-1. We can see that no significant difference in the values of resistances was observed in the two electrodes, which is a clear indication that GnP paper as a current collector has good interaction with the active material and hence demonstrates comparable performance to copper foil.

LITHIUM TITANATE (LTO) ELECTRODE ON GNP PAPER

The use of these GnP Papers as current collector is not restricted to carbon based anode materials, and this was verified by using it as current collector for Lithium Titanate (LTO) anode material. The electrodes were cast by coating NMP based slurry by similar procedures as described above. The cross-sectional morphology of the electrode was compared by cutting the cross-section using FIB and was compared as shown in Figure 4-11.

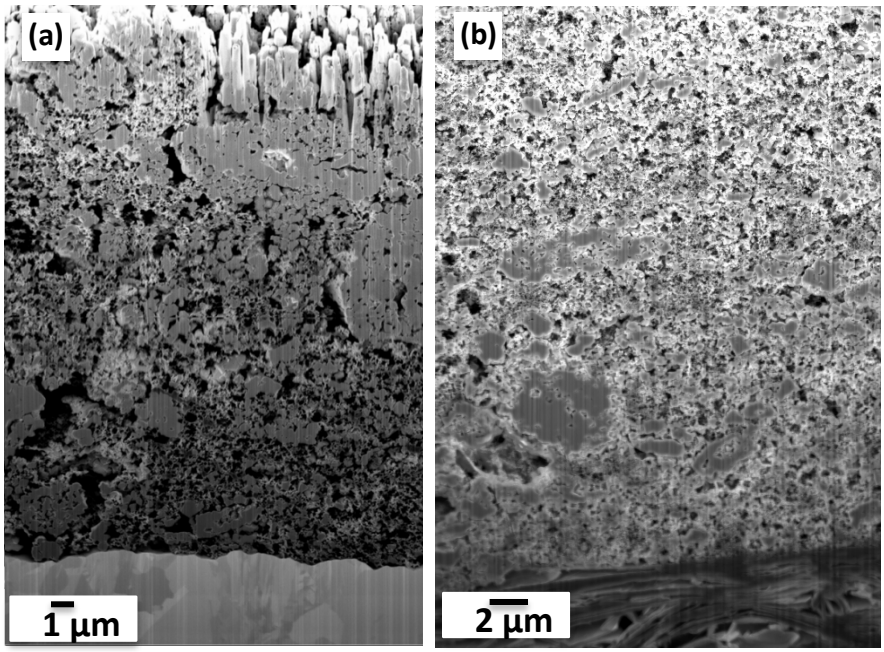

Figure 4-11: SEM images showing cross-sectional view of LTO electrodes on different current collectors (a) On copper (b) On GnP Paper

The analysis below in Figure 4-12 compares the electrochemical performance of LTO electrodes cast on copper foil vs. GnP Paper. From this we can observe that the GnP paper performs very well with LTO as anode material, in fact slightly better than the electrode made on copper. Such an improvement can be a consequence of improved conduction due to better adhesion of electrode with current collector thus providing good electronic conductivity.

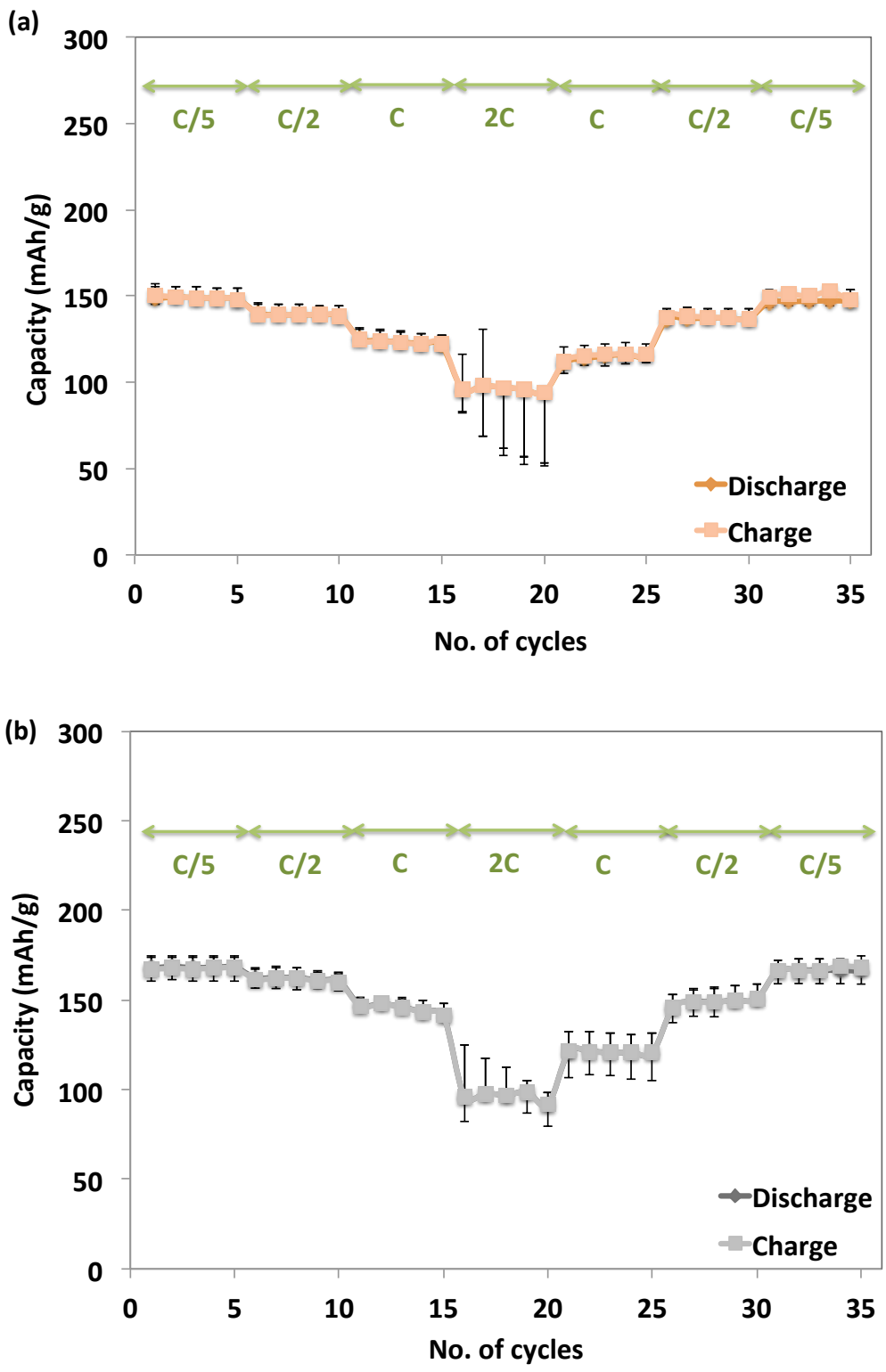

Figure 4-12: Electrochemical Performance of LTO electrodes casted on different current collectors (a) On copper (b) On GnP Paper

This analysis with a non-graphitic anode material operates above the potential range in which carbon gets involved in any interaction with lithium. The results clearly demonstrate the diversity in the use of GnP Paper as current collector even in situations where it has no active electrochemical role to play.

UNIQUE GNP ELECTRODE ON C VEIL

A unique approach was adapted to make a GnP electrode on an Optimat® carbon veil, a lightweight C mat. These carbon veils are 140 µm in thickness and have an electrical conductivity of 12 S/cm and tensile strength of 6.5 MPa. Figure 4-13 below shows the optical microscope images of the C veil, from which we can see that the diameter of the fibers are <10 µm and the veil is highly porous with empty spaces of the order of 50-100 µm. The electrical conductivity of as received C veil was measured at different conditions to ensure that there will not be a degradation of C veil during electrode preparation procedure.

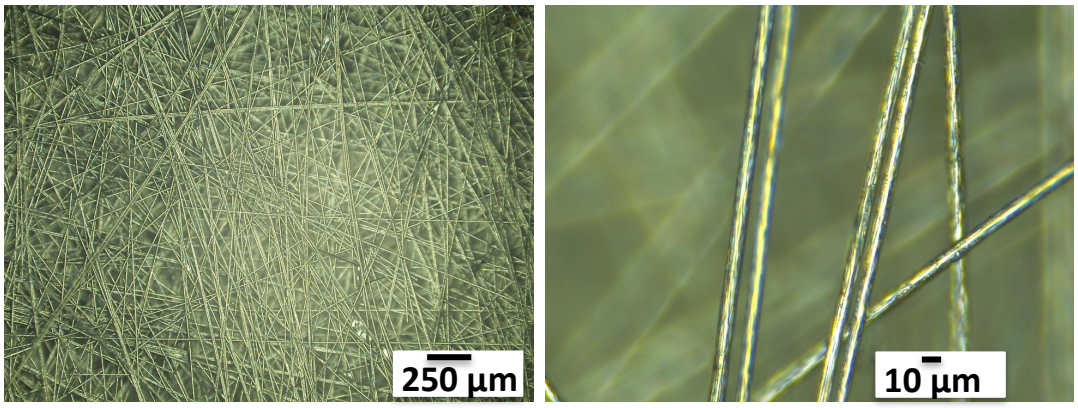

Figure 4-13: Optical Images of the Optimat® carbon veil

The GnP electrode on C veil was prepared by the same methodology as GnP paper synthesis. The carbon veil was placed as a second filter in addition to the Durapore filter paper,

and an aqueous suspension of GnP:PEI:Water was filtered. The GnP collects on the C veil and forms the GnP-veil electrode. The electrode was repeatedly washed with water and then heat treated at 340 °C to remove PEI (the dispersion agent). The electrode was further pressed in the Carver press to achieve good compaction. Figure 4-14 and Figure 4-15 below show the pictures and SEM images of the unpressed and pressed electrodes, respectively. The SEM images show that the GnP penetrates through the veil structure and forms a well-distributed interconnected network. Also, we can observe, that on pressing the uncovered C veil area (the edges) degrade, however, the central portion stay intact. This is possibly due to the mechanical strength imparted by GnP to the C veil structure.

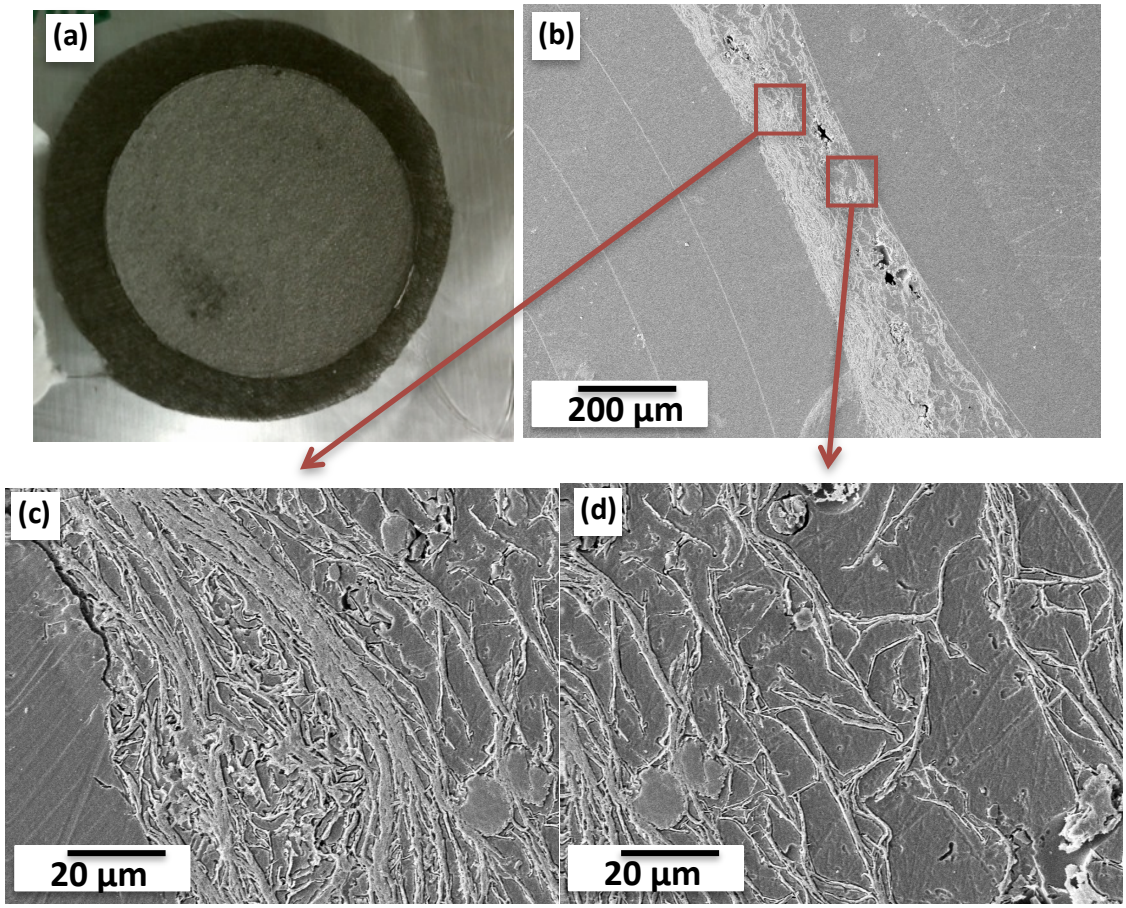

Figure 4-14: (a) Picture and (b),(c),(d) SEM Images of unpressed GnP electrode on C veil as current collector

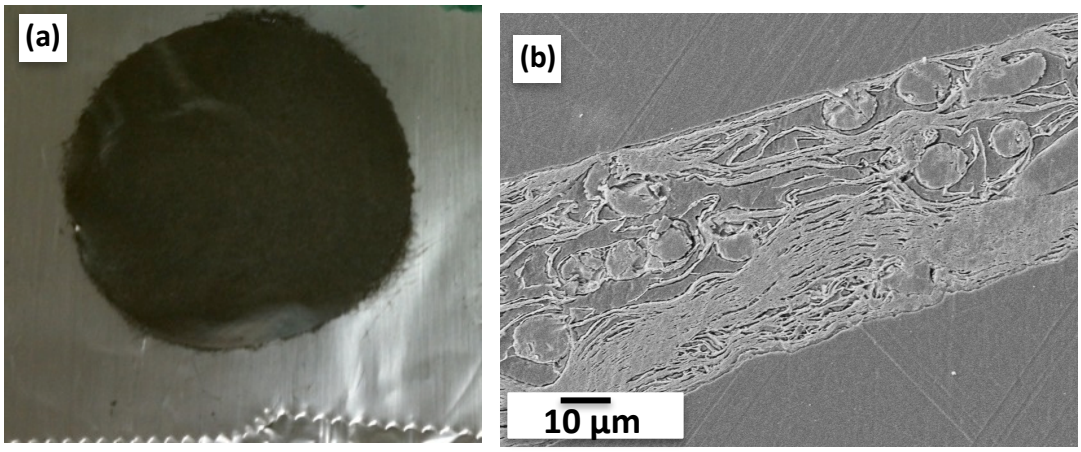

Figure 4-15: (a) Picture and (b) SEM Images of pressed GnP electrode on C veil as current collector (Scale bar- (b): 10 µm)

ELECTROCHEMICAL PERFORMANCE

Electrochemical measurements of this electrode was done in the three electrode Swagelok setup with Li foil as counter and reference and 1M $LiPF_6$ in EC-DMC (1:1v/v) as the electrolyte.

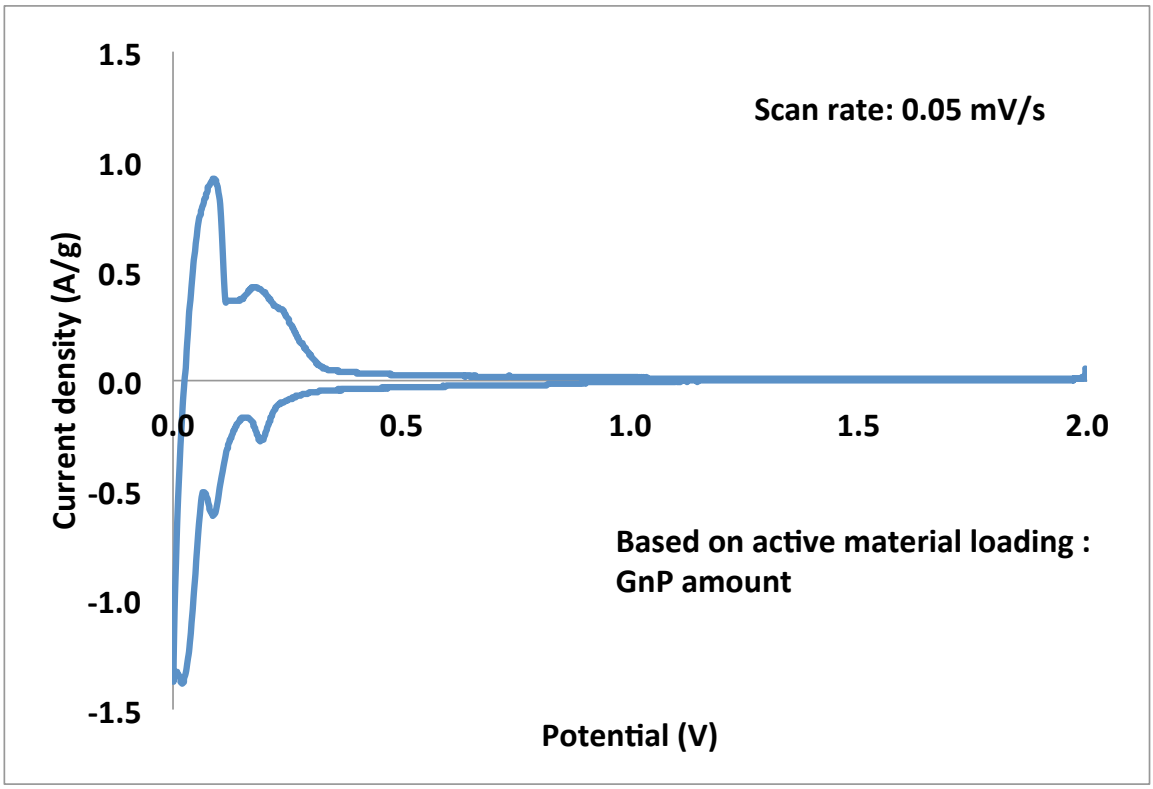

Figure 4-16: Cyclic Voltammogram (third sweep) of GnP on C veil

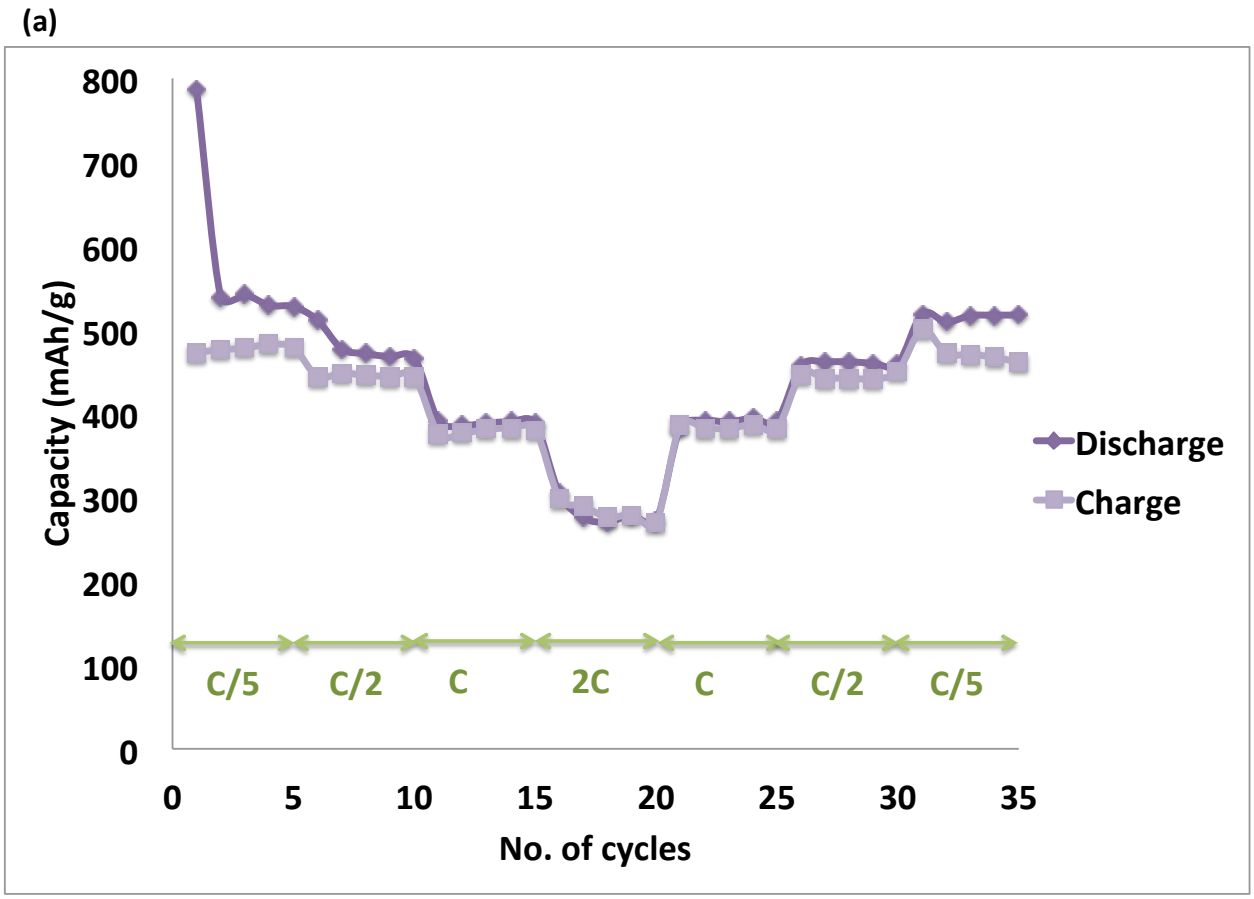

Figure 4-17: Galvanostatic Performance of GnP on C veil electrode (a) based on active electrode material (b) based on complete weight

Figure 4-17 (cont'd)

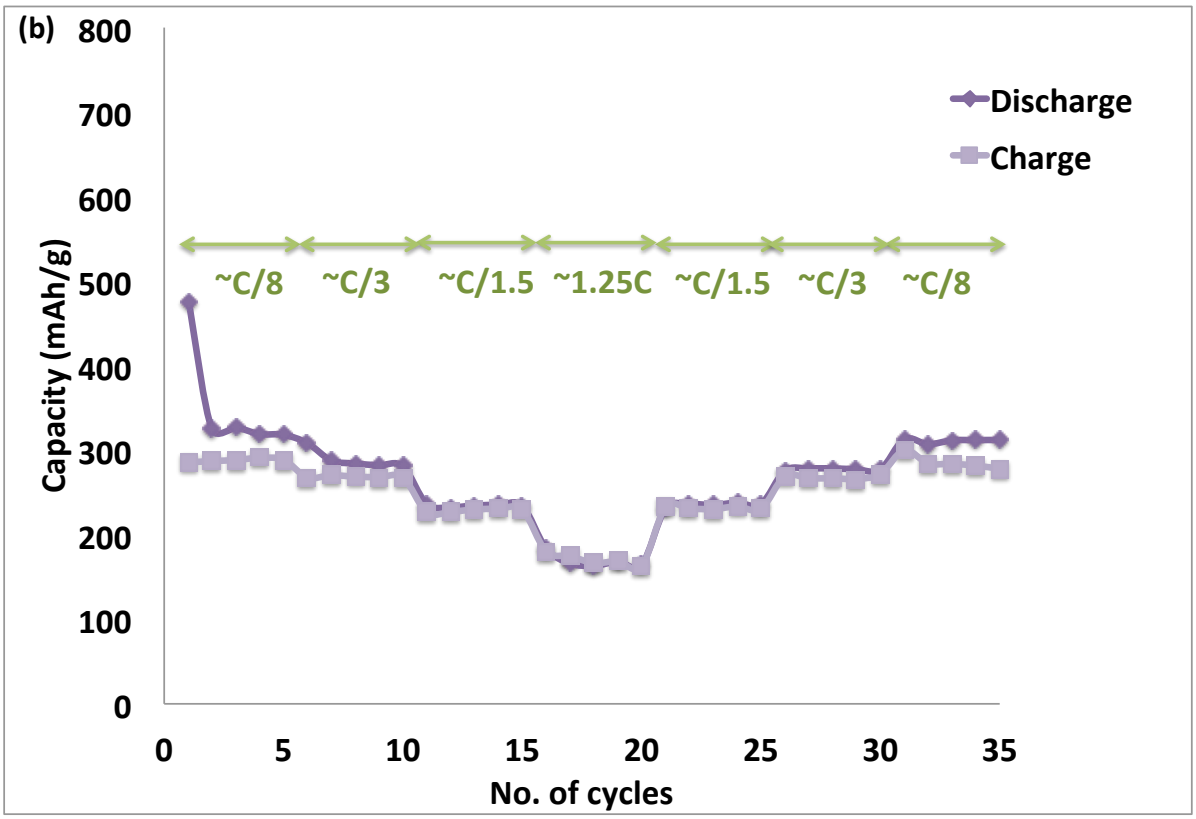

The cyclic voltammogram done at a scan rate of 0.05 mV/s shows the typical carbon intercalation peaks, as shown in Figure 4-16. The galvanostatic performance was done at different charge rates (Figure 4-17), and the capacity based on active material GnP's weight (excluding the C veil weight), was found to be around 450 mAh/g at C/5 charge rate. The additional contribution to lithium capacity is coming from the electrochemical activity of the C veil, which itself is participating in the lithium intercalation-deintercalation process. When the capacity calculations were done with complete electrode weight in mind (GnP+C veil), we see the expected performance of ~310 mAh/g at C/5 charge rate

In summary the GnP-C veil electrode has significant advantages as a lightweight current collector, and improved gravimetric energy density. However, the C veil as current collector has drawbacks of significantly low electrical conductivity and may have some electrode fabrication and processing challenges.

CONCLUSIONS

We have demonstrated, that the GnP paper has the potential to replace copper as current collector and can impart electrical conductivity to the anode material. Based on performance data, it can be asserted that GnP Paper can match and potentially replace the use of copper as current collector. Table 4-2 shows the relative comparison of properties of the two current collectors.

Table 4-2: Comparison of properties of copper foil and GnP paper as current collectors

Properties	Copper Current Collector	GnP Paper Current Collector
Areal density	8.6 mg/cm^2	4.3 mg/cm^2
Electrical Conductivity	8*10^5 S/cm	750 S/cm
Tensile Strength	70 Mpa (Yield)	2.85+/- 0.30 MPa

FUTURE WORK

GnP paper has immense potential as a possible alternative to the currently used copper current collector and will increase the energy density of the battery. The same GnP paper can also be used to eliminate aluminum foil as a current collector for cathodes. Although it has lower conductivity in comparison to its metal foil counterparts, it appears to be capable of

functioning equally well as a current collector. In addition, the use of a GnP based current collector current can eliminate the corrosion associated with metal current collectors, and hence might allow the usage of more aggressive electrolytes.

GnP paper can be easily made as a continuous product with easily scalable and well-established techniques commonly used in paper industry. Since the cost of GnP itself as raw material is very reasonable, and the economics of paper processing methods are optimized, the commercialization of GnP paper can be a feasible alternative to metal based current collector.

The thickness of GnP paper can be easily reduced to around 10 microns, and that should account for around ~75% reduction in weight. However, there are certain challenges that should be addressed, particularly in terms of its mechanical strength and ductility to allow its versatility for industrial scale continuous, roll-to-roll and calendaring processes commonly used in battery fabrication. Also, improvement of conductivity of these papers and improved diffusion through the GnP paper can provide additional benefits for the use of GnP papers as current collectors

To address some of the challenges and further improve the performance, following approaches can be adopted:

i. Mechanical properties of the GnP paper can be modified by selective use of a polymeric binder to make the GnP paper robust enough to be inserted as a replacement for copper foil in current electrode and battery fabrication processes. However the selection of polymeric materials will be restricted based on their reactivity with the electrolyte. Other methodologies involve making polymer-GnP paper composites by

making laminates or cofiltration of co-suspended polymer binder powders or fibers followed by sintering without negatively affecting the lithium extra storage capability provided by the GnP papers itself.

ii. Another way of handling the problem of mechanical strength can be to have the GnP paper supported on another robust and flexible but sacrificial film. Such films will make the processability of GnP paper more feasible, particularly during the electrode preparation and calendaring process, and can eventually be dissolved, etched or peeled off before its assembled into a battery setup. There is a literature report verifying this concept, in which CNT coating on paper has resulted in flexible current collectors [7].

iii. Incorporating GnP paper with additional carbon nanomaterials or metal nanoparticles to improve the conductivity of the paper aiming at improving its performance as a current collector in electrochemical energy storage systems. Also, GnP paper can be coated with metal nanoparticles on one side to get extra conductivity as is done in case of polymeric films for current collector[21].

Based on our results and the scope of further improvements, the GnP paper can be customized to suit its use with varied materials for different applications. Hence, we can foresee the potential of GnP paper for diverse electrochemical applications such as lithium-sulfur, lithium-air or electrochemical capacitors.

REFERENCES

REFERENCES

1. Gaines, L. & Cuenca, R. Costs of Lithium-Ion Batteries for Vehicles. *Energy* **48**, 73 (2000).

2. Futaba, D. O. N. N. *et al.* Shape-engineerable and highly densely packed single-walled carbon nanotubes and their application as supercapacitor electrodes. *Nature materials* **5**, 987–994 (2006).

3. Gowda, S. R. *et al.* Three dimensionally engineered porous silicon electrodes for Li ion battery. *Nanoletters, **12***, 6060-6065 (2012).

4. Guo, J., Sun, A. & Wang, C. A porous silicon–carbon anode with high overall capacity on carbon fiber current collector. *Electrochemistry Communications* **12**, 981–984 (2010).

5. Xiao, F. *et al.* Growth of Metal – Metal Oxide Nanostructures on Freestanding Graphene Paper for Flexible Biosensors. *Adv. Funct. Mater.* (2012).doi:10.1002/adfm.201200191

6. Wang, S., Pei, B., Zhao, X. & Dryfe, R. a. W. Highly porous graphene on carbon cloth as advanced electrodes for flexible all-solid-state supercapacitors. *Nano Energy* (2013). doi:10.1016/j.nanoen.2012.12.005

7. Hu, L. *et al.* Highly conductive paper for energy-storage devices. *PNAS* **106**, (2009).

8. Zhang, H. & Hsing, I.-M. Flexible graphite-based integrated anode plate for direct methanol fuel cells at high methanol feed concentration. *Journal of Power Sources* **167**, 450–454 (2007).

9. Chen, J. *et al.* A flexible carbon counter electrode for dye-sensitized solar cells. *Carbon* **47**, 2704–2708 (2009).

10. Yazici, M., Krassowski, D. & Prakash, J. Flexible graphite as battery anode and current collector. *Journal of Power Sources* **141**, 171–176 (2005).

11. Marschilok, A., Lee, C., Subramanian, A., Takeuchi, J. & Takeuchi, E. S. Carbon nanotube substrate electrodes for lightweight , long-life rechargeable batteries. *Energy Environ. Sci.* ***4***, 2943–2951 (2011).doi:10.1039/c1ee01507a

12. Hu, L., Wu, H., Mantia, F. La, Yang, Y. & Cui, Y. Thin, Flexible Secondary Li-Ion Paper Batteries. *ACS Nano* **4**, 5843–5848 (2010).

13. Wang, K. *et al.* Super-Aligned Carbon Nanotube Films as Current Collectors for Lightweight and Flexible Lithium Ion Batteries. *Advanced Functional Materials* **23**, 846–853 (2013).

14. Lashmore, D. S., Schauer, M. W., Gurau, M. & Dev, B. CNT Current Collectors for Advanced Automotive Batteries. *Available from http://www.speautomotive.com/SPEA_CD/SPEA2012/pdf/NN/NN3.pdf*

15. Hu, L. *et al.* Silicon-conductive nanopaper for Li-ion batteries. *Nano Energy* **2**, 138–145 (2013).

16. Kercher, a. K., Kiggans, J. O. & Dudney, N. J. Carbon Fiber Paper Cathodes for Lithium Ion Batteries. *Journal of The Electrochemical Society* **157**, A1323 (2010).

17. Martha, S. K., Kiggans, J. O., Nanda, J. & Dudney, N. J. Advanced Lithium Battery Cathodes Using Dispersed Carbon Fibers as the Current Collector. *Journal of The Electrochemical Society* **158**, A1060 (2011).

18. Wu, H. & Drzal, L. T. Graphene nanoplatelet paper as a light-weight composite with excellent electrical and thermal conductivity and good gas barrier properties. *Carbon* **50**, 1135–1145 (2012).

19. Xiang, J. & Drzal, L. T. Thermal conductivity of exfoliated graphite nanoplatelet paper. *Carbon* **49**, 773–778 (2011).

20. Gamby, J., Taberna, P. ., Simon, P., Fauvarque, J. . & Chesneau, M. Studies and characterisations of various activated carbons used for carbon/carbon supercapacitors. *Journal of Power Sources* **101**, 109–116 (2001).

21. Yun, J. H. *et al.* Low Resistance Flexible Current Collector for Lithium Secondary Battery. *Electrochemical and Solid-State Letters*, **14** (8) 116-119 (2011).

5 GRAPHENE NANOPLATELETS AS A CONDUCTING TEMPLATE FOR LITHIUM-SULFUR BATTERIES

BACKGROUND

The current Lithium ion batteries are suffering from technological challenges to cater to the increasing high power energy and power demands, for applications such as electric vehicles. Though there are several anode materials, which can deliver high capacity, the main roadblock has been to develop high performance cathode materials. Lithium-sulfur batteries offer a promising solution due to high theoretical capacity of sulfur cathode (1680 mAh/g) with additional benefits of low cost, non-toxicity and ample availability. However, their applicability has been restricted due to challenges faced by different components, which have been discussed in detail in the introduction.

The Lithium-sulfur battery typically consists of a sulfur cathode, combined with binder and conducting carbon material, and lithium metal anode. The electrolyte used is generally a non-aqueous system, and current research focuses on use of solid electrolytes. These batteries are based on the redox reaction mechanism for conversion of Sulfur (S_8 molecule) to Li_2S, delivering a potential of 2.2 V vs. Li^+/Li^0 .

$$S_8 + 16\mathrm{Li} \rightleftharpoons 8\mathrm{Li}_2\mathrm{S}$$

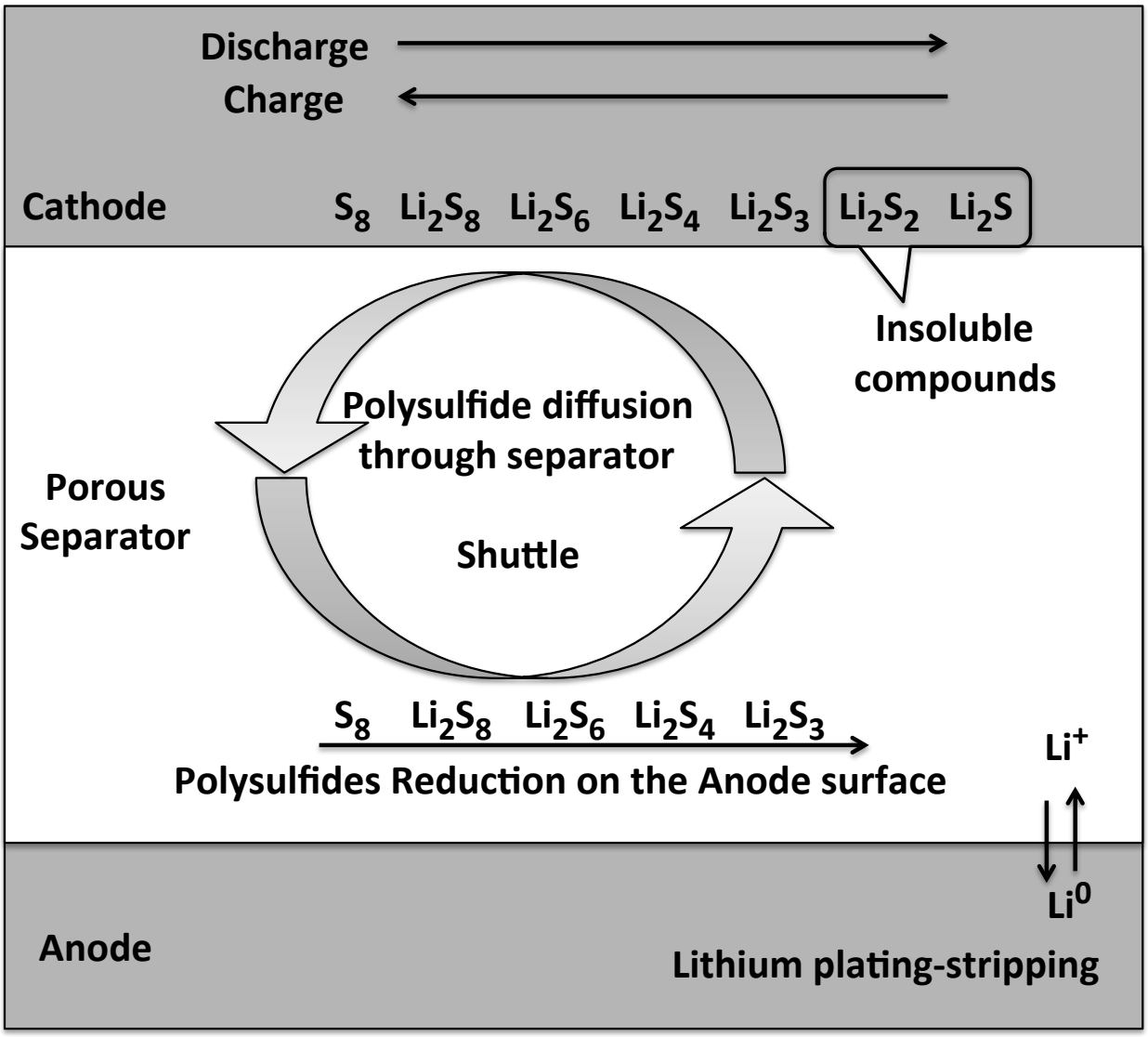

Figure 5-1: Schematic showing the working of Lithium-Sulfur Battery [1]

POLYSULFIDE SHUTTLE

Polysulfide shuttle phenomenon is a concentration driven repeated transfer of polysulfides between cathode and anode, due to solubility of high order polysulfides in the liquid electrolyte (shown in Figure 5-1). This shuttle mechanism leads to capacity fade and loss of active electrode area when the reaction proceeds to form insoluble and insulating Li_2S. The

different reactions involved in polysulfide shuttling have been explained in detail by Liu et. al,[2] and are summarized below:

Cathode- Electrochemical Oxidation

The sulfides and disulfides get oxidized to form high order polysulfides, at the cathode.

$$2\,S^{2-} + \,S_2^{2-} \rightleftharpoons S_h^{2-} \, + xe^-$$

Anode- Chemical Reduction

The soluble high order polysulfides, which are soluble in the electrolyte, diffuse to the anode and react with lithium to form low-order polysulfides.

$$(\,\mathrm{h} - \mathrm{x})S_h^{2-} + \,2xLi^0 \,\rightleftharpoons\, \mathrm{h}S_{h-x}^{2-} + \,2xLi^+$$

Cathode- Electrochemical Oxidation

The low order polysulfides formed at the anode, then shuttle back to the cathode and get oxidized to form high order polysulfides.

$$\mathrm{h}S_{h-x}^{2-} \,\rightleftharpoons (\,\mathrm{h} - \mathrm{x})S_h^{2-} \, + 2xe^-$$

SIGNIFICANCE

Sulfur as a cathode material has high theoretical capacity, but suffers from problems of poor conductivity of sulfur and polysulfides, dissolution of reaction intermediates into the electrolyte, thus compromising the efficiency and reversibility of its electrodes[3–5].To address

these issues, extensive research has been focused on coupling sulfur with conductive materials in a restricted electrode structure[6,7].

Carbon materials are the most attractive candidates; owing to their conductivity, variable pore sizes and electrochemical stability. All kinds of nanographitic system viz. graphene[8–12], carbon nanotubes[13–15], activated carbon, expanded graphite[16] and carbon fibers[17,18] are being explored as conducting additive to sulfur electrodes[10,14,16,17]. Diverse techniques such as melting, sublimation, sulfur infusion, encapsulation[18] or different template methodologies[14,19,20] are being attempted to optimize the interaction between sulfur and nanographitic additive.

Hence, for sulfur cathodes, a conductive yet restricted nanostructure needs to be developed. This nanostructure, should allow for good conduction, enhanced ion transport and volumetric expansion, but on the other hand, should have limited sulfur-electrolyte contact and restricted polysulfide dissolution.

APPROACH

The carbon additive being investigated here is exfoliated graphene nanoplatelets (GnP), Because of its two dimensional morphology and nano-thickness dimension, GnP shows excellent electrical conductivity, which is a necessary requirement of any electrochemical system.

Most of the studies on carbon-sulfur materials follow a melting or sublimation approach by heat treatment around 150°C and 300 °C. This can result in liquid and vapor diffusion of sulfur in pores of the nanocarbon materials. However, melting results in sulfur coating the external surface of carbons, which allows easy dissolution of polysulfides in electrolyte causing shuttling and degradation in performance. However, sublimation conditions (~300°C) help sulfur to penetrate into micropores of carbon hosts, which are small enough to restrict polysulfide dissolution. Heat treatment at even higher temperatures of >450°C, does beyond vapor diffusion and can induce interactions between sulfur and carbon. The S_8 sulfur converts to S_6 and S_2 forms at such conditions, which are more reactive due to a higher fraction of terminal S atoms[14]. There are reports of sulfur forming C-S bonds and intercalating into graphene layers in such high temperature conditions[14].

GnP has a non-porous, platelet type morphology, hence, higher temperature conditions (> 450°C), which are known to create C-S interactions by bonding or intercalation, are being used in our procedure.

EXPERIMENTAL DETAILS

MATERIALS

Sulfur powder, PVDF binder and NMP were obtained from Sigma- Aldrich. Graphene nanoplatelets of 25 µm diameter (xGnP-M-25) and surface area of 100 m^2/g, obtained from XG

Sciences® are used as the carbon host material for this application. GnP-15 (surface area of 25 m^2/g) made in our lab is used as the conducting additive for these electrodes.

ACTIVE MATERIAL PREPARATION

Graphene Nanoplatelets and Sulfur powder were measured in desired weight ratio and were mixed by a simple ball milling process in the SPEX 8000M Mixer Mill. The milling media used for this process was ¼" Polypropylene balls. Further treatment of GnP+S mixture was done in a sealed pressure vessel to avoid loss of sulfur at temperatures greater than sublimation conditions. PARR 4740 High Pressure Vessel with graphite gaskets, compatible for temperatures up to 540 °C, and pressure rating of 1500 psi (at 540 °C) was used for synthesis of composites. The pressure vessel was sealed inside a glove box under Argon atmosphere, to avoid any interference due to ambient moisture. The GnP-Sulfur material sealed in the pressure vessel was subjected to different heat treatment temperatures (300 °C, 500 °C) in the box furnace for 2 hours.

ELECTRODE PREPARATION

The GnP-S composite material composed of 5 wt% GnP-15 and 10 wt % PVDF as binder was combined with NMP as solvent to make a slurry, which was cast on Al foil by procedures described elsewhere. The addition of high aspect ratio GnP-15 as an additive was done to ensure good conductivity throughout the electrode. The electrodes were dried under ambient condition, followed by vacuum annealing at 120 °C for 8 hours.

PHYSICAL CHARACTERIZATION

The morphology of the sulfur electrodes was observed from top view and cross-section view using Auriga FIB SEM. The sample preparation for cross-sectional imaging involved epoxy embedding and polishing procedure (described earlier). The sulfur concentration was also verified by doing Energy Dispersive Spectroscopy, on a pellet formed by compressing the GnP-Sulfur composite powder using a Carl-Zeiss EVO SEM.

Thermogravimetric analysis (TGA) was conducted by heating the material up to 900°C at a ramp rate of 10°C/min, in airflow. The sulfur concentration is evaluated by loss of material at 300 °C, which is the sublimation temperature of Sulfur.

The X-ray diffraction analysis was done on powder samples by a Bruker Davinci Diffractometer, using Cu K α radiation and λ = 1.5418 Å.

ELECTROCHEMICAL CHARACTERIZATION

The electrodes were characterized in a coin cell CR 2032 with Lithium foil as counter electrode and 1M lithium bis-trifluoromethanesulfonylimide (LiTFSI) solution in (1:1 v/v) 1,3-dioxolane (DO) and dimethoxyethane (DME) mixture. The cells were assembled and tested in Argon atmosphere in Braun Glove Box (<2ppm O_2, <2ppm H_2O).

The electrochemical characterization of GnP-S was done using a VersaSTAT MC Instrument. The charge–discharge performance of the electrodes was evaluated by cycling between 1-3.0 V at different charge rates. AC impedance spectra were collected in the

frequency range from 1 Hz-10^6 Hz with amplitude of 5 mV, before and after cycling for 10 cycles at C rate.

RESULTS & DISCUSSION

GNP-SULFUR COMPOSITE SYNTHESIS

GnP-sulfur nanocomposites were synthesized by incorporating sulfur into GnP matrix, by a simple mixing-melting procedure (schematic illustration shown in Figure 5-2).

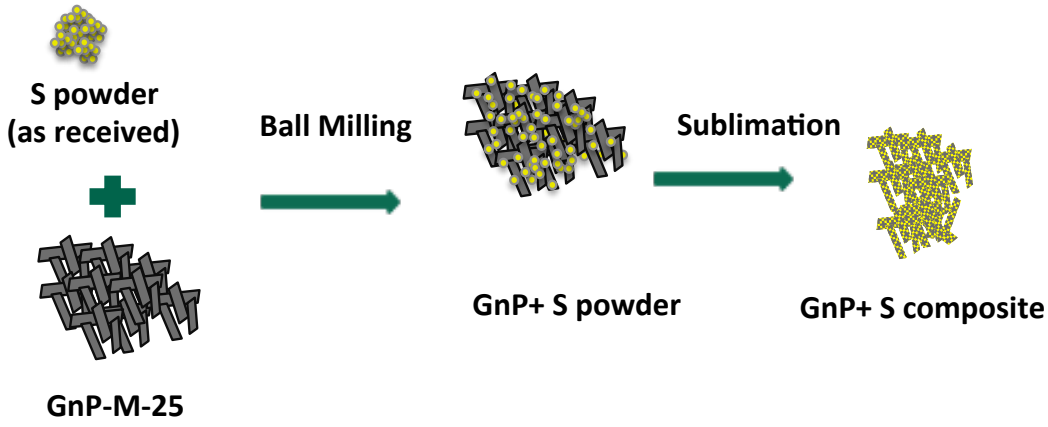

Figure 5-2: Schematic depicting synthesis process for GnP-S composite

PHYSICAL CHARACTERIZATION

The concentration of composite material was investigated by TGA and EDS analysis on the powder. From the TGA analysis (Figure 5-3), it was observed, that the concentration of sulfur in the composite is 10%. Since a starting concentration of 33% was used, there was a loss in sulfur as a result of the fabrication process. A strong sulfur smell was observed on opening the pressure vessel after the heat treatment, which is a probable explanation for volatilization of the sulfur in the process. There is visible corrosion of the stainless steel pressure vessel, due

to high temperature treatment under sulfur, which has led to some iron and chromium contamination.

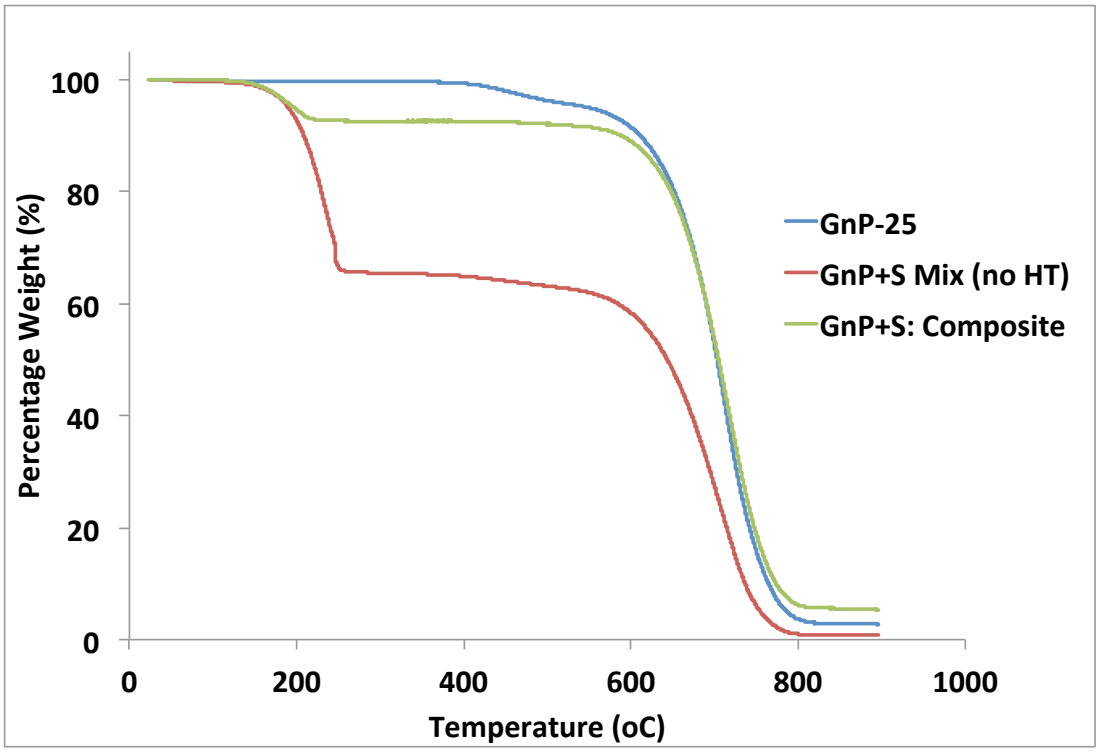

Figure 5-3: TGA Analysis showing the removal of sulfur around 300°C, giving an indication of Sulfur concentration in the composite

For EDS analysis, the powder was compressed to form a pellet to provide bulk and uniform area for X-rays to penetrate, and give a more accurate estimation of sulfur concentration. Also, using a thick pellet helps to eliminate any signal contribution from C tabs used for mounting sample on the SEM stub. THE EDS data shown in Figure 5-4 shows two different regions, one is the most commonly seen GnP surface and the brighter spot is an area observed but in very low concentration which is most likely contamination from pressure vessel corrosion. Area 1 and 2 shows S concentration to be approximately 10% in the composite, with very little impurities. However Area 3 shows a higher concentration of S along with Cr & Fe,

which indicates that S is reacting with the components of pressure vessel and getting sacrificially consumed.

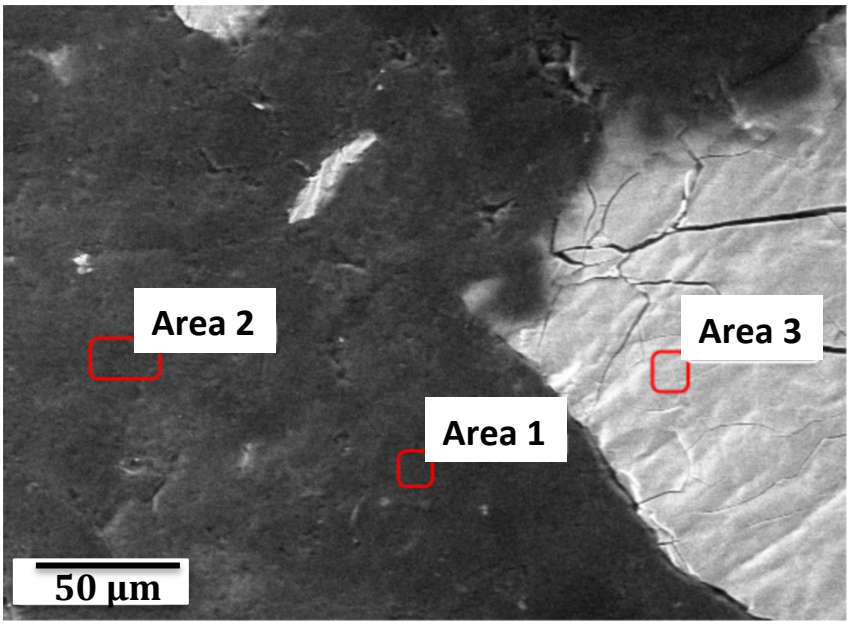

Element	Weight %		
	Area 1	Area 2	Area 3
C K	88.1	88.2	30.7
S K	10.6	8.9	30.6
O K		0.9	3.5
S K	10.6	8.9	30.6
Cr K	1.3	0.7	24.3
PoM		0.7	1.3
Fe K	0.6	0.6	9.0
Si K			0.6

Figure 5-4: EDS Analysis of GnP-S composite material

Further characterization of the composite material was done by X-ray diffraction analysis (Figure 5-5). The XRD pattern of S powder and GnP-S ball milled mixture was done to understand the changes in the composite. As we can see, GnP-S ball milled mixture shows all the peaks corresponding to sulfur powder, in addition to the graphitic peaks at 26° and 55°. Most of the prominent S_8 peaks disappear in GnP-S composite (prepared by heat treatment), however there are some minor peaks and additional peaks can be observed which indicates some kind of sulfur or its compounds still exists. However, these peaks could not be interpreted completely to give an indication of the composition of the material.

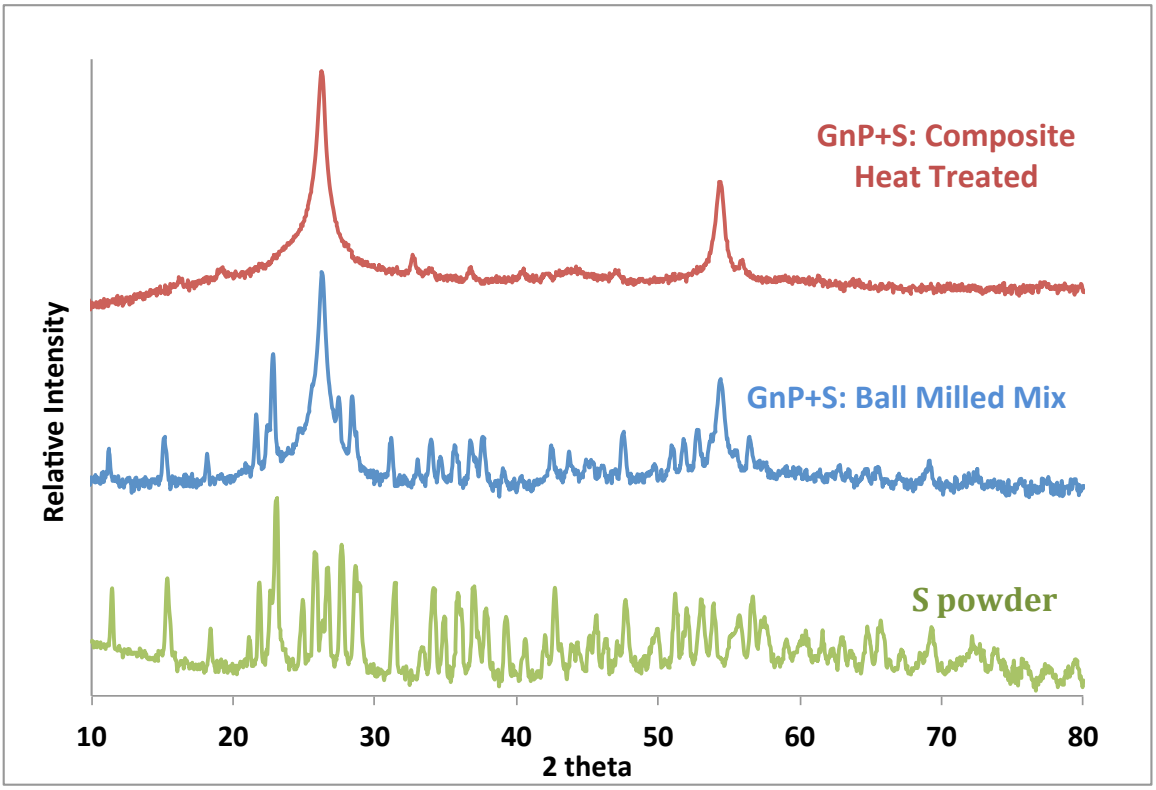

Figure 5-5: XRD Diffraction of GnP-S composite compared to the as received sulfur and intermediate ball milled mixture

ELECTRODE MORPHOLOGY

The electrodes were prepared by making slurry of the composite in NMP with PVDF as the binder and 5 weight % of GnP-15 (schematic shown in Figure 5-6). The addition of small amounts of GnP-15 was done to form an interconnected network through the electrode structure, which can ensure good conductivity throughout the electrode structure and also hinder the polysulfide dissolution.

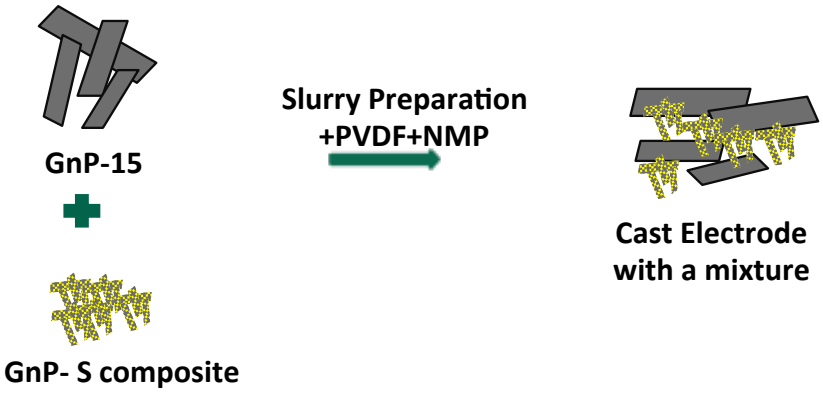

Figure 5-6: Schematic showing the electrode preparation of GnP-S composite

The morphology of the electrodes was observed from top view (Figure 5-7) and cross-sectional view (Figure 5-9) to understand the arrangement of GnP-S material in the electrode. The top view of the electrode shows a uniform distribution of sulfur throughout the GnP-S surface. Also, the backscatter electron image shown in Figure 5-8, emphasizes the different phases based on their atomic number. The sulfur phase is highlighted (grey regions) and shows good dispersion throughout the electrode. The very bright areas might be due to chromium or iron contamination from the pressure vessel. Figure 5-9 shows the cross-sectional view of the GnP-S electrodes which shows aligned and interconnected structure, characteristic of GnP

based electrodes. We can see good connectivity throughout the electrode, however there are some regions showing aggregation.

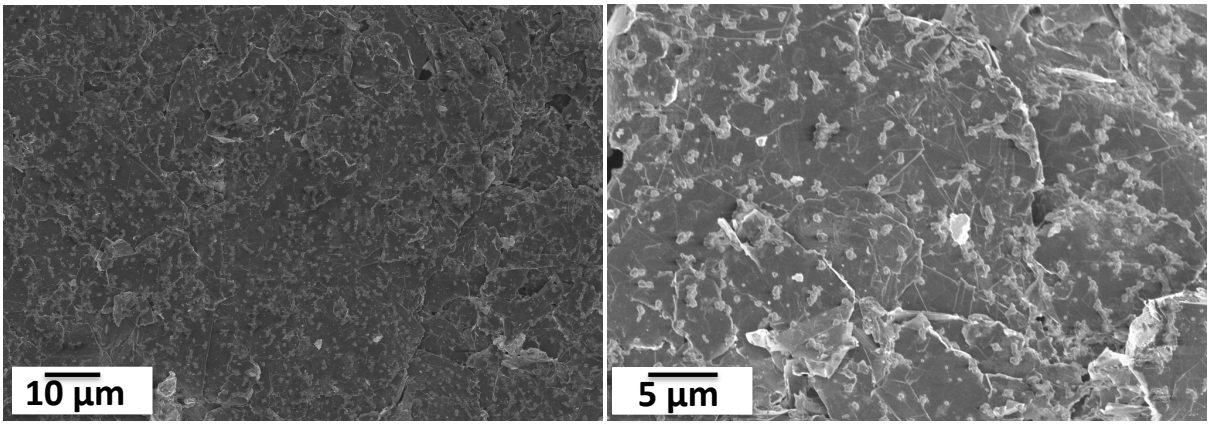

Figure 5-7: Top-view of GnP-S electrode

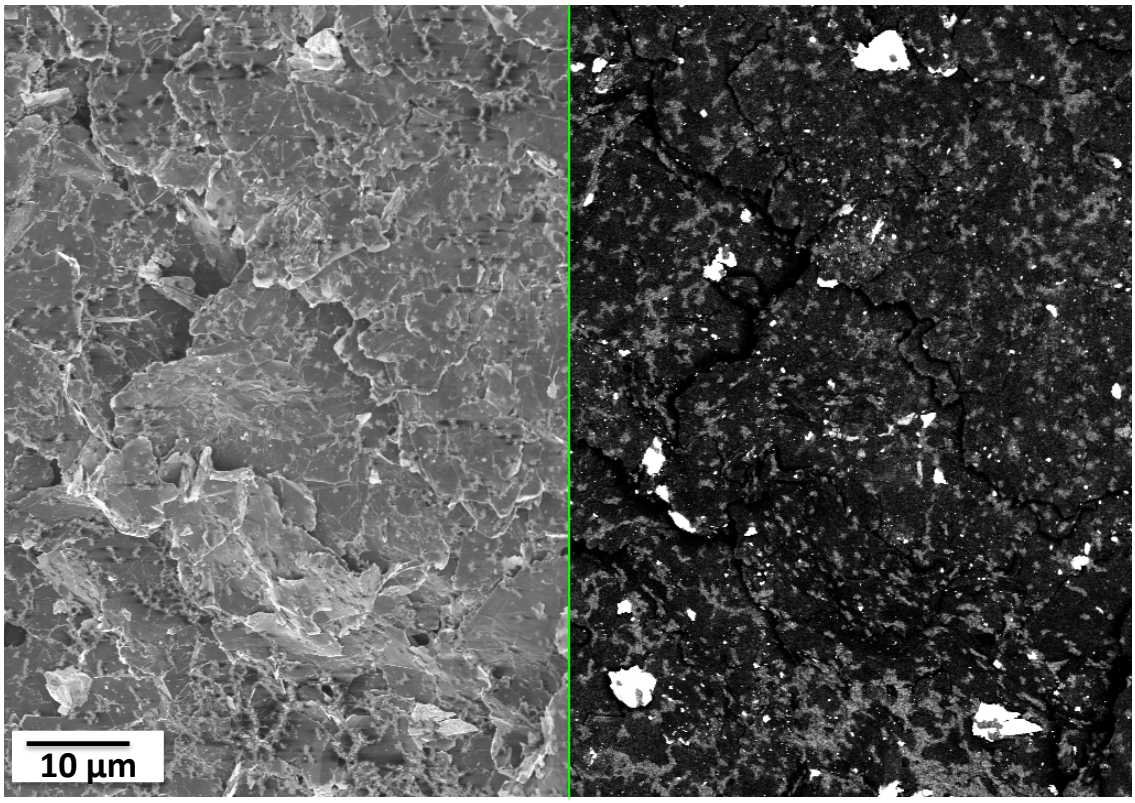

Figure 5-8: Secondary electron and Back-scatter electron images of GnP+S electrode

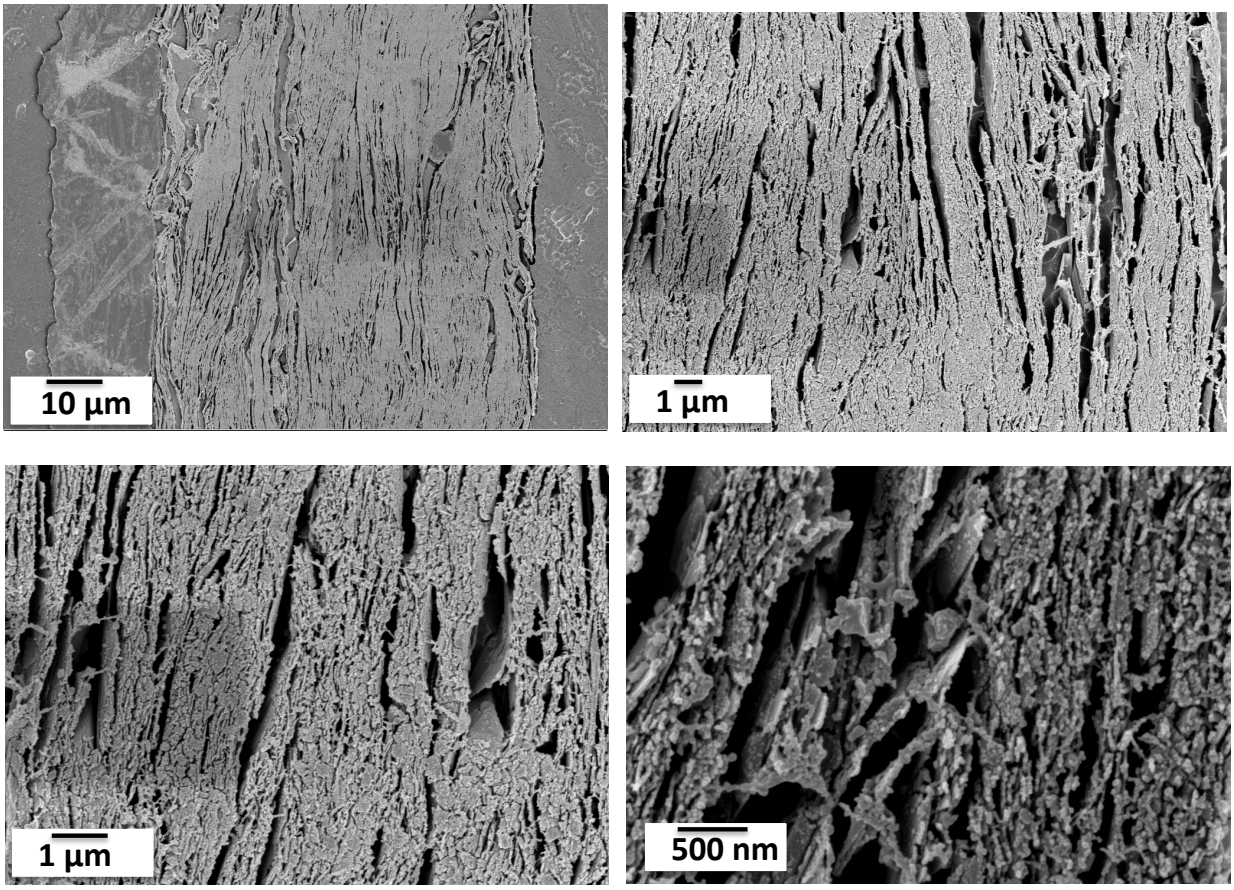

Figure 5-9: Cross-sectional Image of GnP-S electrode at different magnifications

ELECTROCHEMICAL CHARACTERIZATION

The charge discharge performance of GnP+S electrode was evaluated at different charge rates (Figure 5-10 (a)). The performances, shown in Figure 5-10 represent the mean value of the capacities obtained, with the error bars representing the range of data. We can observe that there is significant degradation in capacity for the first cycle and eventually the capacity becomes stable. At C charge rate, the first cycle shows capacity is around 1500 mAh/g, which degrades considerably on cycling to 1100 mAh/g after 10 cycles. The capacity values reduce to ~900 mAh/g and ~450 mAh/g at faster charge rates of 2C and 5C rates respectively.

We can notice some erratic behavior around cycle 17, which was visible in all the cells. The exact cause of this change could not be determined and was probably an artifact due to external factors like instrument error and vibrations. The cell continued to function properly even after this event. More testing is being done, to rule out any other reasons. Further, long term cycling was continued by charging the cell up to 100 cycles at C rate (Figure 5-10 (b)). At the end of 100 cycles, the capacity of the GnP-S composite was equal to 900 mAh/g.

It is also important to mention that cycling at low charge rates (C/5) gave unrepeatable capacity values and showed a significant degradation. This is probably a consequence of increased polysulfide dissolution due to long reaction times, thus resulting in loss of active material and capacity degradation.

The charge –discharge capacity profiles of 5th cycle of every charge rate are shown in Figure 5-11. The profiles do not have the typical plateau type behavior, and instead have sloping curves. The plateau type profiles shown in most of the literature[8,16,18,21,22], can be attributed to the conversion of $S_8 \rightarrow S_6^{2-}$ (at 2.4 V), $S_6^{2-} \rightarrow S_4^{2-}$ (at 2.1 V) and $S_4^{2-} \rightarrow S_2^{2-}$ (at 2.05 V); and their conversion back during charging. However, sloping curves have been observed in composite materials, which are heat treated at temperatures higher than S sublimation[14,23]. It has been predicted that at very high temperatures (>450°C), sulfur doesn't exist in S_8 form and some interaction between carbon and sulfur can happen such as a weak bond or intercalation of sulfur into graphite[14]. However, in our case, no signs of further intercalation are observed from the XRD data. Such a change in the initial C-S interaction can change the pathway of the

reaction during galvanostatic cycling. These materials act similar to Ni-S alloys and follow a reaction pathway $S_4^{2-} \rightarrow S_2^{2-} \rightarrow S^{2-}$, which can explain the sloping profile.

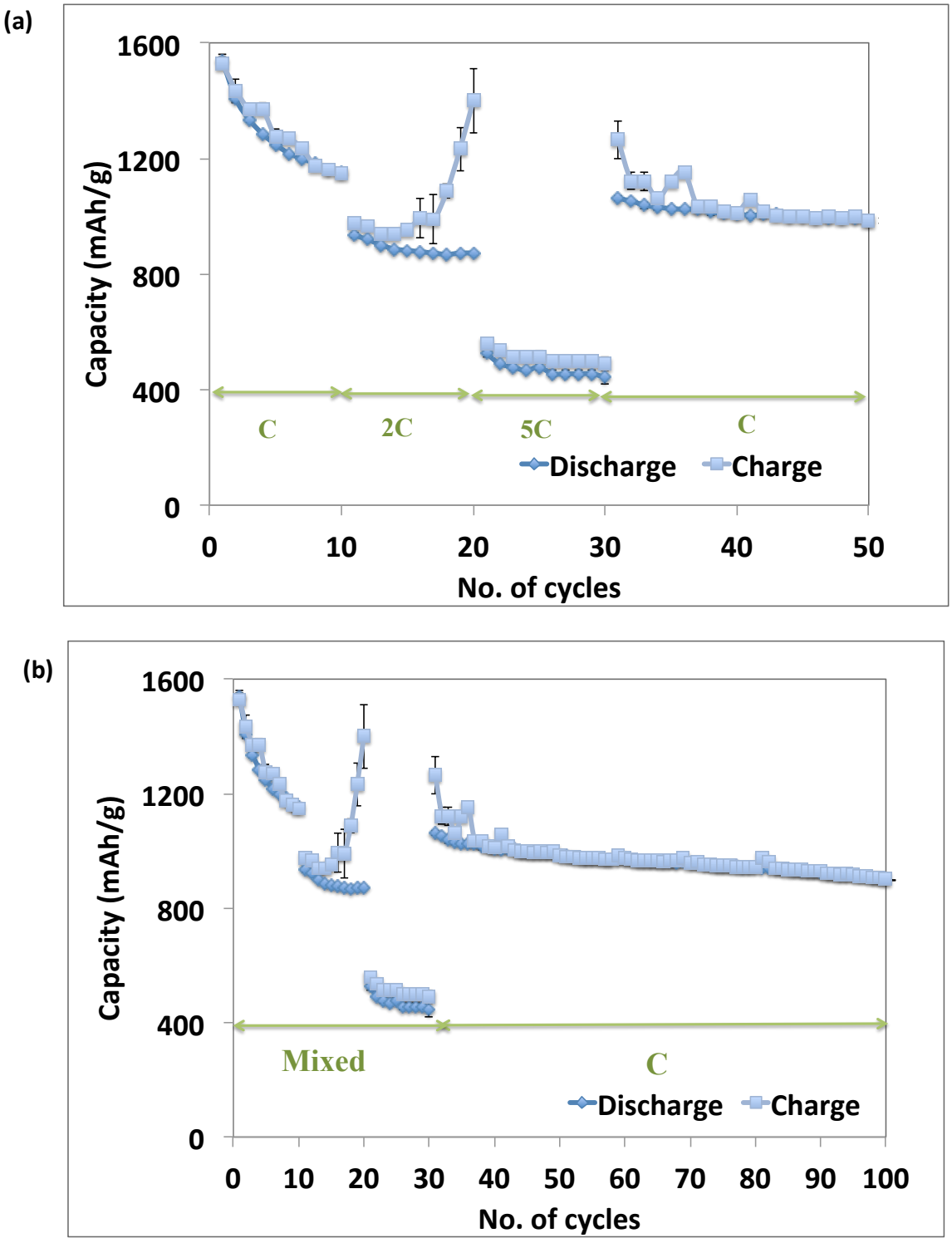

Figure 5-10: Galvanostatic Performance of GnP-S composite electrode for (a) different charge rates (b) long cycling

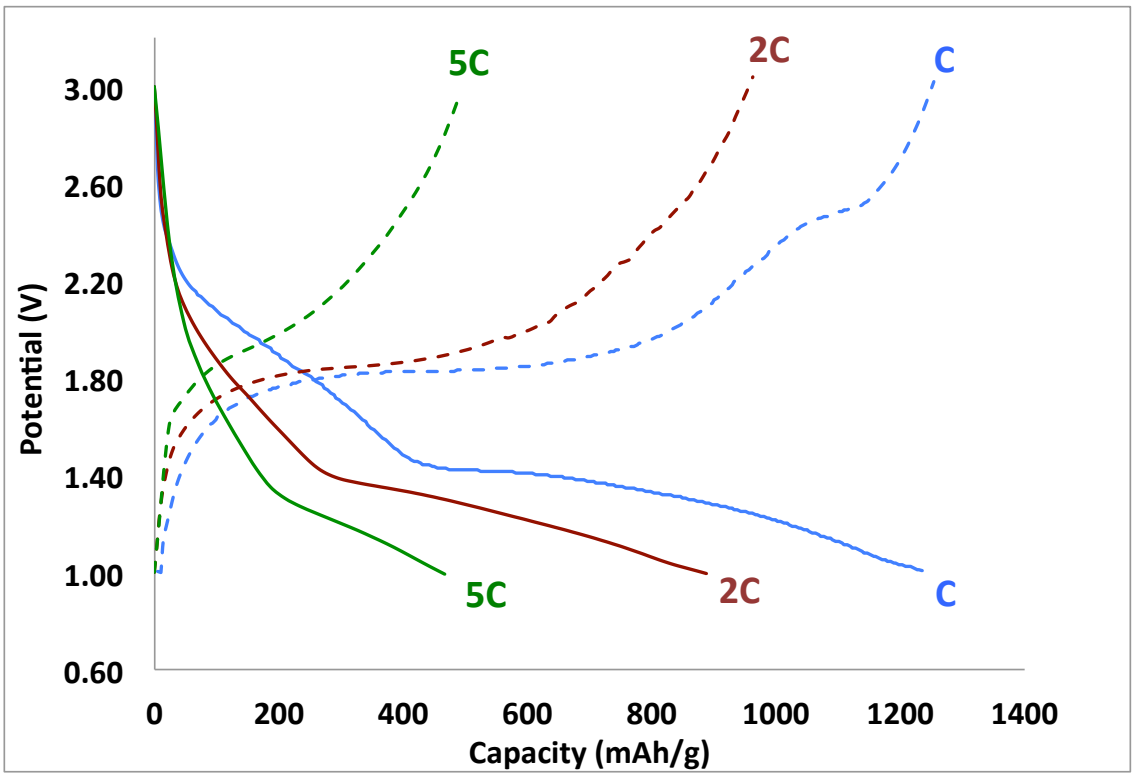

Figure 5-11: Charge-Discharge capacity profiles at different charge rates C, 2C, 5C.

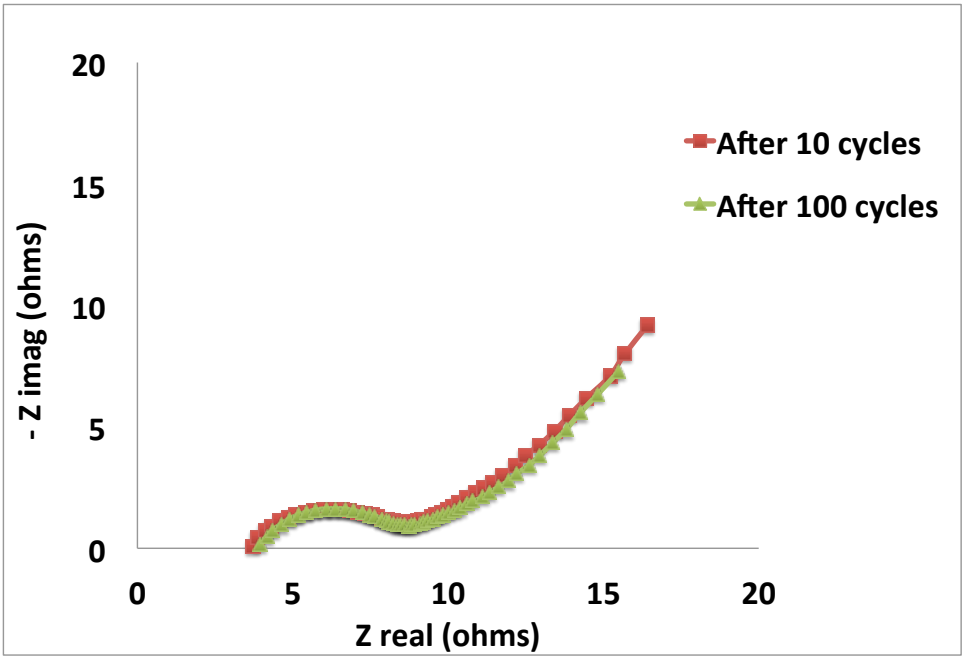

Figure 5-12: Nyquist plot of GnP+S electrode before and after 10 and 100 cycles

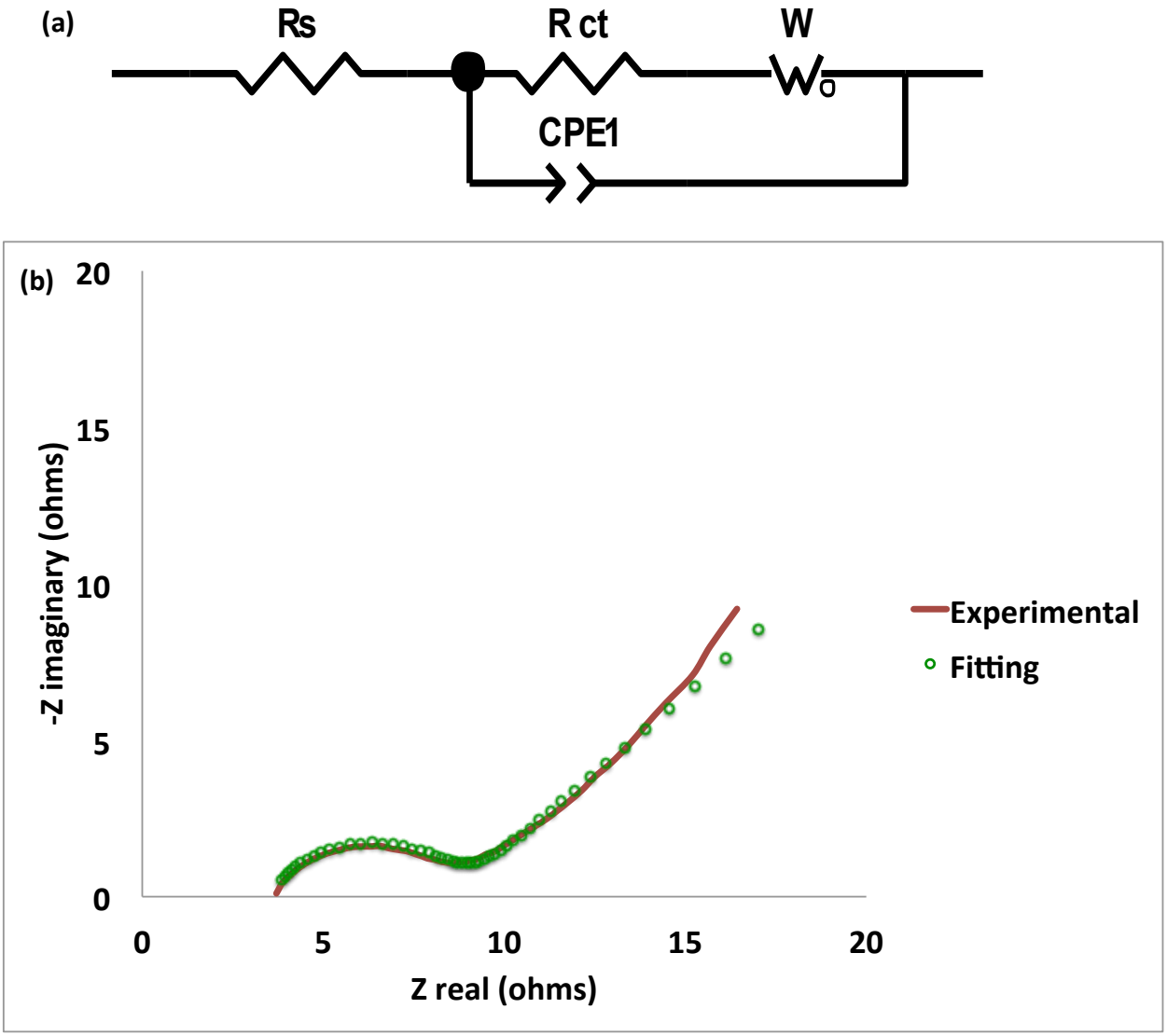

Figure 5-13: (a) Equivalent circuit used for fitting impedance data (b) Comparison of experimental and fitted impedance data for GnP-S electrode after cycling for 10 cycles

Table 5-1: Resistance values obtained by fitting impedance data using the equivalent circuit

	Rs	Rct
GnP+S-10cyc	3.5	5.3
GnP+S-100cyc	3.8	5.1

EIS analysis was conducted to evaluate the presence of insulating polysulfide products deposited on the electrode surface. Figure 5-12 below shows the Nyquist plots of GnP-S electrode after 10 and 100 cycles. The intercept of the curve on the Z real axis gives us the bulk or solution resistance of the cell, which is a combination of the electrolyte resistance and intrinsic resistance of the electrode[24]. The charge transfer resistance associated with the kinetics of charge transfer is indicated by the semi-circular part of the curve at medium frequencies[10,24]. The inclined line at low frequencies corresponds to the Warburg impedance, which is a measure of the diffusion of Li ions in the electrode[24]. The experimental impedance data obtained was fitted with Zview software using the equivalent circuit[12,25] shown in Figure 5-13(a). A comparison of experimental and equivalent circuit calculated data for GnP-S electrodes after 10 cycles is shown in Figure 5-13(b). Very good fitting in the high and medium frequency range was obtained, however there was only reasonable fitting with 15-20% error for the diffusion region, which is a complex process in lithium-sulfur system. Based on the values of the solution and charge transfer resistance (Table 5-1) obtained from this analysis, we can observe that there is no significant increase in resistance after 100 cycles. This confirms that the interconnected network of GnP particles imparts good conductivity to the electrode over long cycling.

CONCLUSIONS

From the above results, we can infer that GnP can act as a good conducting host for Lithium-sulfur batteries. We have demonstrated good performance of 900 mAh/g after 100

cycles at C charge rate. However, the sulfur loading in these experiments is quite low and focus should be on improving the overall sulfur percentage in the electrode for better gravimetric capacity.

FUTURE WORK

Based on our understanding of the lithium-sulfur batteries, we have concluded that the potential sulfur electrode should be sulfur encapsulated in a conducting but flexible or spacious matrix, which will allow for volumetric expansion, but restrict the interaction of sulfur with the electrolyte. We have demonstrated that graphene nanoplatelets have good electrical conductivity and can be arranged into a nanostructure with controlled porosities. Hence, from previous experiments and current progress in the field, GnP Paper can be used as a conducting template for lithium sulfur batteries, capable of delivering high performance and good cycle life. The process approach is schematically shown in Figure 5-14.

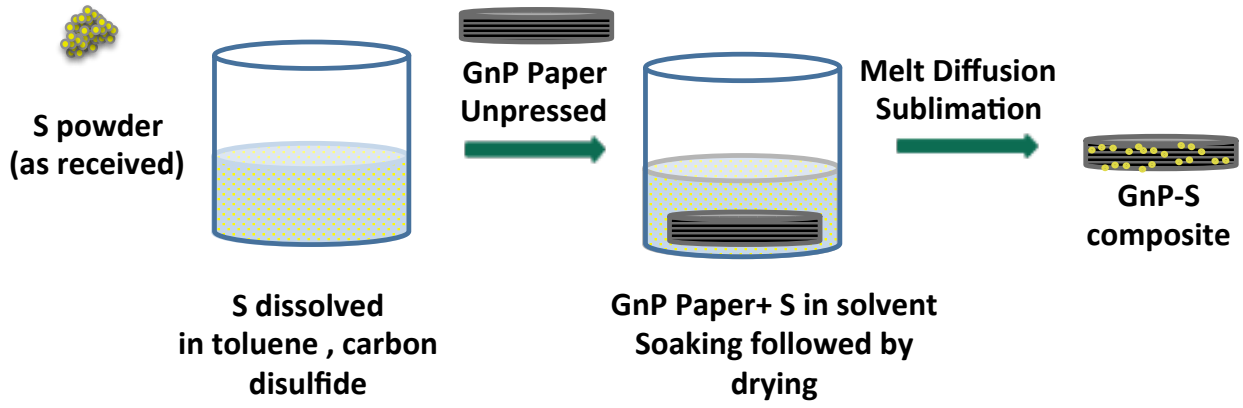

Figure 5-14: Schematic depicting the synthesis of sulfur impregnated GnP Paper

This conducting template can be altered in porosity and hence can be made selectively permeable to lithium ions, but not to the undesirable polysulfides reaction intermediates. Such a structure can entrap the active sulfur material and will prevent it from dissolving into the

active electrolyte during the reaction, in the form of polysulfides. Literature references show a retention of 80% of theoretical capacity of sulfur by ensuring restricted polysulfide dissolution by having a polymer coated carbon nanostructure[26].

Future work in this application will revolve around encapsulating sulfur in a GnP matrix for enhanced conduction and tailoring the GnP paper to desired porosities for achieving maximum performance for lithium sulfur cathodes.

REFERENCES

REFERENCES

1. Mikhaylik, Y., Kovalev, I., Schock, R. & Affinito, J. High Energy Rechargeable Li-S Cells for EV Application. Status, Challenges and Solutions. *Sion Power Corporation* . Available from http**:**//sionpower.com/pdf/articles/SionPowerECS.pdf

2. Liu, Z., Fu, W. & Liang, C. *Handbook of Battery Materials*. 811–840 (2011).

3. Evers, S. & Nazar, L. F. New Approaches for High Energy Density Lithium Sulfur Battery Cathodes. *Accounts of Chemical Research* , (2012). **DOI:** 10.1021/ar3001348

4. Manthiram, A., Fu, Y. & Su, Y. Challenges and Prospects of Lithium-Sulfur Batteries. *Accounts of Chemical Research*, (2012). **DOI:** 10.1021/ar300179v

5. Bruce, P. G., Freunberger, S. A., Hardwick, L. J. & Tarascon, J. Li – O 2 and Li – S batteries with high energy storage. *Nature materials* **11**, 19–30 (2012).

6. Zhang, Y., Zhao, Y., Sun, K. E. & Chen, P. Development in Lithium / Sulfur Secondary Batteries. *The Open Materials Science Journal* **5**, 215–221 (2011).

7. Song, M.-K., Cairns, E. J. & Zhang, Y. Lithium/sulfur batteries with high specific energy: old challenges and new opportunities. *Nanoscale* **5**, 2186–204 (2013).

8. Cao, Y. *et al.* Sandwich-type functionalized graphene sheet-sulfur nanocomposite for rechargeable lithium batteries. *Physical chemistry chemical physics : PCCP* **13**, 7660–5 (2011).

9. Chuvilin, a *et al.* Self-assembly of a sulphur-terminated graphene nanoribbon within a single-walled carbon nanotube. *Nature materials* **10**, 687–92 (2011).

10. Wang, J.-Z. *et al.* Sulfur-graphene composite for rechargeable lithium batteries. *Journal of Power Sources* **196**, 7030–7034 (2011).

11. Wang, H. *et al.* Graphene-Wrapped Sulfur Particles as a Rechargeable LithiumÀSulfur Battery Cathode Material with High Capacity and Cycling Stability. *Nano Letters* **11**, 2644–2647 (2011).

12. Zhang, F. *et al.* Preparation and performance of a sulfur/graphene composite for rechargeable lithium-sulfur battery. *Journal of Physics: Conference Series* **339**, 012003 (2012).

13. Zhou, G. *et al.* A flexible nanostructured sulphur–carbon nanotube cathode with high rate performance for Li-S batteries. *Energy & Environmental Science* **5**, 8901 (2012).

14. Guo, J., Xu, Y. & Wang, C. Sulfur-impregnated disordered carbon nanotubes cathode for lithium-sulfur batteries. *Nano letters* **11**, 4288–94 (2011).

15. Kim, H., Lee, J. T. & Yushin, G. High temperature stabilization of lithium–sulfur cells with carbon nanotube current collector. *Journal of Power Sources* **226**, 256–265 (2013).

16. Li, S., Xie, M., Liu, J., Wang, H. & Yan, H. Layer Structured Sulfur/Expanded Graphite Composite as Cathode for Lithium Battery. *Electrochemical and Solid-State Letters* **14**, A105 (2011).

17. Elazari, R., Salitra, G., Garsuch, A., Panchenko, A. & Aurbach, D. Sulfur-impregnated activated carbon fiber cloth as a binder-free cathode for rechargeable Li-S batteries. *Advanced materials* **23**, 5641–4 (2011).

18. Zheng, G., Yang, Y., Cha, J. J., Hong, S. S. & Cui, Y. Hollow carbon nanofiber-encapsulated sulfur cathodes for high specific capacity rechargeable lithium batteries. *Nano letters* **11**, 4462–7 (2011).

19. Ji, X., Evers, S., Black, R. & Nazar, L. F. Stabilizing lithium-sulphur cathodes using polysulphide reservoirs. *Nature communications* **2**, 325 (2011).

20. Xin, S., Guo, Y.-G. & Wan, L.-J. Nanocarbon networks for advanced rechargeable lithium batteries. *Accounts of chemical research* **45**, 1759–69 (2012).

21. Wu, F., Wu, S. X., Chen, R. J., Chen, S. & Wang, G. Q. Electrochemical performance of sulfur composite cathode materials for rechargeable lithium batteries. *Chinese Chemical Letters* **20**, 1255–1258 (2009).

22. Wang, J. L., Yang, J., Xie, J. Y., Xu, N. X. & Li, Y. Sulfur – carbon nano-composite as cathode for rechargeable lithium battery based on gel electrolyte. *Science And Technology* **4**, 499–502 (2002).

23. Yu, X. *et al.* Stable-cycle and high-capacity conductive sulfur-containing cathode materials for rechargeable lithium batteries. *Journal of Power Sources* **146**, 335–339 (2005).

24. Wang, Y.-X. *et al.* Facile synthesis of a interleaved expanded graphite-embedded sulphur nanocomposite as cathode of Li–S batteries with excellent lithium storage performance. *Journal of Materials Chemistry* **22**, 4744 (2012).

25. Zhang, B., Qin, X., Li, G. R. & Gao, X. P. Enhancement of long stability of sulfur cathode by encapsulating sulfur into micropores of carbon spheres. *Energy & Environmental Science* **3**, 1531 (2010).

26. Ji, X., Lee, K. T. & Nazar, L. F. A highly ordered nanostructured carbon-sulphur cathode for lithium-sulphur batteries. *Nature Materials* **8**, 500–506 (2009).

6 CONCLUSIONS

The increasing energy and power requirements for portable devices have driven strong interest in the development and efficient utilization of active materials for all parts of lithium ion batteries. The direction of current research is oriented towards development of nanomaterials and structured electrodes for improved performance.

Graphene Nanoplatelets (GnP) are a promising nanocarbon material, which can be integrated into different lithium ion battery components and because of its morphology, can be nano-structured to enhance battery performance in a variety of ways. We have demonstrated the potential of GnP as an active anode material. Also, GnP can be combined with metal or metal oxide nanoparticles (with inactive or inherent lithium storage capacity) to form composite electrodes with high performance. Nickel doped graphene nanoplatelets, with 60 nm nanoparticle size have shown improved capacity, around 300 mAh/g at fast charge rates of C and 2C. This improvement has been attributed to a tailored nanostructures with benefits of short diffusion length, ordered porosity and interconnectivity.

The role of different sizes of GnP as a conducting additive has been evaluated for Lithium Titanate electrodes. LTO-GnP electrodes (using GnP-25 and GnP-5) have shown up to 10% improvement in capacity with reference to the use of commercial Super P carbon additives. Based on our results, we can infer that GnP, because of its high aspect ratio and excellent conductivity can provide efficient contact with active materials and thus, is a strong contender for conducting additives for different electrode materials.

GnP can be easily fabricated into free-standing 'paper' films as a current collector. The GnP current collector has ~50% the areal density of copper, and hence can help reduce the dead weight in the batteries. Moreover, the current collector itself can contribute to increased lithium storage capacity in graphite based anode systems. The GnP current collector can be extended to the cathode side and replace the aluminum current collector, thus eliminating any corrosion problems with metal current collectors. Free standing GnP papers can be customized for use in various components of battery systems and other electrochemical systems such as sensors and supercapacitors as well.

Lithium sulfur batteries are being envisioned as the future of portable energy storage because of their low predicted cost and high performance. The use of GnP as a conducting host material for lithium sulfur batteries enables this chemistry to be capable of delivering high performance at fast charge rates because of its nanostructuring and conductivity. High capacity of 900 mAh/g after 100 cycles at C charge rate has been delivered by the GnP-S composite.

ACKNOWLEDGEMENT

This material is based upon work supported in part by the U. S. Army Research Laboratory and the U. S. Army Research Office under contract/grant number No. W911NF0910451. The support for the A123 Michigan Center of Energy Excellence Grant 106979 is also greatly acknowledged.